NASA CONTRACTOR REPORT

THERMOPHYSICAL PROPERTIES OF A LOW-DENSITY PHENOLIC-NYLON ABLATION MATERIAL

by W. T. Engelke, C. M. Pyron, Jr., and C. D. Pears

Prepared by
SOUTHERN RESEARCH INSTITUTE
Birmingham, Ala.
for Langley Research Center
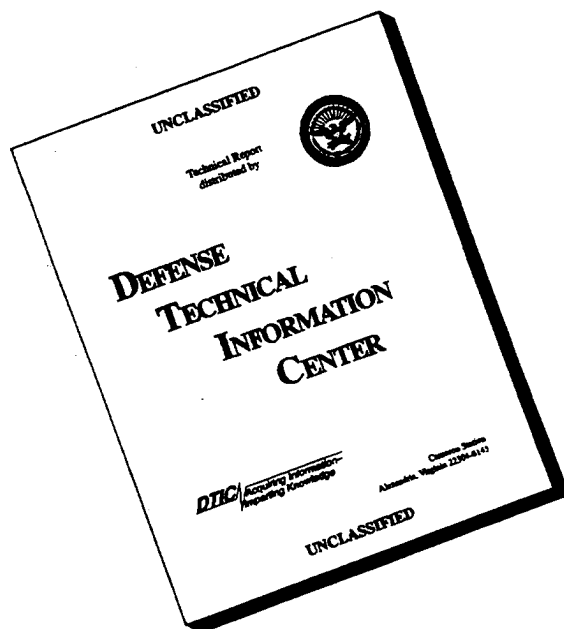
NATIONAL AERONAUTICS AND SPACE ADMINISTRATION • WASHINGTON, D. C. • JULY 1967

DISCLAIMER NOTICE

THERMOPHYSICAL PROPERTIES OF A LOW-DENSITY

PHENOLIC-NYLON ABLATION MATERIAL

By W. T. Engelke, C. M. Pyron, Jr.,
and C. D. Pears

THERMOPHYSICAL PROPERTIES OF A

LOW-DENSITY PHENOLIC-NYLON ABLATION MATERIAL

By W. T. Engelke,
C. M. Pyron, Jr., and C. D. Pears
Southern Research Institute

SUMMARY

Some physical properties were determined on a low-density phenolic-nylon that was both nondegraded (virgin) and thermally degraded (charred). The work was performed under Task Order 4 of Contract NAS 1-2978, which was a continuation of similar studies under previous Task Orders 1 through 3. Task Orders 1 through 3 have been reported in NASA TN D-2991 (Reference 1).

The low-density phenolic-nylon was a molded composite consisting of 25% phenolic resin, 35% phenolic Microballoons, and 40% powdered nylon. The material was thermally charred in an arc tunnel.

The thermal conductivity of the virgin material from -200°F to 750°F ranged from 1.27×10^{-5} Btu/sec/ft/°F (7.91×10^{-2} W/m/°K) to a maximum of 1.69×10^{-5} Btu/sec/ft/°F (10.5×10^{-2} W/m/°K). These values were lower than those exhibited for the low-density phenolic-nylon evaluated under Task Order 1. The reason for the lower conductivity appears to be the weaker structure of the material evaluated under this program.

The thermal conductivity from 1000°F to 5000°F of the charred material increased from 11.5×10^{-5} Btu/sec/ft/°F (0.72 W/m/°K) to 76×10^{-5} Btu/sec/ft/°F (4.73 W/m/°K). During cooling the values were higher and more scattered, indicating further degradation at the higher temperatures and some shrinking and cracking of the specimens upon cooling.

The heat capacity of the virgin material increased from 0.20 Btu/lb/°F (837 J/kg/°K) at -200°F to 0.58 Btu/lb/°F (2427 J/kg/°K) at 600°F. Due to the carbonaceous character of the charred material, the heat capacity compared well with that of graphite. The values increased from 0.39 Btu/lb/°F (1632 J/kg/°K) at 1000°F to 0.57 Btu/lb/°F (2385 J/kg/°K) at 5000°F.

The coefficient of thermal expansion at 70°F for the virgin material was 23.5×10^{-6} in./in./°F (42.3×10^{-6} m/m/°K). The data indicated slight anisotropy of the material and also demonstrated a transformation of the material above 230°F which caused the material to contract.

The permeability of both the virgin and charred material was obtained at low pressure drops across the specimen with helium and nitrogen used as the permeating gases. The admittance of the virgin specimens ranged from 3.6×10^{-4} m²/sec to 5.2×10^{-4} m²/sec, and the charred material exhibited values from 0.81 m²/sec to 1.87 m²/sec. The flow through the charred specimen was transitional and turbulent.

The total normal emittance of the char from 1500°F to 5000°F ranged from 0.79 to 0.87.

The mechanical properties of the virgin material from -200°F to 750°F were determined. The ultimate tensile strength decreased from 570 psi (3.93×10^6 N/m²) at -200°F to below 100 psi (0.69×10^6 N/m²) at 500°F. The ultimate compressive strength decreased from 2600 psi (17.03×10^6 N/m²) at -200°F to approximately 200 psi (1.38×10^6 N/m²) at 750°F. Both tensile and ultimate strength values were lower (about one-half) than those of the phenolic-nylon evaluated under Task Order 1. The weaker structure, mentioned before, was apparently the reason for the lower values.

INTRODUCTION

This is the final report on the thermophysical property evaluation of a low-density phenolic-nylon ablation material performed for the NASA Langley Research Center under Contract No. NAS 1-2978, Task Order 4. The physical properties of the low-density phenolic-nylon in both the non-degraded (virgin) and thermally degraded (charred) forms were determined and analyzed. This investigation was performed to characterize the material for its reentry application as an ablative heat shield. The program was a continuation of similar studies performed under the previous Task Orders 1 through 3 reported in NASA TN D-2991 (Reference 1).

Specifically, the thermal conductivity, heat capacity, thermal expansion, density, permeability, and mechanical properties were determined on the virgin material; and the thermal conductivity, heat capacity, total normal emittance, density, porosity, and permeability were determined on the charred

2

material. The temperature ranges were -200°F to 750°F for the evaluation of the virgin material and 1000°F to 5000°F for the charred material. Reference 1 briefly describes the apparatuses and summarizes the measurement procedures that were applied, except for the permeability measurements. Additional details concerning the test methods may be found in references cited in the discussion of data.

SPECIMEN MATERIAL

The low-density phenolic-nylon material was supplied by the NASA Langley Research Center in both the nondegraded and thermally degraded forms. The nondegraded material was supplied in a block 12 inches in diameter and 4 inches thick. The thermally degraded material was supplied in 3 inch diameter discs with the charred area approximately $\frac{1}{4}$ inch deep.

This low-density phenolic-nylon composite was molded and consisted of the following materials: (1) 40% (weight) powdered 66 nylon, DuPont's Zytel 103; (2) 25% (weight) phenolic resin, Union Carbide Corporation's BRP-5549; (3) 35% (weight) phenolic Microballoons, Union Carbide Corporation's BJO-0930. The molding was performed at a maximum pressure of 2200 psi (15.17 x 10^6 N/m²) and temperature of 340°F. The material was also post cured at a maximum temperature of 300°F. The complete molding and post curing history are shown in Figures 1 and 2.

A more thorough description of the individual constituents is included in Appendix A. The difference in composition noted between this material and the low density phenolic-nylon evaluated under Task Order 1 is the different percentages of the constituents. The material under Task Order 1 contained 50% nylon, 25% resin and 25% Microballoons, and as discussed later, was stronger and exhibited a higher thermal conductivity. Under a separate contract study, reported in Reference 2, it was concluded that the formulation and processing of the material under this present program were less than optimum for a plastic composition. The formulation was low in volume fraction of phenolic resin and the processing method caused mechanical damage to the Microballoons and large temperature gradients during processing. Thus as reported in subsequent sections, the lower mechanical strength and thermal conductivity of this material when compared to the material evaluated under Task Order 1, may be directly correlated with the formulation and processing of the ablation material.

3

The thermally degraded material was produced in an arc tunnel. The three inch diameter discs of the phenolic-nylon were exposed to the following test conditions to form the chars: a stagnation enthalpy of 2800 Btu/lb (6.5 x 10^6 J/kg), stagnation pressure of 0.57 atm (5.8 x 10^4 N/m^2), thermal flux at the material surface of 140 Btu/ft^2/sec (1.58 x 10^6 W/m^2), freestream Mach number of 3.0 with nitrogen gas and an exposure time of 90 seconds. The arc tunnel is that described in NASA TN D-1621 with modifications to provide for supersonic flow.

To further define the as received material, the densities of both the virgin and charred materials were obtained. For the virgin material, the bulk density was determined at room temperature by the water displacement of a paraffin coated specimen in accordance with the ASTM D311-58 procedure. The duplicate values obtained from two pieces selected at random were 36.8 lb/ft^3 (589 kg/m^3) and 36.3 lb/ft^3 (582 kg/m^3) providing an average density of 36.6 lb/ft^3 or 586 kg/m^3. The density above and below room temperature was adjusted with the thermal expansion data (reported under the thermal expansion section) and is shown in Table 1. The density was not calculated above 200°F since the thermal expansion data indicated a transformation or initial degradation above this temperature which was accompanied with some weight loss as indicated in the heat capacity data. This, along with erratic expansion observed above 200°F, would make calculations meaningless.

The bulk density of the char was also determined in accordance with ASTM D311-58, and the true density was determined from a pulverized sample by employing a pycnometer. The average bulk density, determined from duplicate measurements, was 15 lb/ft^3 (240 kg/m^3), and the average true density was 93.6 lb/ft^3 (1500 kg/m^3). The volume percentage of porosity, which is the ratio of the difference between the true and bulk densities over the true density, was 84%.

A micrographic evaluation was also performed on the char to determine the average pore size and relative frequency distribution. The two specimens ($\frac{3}{32}$ in. thick) evaluated were taken from the top surface of the char. The specimens were impregnated with polyalphamethylstyrene and polished. The specimens were viewed at 100X magnification in a plane parallel to the thickness direction, and the pores were counted and measured with a calibrated eye-piece. Figure 3 is a typical photomicrograph of the char structure. The average pore diameter was 28.8 microns, and the histogram of pore diameters is shown in Figure 4. As can be seen in Figure 3, the pore structure is rather irregular with wide variation in size.

4

In comparing this char with the previous degraded low-density phenolic-nylon evaluated under Task Order 3, it was observed that the average pore size was larger for this material; however, the density and porosity were the same.

THERMAL CONDUCTIVITY

The thermal conductivity was determined in one direction (thickness of the supplied block) on both the virgin and charred material. For the virgin material, data were obtained from -200°F (144°K) to 750°F (673°K). The temperature range for the charred material was from 1000°F (811°K) to 5000°F (3033°K) with the data being obtained during heating and cooling cycles. The thermal conductivity of the virgin material was determined using an ASTM C177 guarded hot plate apparatus. The char specimens were evaluated in the radial inflow apparatus.

Apparatus and Procedure

ASTM guarded hot plate. - The 7-inch diameter ASTM C177 guarded hot plate apparatus employed for the thermal conductivity evaluation of the virgin material is described fully in Reference 3 and briefly below.

Basically this apparatus consisted of a central heater plate surrounded by a guard heater, each separately controlled. The guard ring was maintained at the same temperature as the central heater so that all of the heat flow was normal to the specimen surfaces. The heater plate was centrally sandwiched between layers of filler material, hot face thermocouples, the specimen, cold face thermocouples, filler material, a copper plate, and finally a cold plate to dissipate the heat. In addition to the thermocouples in contact with the specimen, thermocouples were located in the central heater and the outer copper cold plates. Intimate contact was provided at all interfaces by pressing the entire assembly together with a screw loaded frame.

Filler pads of gum rubber were used from -200°F to 150°F. Above 150°F, Fiberfrax paper was used for the filler pads with a sheet of gum rubber at the cold plate. Overlapping data were obtained at the 150°F temperature level for both filler arrangements, providing a check on contact resistance resulting from irregularities of the specimen surface.

To obtain mean temperatures of -200°F, liquid nitrogen was circulated through the cold plate. For higher temperatures, chilled trichloroethylene and water cooling were employed. When data points were obtained below room temperature, the apparatus was enclosed in a plastic bag which was purged with dry helium to eliminate frosting and moisture condensation.

During the run on Specimen 2, the change in thickness at the higher temperature levels was monitored. This was accomplished by cutting slots in the edge of the specimens. Small pads of 5 mil stainless steel shim stock were placed above and below the specimen, and the distance between these was measured with a hole gage. Measurements were taken at each temperature level. There was some uncertainty in these measurements since the specimen degraded and collapsed more rapidly at the edge than at the center due to the greater oxidation at the edge. This uncertainty was corrected at the last point by measuring the thickness at the center of the specimen after the completion of the run. The measurements taken at the intermediate temperatures were corrected in proportion to the difference obtained on this last point between the thickness change at the edge and at the center. The uncertainties resulting from this procedure are recorded with the data. In general, the thickness changed by about 20% during the run, and this change could be measured within an uncertainty of 3% at temperatures below about 400°F and within 8% at higher temperatures where degradation of the material was more severe.

Radial inflow apparatus. - To determine the thermal conductivity of the char specimens a modified procedure of the radial inflow apparatus was employed. The basic apparatus is fully described in Reference 1 and Reference 4.

Briefly, the test section was heated radiantly in a high temperature furnace which employed a cylindrical graphite resistance heating element. The heat flowed radially inward through the specimen to a central water flow calorimeter. Water temperatures in the calorimeter were indicated by thermocouples in the water stream located one-half inch apart, axially, and heat flow through the specimen gage section was computed from measurements of water flow rate and temperature rise. Specimen temperatures were measured in two axially drilled holes located on two different radii. Below 2000°F, temperature measurements were taken with chromel-alumel thermocouples; above this temperature, measurements were taken by sighting the bottom of the holes, by using an optical pyrometer and a right angle mirror device. Axial conduction in the specimen is minimized by (1) insulating the specimen on each end with graphite sleeves filled with thermatomic carbon, (2) by making the specimen length at least twice the gage length, and (3) by providing an isothermal hot zone over at least twice the specimen length.

6

Thermal conductivity is calculated from the standard relation

$$k = \frac{ql}{A\Delta T} \tag{1}$$

where k is the thermal conductivity, A is the log mean cylindrical area, and l is the radial distance over which ΔT is measured.

To measure the thermal conductivity of the char specimens, the technique described above was modified as follows: Four char strips, approximately $\frac{3}{8}$ inch wide by $\frac{3}{16}$ inch thick by 2 inches long were arranged symmetrically as shown in Figure 5. For this configuration, it was necessary that isothermals in the specimen be perpendicular to the thickness direction. This condition was achieved by placing thin strips of pyrolytic graphite at the inner surfaces of the char strips. Because of the high anisotropy of this material (the conductivity is approximately 50 times greater in the "a" direction than in the "c", or thickness, direction) the isotherms were forced to assume a square configuration. Heat flow other than through the specimen was eliminated essentially by using thermatomic carbon of extremely low thermal conductivity (approximately 0.1 Btu/hr/ft^2/°F/in.) as packing at the edges of the specimens. The space around the calorimeter was packed with graphite. Temperatures were measured at two locations in the strips, using the methods described above. This procedure was employed with good results under previous Task Orders 2 and 3, and is reported in NASA TN D-2991.[1]*

During each run, the thermal conductivity was determined while the specimen was heated from 1000°F to 5000°F at 500°F intervals and cooled from 5000°F to 1000°F at 1000°F intervals. This was done to determine any alterations of the char after heating to the higher temperatures.

The machining of the conductivity specimens was performed after impregnating the char with polyalphamethylstyrene to provide sufficient mechanical strength. The evaluations were made after installing the specimens in the apparatus and heat soaking them at 1000°F. At this temperature, polyalphamethylstyrene effectively vaporized, leaving no residue. This technique was also employed successfully under Task Orders 2 and 3. The impregnation of the char was required only on the thermal conductivity specimens and the photomicrographic samples.

---

*See REFERENCES

Data and Results

Virgin material. - The thermal conductivity data for the virgin material are presented in Figure 6 and Table 2. As shown in the figure, the conductivity increased sharply from 1.27×10^{-5} Btu/sec/ft/°F (7.91 x 10^{-2} W/m/°K) at -250°F to 1.69×10^{-5} Btu/sec/ft/°F (10.52 x 10^{-2} W/m/°K) at -100°F, then decreased to 1.27×10^{-5} Btu/sec/ft/°F (7.91 x 10^{-2} W/m/°K) at 0°F. From 0°F to 750°F the values increased steadily to 1.49×10^{-5} (7.73 x 10^{-2} W/m/°K). These values were lower than those exhibited by the phenolic-nylon material evaluated under Task Order 1; however, the characters of the curves were very similar. The lower conductivity of this material, which exhibited the same density as the previous phenolic-nylon, may have resulted from weaker bonding (higher thermal contact resistance) between the resin and filler. This obviously resulted from the formulation and processing being less than optimum for a plastic composition as discussed previously. As discussed in a subsequent section, the lower mechanical properties exhibited by this material also indicate the weaker bonding.

Charred material. - The thermal conductivity values of the charred material are shown in Figure 7 and Table 3. The conductivity and mean temperature were computed by assuming a linear gradient through the specimen as has been done in the past. As shown in the figure, the values increase steadily from 11.5×10^{-5} Btu/sec/ft/°F (0.72 W/m/°K) at 800°F to 76×10^{-5} Btu/sec/ft/°F (4.73 W/m/°K) at 5000°F during the heating cycle and during cooling the values decreased from 85.6×10^{-5} Btu/sec/ft/°F at 4300°F to 34.7×10^{-5} Btu/sec/ft/°F at 1500°F. It was found that the thermal conductivity of the material during heating could be described by the equation,

$$k = 11.57 \times 10^{-5} + 5.3 \times 10^{-15} T^3 \qquad (2)$$

where

k = thermal conductivity, Btu/sec/ft/°F

T = mean temperature of specimen, °F

Because of the scatter in the cooling data, these are not represented by an equation but are shown as a band in Figure 7. During heating the runs on three separate specimens agreed well; however, the cooling data were scattered and higher than the conductivity during the heating cycle.

8

Examinations of the specimens after the run revealed that cracking and shrinkage had occurred during cooling, and the structure appeared to be more porous. These effects would tend to scatter the data and cause higher indicated conductivities due to the increased radiant (and possibly convective) heat transport. The values obtained on cooling should be treated with caution. Figure 8 illustrates the structural changes of the specimens after exposures to 5000°F. Some erosion can be observed near the ends of the strips, however, the central $\frac{1}{2}$ inch gage lengths through which the conductivity was measured appear to be undamaged.

HEAT CAPACITY

The enthalpy and heat capacity were determined on both the virgin and charred material. The data were determined from -200°F to 750°F for the virgin material and from 1000°F to 5000°F for the charred material.

Two apparatuses were used in the determinations. For the evaluations of the virgin material, a drop type adiabatic calorimeter was employed. A drop type ice calorimeter was utilized in the evaluations of the char material.

Apparatus and Procedure

Adiabatic calorimeter. - This apparatus is fully described in Reference 3 so that only the major features are discussed here. Briefly, the enthalpy of a specimen at a particular temperature was determined by dropping the heated or cooled specimen into a cup which was maintained adiabatic. Enthalpy was determined from the weight of the specimen and the temperature change of the cup. The calorimeter cup was placed in an insulated container which was immersed in a bath of ethylene glycol. Adiabatic conditions were maintained by heating or cooling the bath. The specific heat was calculated from the slope of the enthalpy versus temperature curve. This slope was determined by averaging both a graphical solution and an analytical solution in which the enthalpy curve was fitted by a least squares approach, and the resulting equation differentiated to obtain the specific heat.

The temperature range of the adiabatic calorimeter equipment was extended from -50°F to -250°F. This was accomplished by cooling the specimen in a cooling chamber specially designed for inserting within the standard cold box. The cooling chamber is constructed of two concentric

9

cylinders in which the specimen was inserted within the central cylinder, and liquid nitrogen was placed in the annulus between the cylinders. With this system, temperatures of -250°F were readily obtained. A continuous dry helium purge was maintained eliminating any "frosting" on the specimen.

Ice calorimeter. - The drop type ice calorimeter employed to determine the enthalpy of the degraded material is fully described in Reference 4.

This calorimeter employed a cup surrounded by an ice mantle. The enthalpy determinations were made by dropping the heated specimen into the apparatus and measuring the volume of ice melted as the specimen cooled to 32°F. Specific heat was calculated from the slope of the enthalpy versus temperature curve.

Data and Results

Virgin material. - The enthalpy and heat capacity data of the virgin material are included in Figure 9 and Table 4. The heat capacity values increased from 0.20 Btu/lb/°F (837 J/kg/°K) at -200°F to 0.58 Btu/lb/°F (2427 J/kg/°K) at 600°F, with the values above 600°F becoming erratic due to the excessive degradation of the material. The data up to 600°F agreed well with the previous values obtained on the low-density phenolic-nylon evaluated under Task Order 1. In comparison with the heat capacity of phenolic-carbons, graphites, and silicas evaluated here previously, the phenolic-nylon exhibited higher values. This was expected since the heat capacity of nylon is significantly higher than that of carbon, graphite, or silica.

Charred material. - The enthalpy and heat capacity data for the charred phenolic-nylon are included in Figure 10 and Table 5. As shown in the figure, the heat capacity increased from 0.39 Btu/lb/°F (1632 J/kg/°K) at 1000°F to 0.57 Btu/lb/°F (2385 J/kg/°K) at 5000°F. This compares favorably with the heat capacity obtained on the degraded phenolic-nylon evaluated under Task Order 3, which remained a constant 0.52 Btu/lb/°F (2175 J/kg/°K) from 1200°F to 5000°F. As was expected, due to the carbonaceous character of this material, the values obtained also compared well with those of graphite (0.4 Btu/lb/°F at 2000°F to 0.55 Btu/lb/°F at 5000°F for CFZ).

The scatter of the enthalpy data was relatively high due to the small mass of the specimens; therefore, four specimens were evaluated in order to reduce the uncertainty.

10

THERMAL EXPANSION

The thermal expansion of only the virgin material was determined from -200°F to 750°F employing the precision quartz tube dilatometer.

Apparatus and Procedure

A complete description of the quartz tube dilatometers is included in Reference 3. Briefly, the specimen was placed in the bottom of a quartz cylinder and a quartz rod placed on the specimen extended to the open end of the cylinder. The thermal expansion was indicated by a precision dial gage mounted to the cylinder with its stylus bearing on the rod. The specimen, which was heated in a tube type furnace, was instrumented with thermocouples at three locations along its length to minitor temperatures and temperature gradients. From calibration with standards such as "A" nickel, the precision of the measurements has been confirmed within 0.0001 inch scatter at any level and the total uncertainty within ± 5%.

The cryogenic temperatures were obtained by two methods for Specimens 1 and 2. The first was performed by immersing the quartz dilatometer in a dewar filled with liquid nitrogen. The second utilized a coil with several orifices drilled on the inside diameter which provided a surrounding spray of the liquid and gaseous nitrogen on the outside of the quartz tube. The second method provided better control of the temperatures desired.

Data and Results

The thermal expansion data are shown in Figure 11 and Tables 6 and 7. Duplicate data were obtained in the direction perpendicular to the 4 inch thickness defined as "ab" direction, and singular data from room temperature to 750°F were obtained in the thickness direction defined as the "c" direction. The determination in the thickness direction was not required under the contract but was performed in order to determine if any anisotropy of expansion existed in this material.

As can be seen from the figure, in the "ab" direction the material expanded steadily from -200°F to 230°F at which point contraction occurred and continued until 750°F. The coefficient of expansion in the "ab" direction at room temperature was 23.5×10^{-6} in./in./°F (42.3×10^{-6} m/m/°K).

The expansion in the "c" direction, also shown in Figure 11, differed from that in the "ab" direction above 150°F, being about 20% greater at 230°F. Above 230°F, contraction in the "c" direction occurred in a manner similar to the behavior in the "ab" direction; however, above the cure temperature (340°F) of the material, erratic data were obtained.

The difference in the observed expansions in the "ab" and "c" directions may have been due to some anisotropy in the material, but more likely these differences, particularly above the cure temperature of 340°F, were the result of degradation of the material. We have noted with previous expansion evaluations on reinforced plastics that erratic and unrepeatable data are usually obtained above the material's cure temperature due to the spurious thermal motions associated with degradation. More evaluations, which were beyond the scope of this contract, would be required to fully define the anisotropy that does exist.

In comparing the above values with those obtained on the phenolic-nylon evaluated under Task Order 1, the prior phenolic-nylon exhibited expansions about 10% higher over the range from -300°F to room temperature. From room temperature to about 150°F the curves for the two materials were almost identical. Above 150°F the prior phenolic-nylon also behaved erratically but did not begin to contract until about 400°F.

PERMEABILITY

The permeability on both the virgin and charred materials was determined at room temperature.

Apparatus and Procedure

The apparatus employed for both virgin and charred material is completely described in Appendix B. The procedure simply provides a pressure drop across the specimen by mounting and sealing the specimen between two chambers at different pressures. The flow of the permeating gas through the specimen is monitored downstream from the specimen. The measurement of the flow, specimen mean pressure, and pressure drop across the specimen provided the data required to investigate the permeability of the material. These data can be utilized in various equations to provide permeability coefficients which are applicable for various flow conditions. We chose to determine the admittance (K_{mv}) defined in the equation

12

$$K_{mv} = \frac{P_m Q_m}{\Delta P} \frac{L}{A}$$

where

K_{mv} = admittance, cm^2/sec

P_m = mean pressure in specimen

Q_m = flow rate through specimen, defined at mean pressure cm^3/sec

L = thickness of specimen, cm

A = cross sectional area of specimen exposed to flow, cm^2

ΔP = pressure drop through specimen

This admittance value is applicable to the combined Poiseuille (viscous) and Knudsen (molecular) flows.

Permeating gases of helium and nitrogen were used in this investigation. Gas flow rates through the virgin material were measured with a bubble flowmeter; the higher flow rates through the more porous char material were monitored with a precision Rotameter made by Fischer and Porter Company. Pressure differentials across the specimen ranged from 1.5 to 9.8 inches of water. Two thicknesses (approximately 0.25 and 0.43 inches) of the virgin phenolic-nylon and only one thickness (0.25 inch) of the char were evaluated.

Data and Results

The pressure drop across, flow through, and mean pressure of both the virgin and charred specimens are shown in Tables 8 and 9. The calculated admittance is also included in the table to facilitate a comparison of the data obtained under the various conditions for the two materials.

Virgin material. - It was observed that for the virgin material the admittance did not change (within the limits of uncertainty of the equipment) with the two purge gases or with the variation in pressure differentials across the specimen. However, some increase in values was noted for the thicker specimens. The average values of the thinner Specimens 1, 4, and 5 were 4.15×10^{-4}, 3.88×10^{-4}, and 4.10×10^{-4} m²/sec, respectively; whereas, the average values of the two thicker specimens were 4.29×10^{-4} and 5.07×10^{-4} m²/sec, respectively.

Charred material. - For the degraded material, the admittance was higher due to the cracked and porous structure and varied depending on the permeating gas used and pressure gradient across the specimen. Nitrogen provided lower values (approximately 0.8 to 1.0 m²/sec) than those exhibited with helium (approximately 1.4 to 1.9 m²/sec), and there also was a drop of 20% in the admittance as the pressure drop across the specimen was increased from 1.5 to 3.0 inch of water.

It is important to know the type of flow that occurs within the char in studying the effectiveness of transpirational cooling during ablation. Due to the size variations of the pores and channels within the material, the type of flow will naturally vary between turbulent, transitional, and laminar within the different passages. The data obtained on this char do indicate that most of the flow was either transitional or turbulent. This was demonstrated by the fact that the helium provided higher flow rates through the char when compared with nitrogen. In a flow regime of mostly turbulent flow, the volume flow rate is inversely proportional to the square root of the gas density, and for laminar flow the flow rate is inversely proportional to the viscosity. This can be seen from Darcy's equation (valid here due to the low pressure drop) and was also illustrated by Creutz.[5] Since there is a wide variation in density (nitrogen 0.072 lb/ft³; helium 0.010 lb/ft³) and only a slight difference in viscosity (nitrogen 1770×10^7 poise; helium 1960×10^7 poise) of the two gases, the higher flow of the helium indicated that very little laminar flow occurred.

The same conclusion can also be drawn by applying the data to the following relation offered by Creutz:

$$Q \alpha (P \Delta P)^{\delta}$$

where

    Q = flow of gas through the sample (corrected for Knudsen and slip flow rates)

P   =   mean pressure of the specimen

ΔP =   pressure drop across the specimen

δ =   exponent which is 0.5 for turbulent and 1.0 for laminar flow

Using the data shown in Table 9, an approximate value of δ can be obtained by plotting Q vs (PΔP) on logarithmic coordinates and determining the slope, which is the exponent δ. This was done, without correcting for Knudsen or slip flow (which would be relatively small at these large flows), and the slopes were about 0.9 for helium and 0.7 for nitrogen. This value indicates the flow to be transitional. Therefore, for the pressure drops between 1.5 to 3.0 inches of water, the flow should be considered transitional or turbulent for this char.

TOTAL NORMAL EMITTANCE

The total normal emittance of the degraded material from 1500°F to 4000°F was determined. This was performed by comparing the irradiance from the specimen to that from a cavity-type blackbody maintained at the same temperature.

Apparatus and Procedure

A complete description of the apparatus and procedure employed for the emittance determinations is included in Reference 4. Briefly, the specimen was heated in an induction furnace and its irradiance was monitored by a 160-junction thermopile calibrated against a cavity type blackbody to about 5200°F. An optical pyrometer was employed to monitor temperature of the specimen. The assumption of graybody emittance and the use of the Wein and Stefan-Boltzmann equations permitted an iterative calculation of true temperature and emittance.

Temperatures below 1500°F were not obtained since the irregular surface of the char and its weak structure inhibited the proper contact required for a surface thermocouple. Temperatures above 4000°F were not obtained due to the destruction of the tungsten heating discs under the specimen. The high heat flux and low conductivity of the char created a very high temperature gradient across the specimen which accounted for the melting of the tungsten disc while the specimen surface temperature was about 4000°F.

15

The specimens were prepared by carefully cutting the discs ($\frac{1}{2}$ inch diameter by $\frac{3}{16}$ inch to $\frac{1}{8}$ inch thick) from the charred material. The top surface of the char was unaltered from the as received condition and no resin impregnant was used.

Data and Results

The total normal emittance data are shown in Figure 12 and Table 10. The emittance increased slightly from 0.79 at 1550°F to 0.87 at 3300°F and then decreased to 0.79 at 4000°F. These values were, over most of the temperature range, slightly lower than those obtained on the low-density, phenolic-nylon char evaluated under Task Order 3. The significant difference between the emittances of the two materials occurred between the temperatures of 3000°F and 3500°F, where the emittance of the char under Task Order 3 decreased due to the formation of a white residue. The same residue was noted on Specimen 1 (see remarks in Table 10); however, its effect on emittance was negligible for this char since the amount of residue formed on the present specimens was probably less. It was noted during the runs that the "speckled" appearance of the specimen viewed through the optical pyrometer was not as noticeable for these runs when compared with the runs performed under Task Order 3 indicating less residue formation. Apparently the residue was formed by impurities within the char as discussed in Reference 6.

Extra specimens were evaluated for emittance to obtain a representative mean due to the higher than normal data scatter which resulted from the varying surface structure and the gray to black color variation. The variation in the porous surface structure apparently caused different degrees of subsurface radiation.

MECHANICAL PROPERTIES

On the nondegraded material, the tensile and compressive strength properties in one direction were obtained from -200°F to 750°F. The specific properties determined were ultimate strength, yield strength at 0.2% offset, Poisson's ratio, Young's modulus, total elongation or compression, and stress-strain curves.

16

Apparatus and Procedure

The apparatus and procedures employed for the mechanical property determinations are completely described in Reference 3. The specimens were loaded in a Tinius-Olsen universal testing machine. Curves of stress versus strain and lateral versus axial strain were continuously plotted to failure on X-Y recorders. Strains were measured axially and laterally in one direction. Triaxial strains were recorded during the initial tests until it was confirmed that the material was essentially isotropic for this property. Temperatures were obtained by programmed heating above 70°F using tungsten filament radiation lamps controlled by a Powerstat. For cooling, the specimen was surrounded by cotton sprayed with liquid or gaseous nitrogen at a rate sufficient to provide the desired temperature. The load was programmed to provide a given stress rate for failure at approximately 5 minutes, thus the stress rates differed at different temperatures. The strain in the direction of loading was measured by dual "strain gage" clip-on extensometers mounted on lugs clamped to the specimen. The strain in the lateral direction (perpendicular to the loading direction) was measured by mechanical extensometers in contact with the specimen which transmitted the lateral motion to a differential voltage transformer.

This type of instrumentation provided precision recordings of the load and the biaxial strains, continuously, to failure of the specimen. The Young's modulus, ultimate strength, yield strength, Poisson's ratio, and total elongation or compression were obtained from the curves.

The tensile specimens employed were $8\frac{1}{4}$ inches long containing a gage section $2\frac{1}{2}$ inches long by $\frac{1}{2}$ inch wide by $\frac{1}{4}$ inch thick. The compressive specimens were $\frac{1}{2}$ inch by $\frac{1}{2}$ inch in cross section by 1 inch in the loading direction.

Data and Results

Tensile properties. - All the tensile property values are shown in Figures 13 and 14 and Table 11. Data were obtained to only 600°F since burning of the specimens at higher temperatures caused premature breaking. The tensile stress-strain curves, which are direct tracings from the X-Y recordings, are included in Figures C1 through C22 of Appendix C. Yield strength was not obtained on all runs in tension since fracture occurred in most cases before the 0.2% offset.

As can be seen from Figures 13 and 14, the tensile strength and elastic modulus decreased with an increase in temperature, with a sharp drop occurring between 200°F and 300°F. The ultimate strength decreased from 570 psi (3.93×10^6 N/m^2) at -200°F to below 100 psi (0.69×10^6 N/m^2) at 500°F. These values were about 50% lower than values obtained on the low-density phenolic-nylon evaluated under Task Order 1. The lower elastic modulus, yield strength and total elongation indicate the significantly weaker structure of this material when compared with the previous low-density phenolic-nylon. The weaker structure obviously resulted from the formulation and processing being less than optimum for this material.

Considerable scatter was observed in the ultimate strength values between -200°F and 200°F, and in elastic modulus and Poisson's ratio at -200°F. This scatter may have resulted from several factors, such as variations in stress rates (recall that these were varied to maintain the loading period constant at about five minutes) or in the geometry of the specimens which may have resulted in nonuniformities in stress and strain. Unfortunately, time and funds did not permit an evaluation of these parameters; however, such a study will be performed on a low-density phenolic-nylon of similar composition under a follow up task order (Task Order 4 under Contract No. NAS 1-5448).

The sharp drop in the strength and modulus above 200°F correlates with the contraction at 230°F observed in the thermal expansion measurements. Apparently the material undergoes a transformation above 200°F, even though this temperature is below the cure temperature. Above the cure temperature deterioration of the material contributed to the decrease in strength. Typical photographs of the specimens after the run illustrating the deterioration are shown in Figure 15. Also illustrated are the types of fracture that occurred. The relatively flat breaks obtained did indicate good tensile failure for most of the specimens.

Compressive properties. - All compressive property values are shown in Figures 16 and 17 and Table 12. The compressive stress-strain curves are included in Figures C23 through C48 of Appendix C. Some of these curves are direct tracings of the X-Y recorder; however, the others were plotted since the lateral strains were obtained on a recording oscillograph.

As shown in Figures 16 and 17, the strengths and moduli decreased steadily with an increase in temperature. The ultimate strength decreased from 2600 psi (17.93×10^6 N/m^2) at -200°F to approximately 200 psi (1.38×10^6 N/m^2) at 750°F. As was the case with the tensile properties, these values were considerably lower (again by approximately one-half) than

18

those exhibited for the previous phenolic-nylon evaluated under Task Order 1. As did the tensile strengths, the compressive strength values exhibited considerable scatter below 200°F. The elastic modulus and Poisson's ratio values were also scattered, though not as much as the values measured in tension. Further studies are needed to isolate variations in the test methods from those inherent in the material.

DISCUSSION OF RESULTS AND A COMPARISON
WITH PROPERTIES OF PRIOR PHENOLIC - NYLON

Some correlation of the properties can be made from a review of the data. For purposes of comparison, comprehensive plots of the properties of the virgin low-density phenolic-nylon are presented in Figures 18 and 19. Properties of the prior low-density phenolic-nylon evaluated under Task Order 1 of Contract No. NAS 1-2978, are also shown.

Reference to Figure 18 shows that the thermal conductivity of the phenolic-nylon evaluated in this task order ranged from 7 to 23 percent lower than that of the phenolic-nylon evaluated under the prior Task Order 1. As discussed earlier, the lower conductivity may have resulted from the high percentages of filler and poorer bonding between resin and filler in this material. The characters of both curves were similar, both exhibiting a sharp peak in the vicinity of -100°F. The reason for this peak, which is about 30 percent higher than the values on either extremity, is not known.

The enthalpies of the current and prior materials were essentially the same.

The thermal expansion of the current phenolic-nylon was lower than that of the prior material over the temperature range from -300°F to 150°F. Both materials exhibited erratic behavior above 150°F.

Figure 19 shows composite plots of the mechanical properties of the current and prior (Task Order 1) phenolic-nylons. The ultimate tensile and compressive strengths of the current material were about 50 percent lower at -200°F than those of the prior material but decreased less with temperature, so that at 600°F the two materials exhibited about the same strengths. The tensile modulus exhibited a rather sharp decrease at 200°F (recall that thermal expansion exhibited a reversal near 200°F). The moduli were lower than those of the prior material from -200°F to 200°F and about the same at higher temperatures.

Figure 20 shows a composite plot of the thermal properties of the low-density phenolic-nylon char. For comparison, data are presented for a high-density and a low-density phenolic-nylon char evaluated under prior Task Orders 2 and 3, respectively, of Contract No. NAS 1-2978.

Observe that the emittance of this char remained more nearly constant with temperature than that of the prior low-density char, but was slightly lower over most of the temperature range.

The thermal conductivity of this char was lower than that of either of the prior chars. As expected, the characters of the three curves were similar with the values increasing rapidly with temperature due to radiation. The differences in the conductivities of this and the prior low-density char can probably be attributed to differences in microstructures, even though the densities and porosities of the two materials were about the same. The current material was more heterogeneous, containing areas of relatively dense char separated by large voids (see the prior Figure 3). The median pore size, which is probably more representative of the relatively dense areas than the mean pore size, was 18.2 microns. Reference to Figure 4 shows that the majority of the pores are clustered around this size. On the other hand, the prior low-density char was more uniform in appearance, exhibiting few large voids. The average pore size of the prior material was also larger at 24.2 microns. At higher temperatures, radiant heat transfer would be larger through the char having the larger pore size, other factors being equal. At lower temperatures differences in conductivities could result from such factors as degree of graphitization of the matrix. X-ray diffraction patterns, not obtained in these programs, might detect such differences.

The current low-density char also exhibited the lowest enthalpy of the three chars, although the heat capacities of the two low-density chars were about the same. The heat capacity of the high-density char increased more with temperature, being about 20 percent greater at 4000°F than that of the low-density chars.

Southern Research Institute
    Birmingham, Alabama
        February 24, 1967

REFERENCES

1. Wilson, R. Gale: Thermophysical Properties of Six Charring Ablators from 140° to 700°K and Two Chars from 800° to 3000°K. NASA TN D-2991, October 1965.

2. Keller, L. B.: Development of Characterized and Reproducible Syntactic Foam of Phenolic-Nylon for Heat Shields. NASA CR-73041, 1966.

3. Pears, C. D.; W. T. Engelke; J. D. Thornburgh: The Thermal and Mechanical Properties of Five Ablative Reinforced Plastics from Room Temperature to 750°F. AFML TR 65-133, April 1965.

4. Pears, C. D. and J. G. Allen: The Thermal Properties of Twenty-Six Solid Materials to 5000°F or Their Destruction Temperatures. ASD TDR 62-765, August 1962.

5. Creutz, E.: Laminar, Turbulent, and Transition Gas Flow in Porous Media. Nuclear Science and Engineering, vol. 20, 1964, pp. 28-44.

6. Pyron, C. M., Jr.; and C. D. Pears: Some Thermophysical Properties of a Low-Density, Phenolic-Nylon Char. Final report under NASA Contract NAS 1-2978, Task Order 3, January 1965.
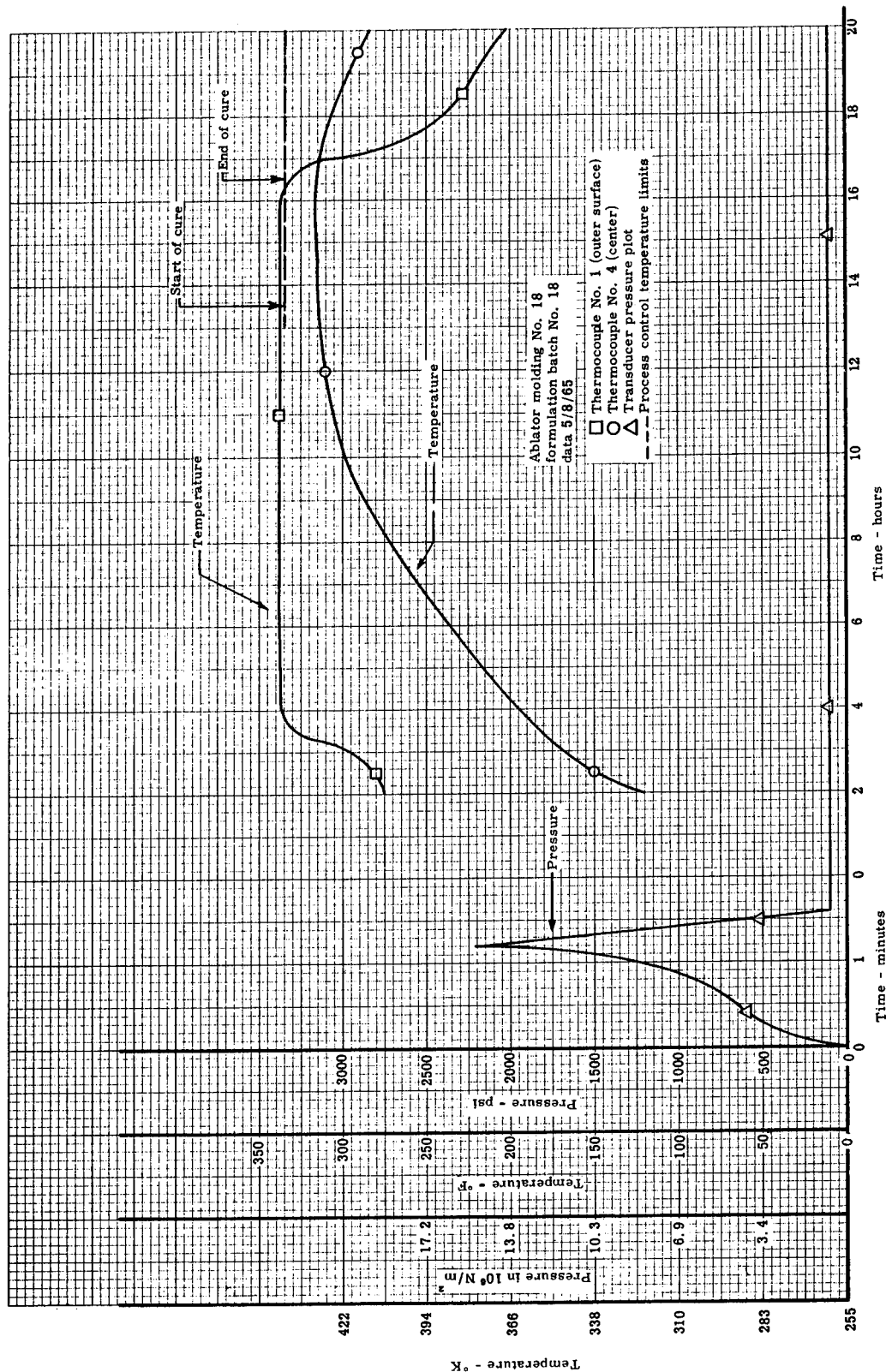
Figure 1. Molding conditions for the low-density phenolic-nylon (data supplied by NASA, Langley Research Center)

22
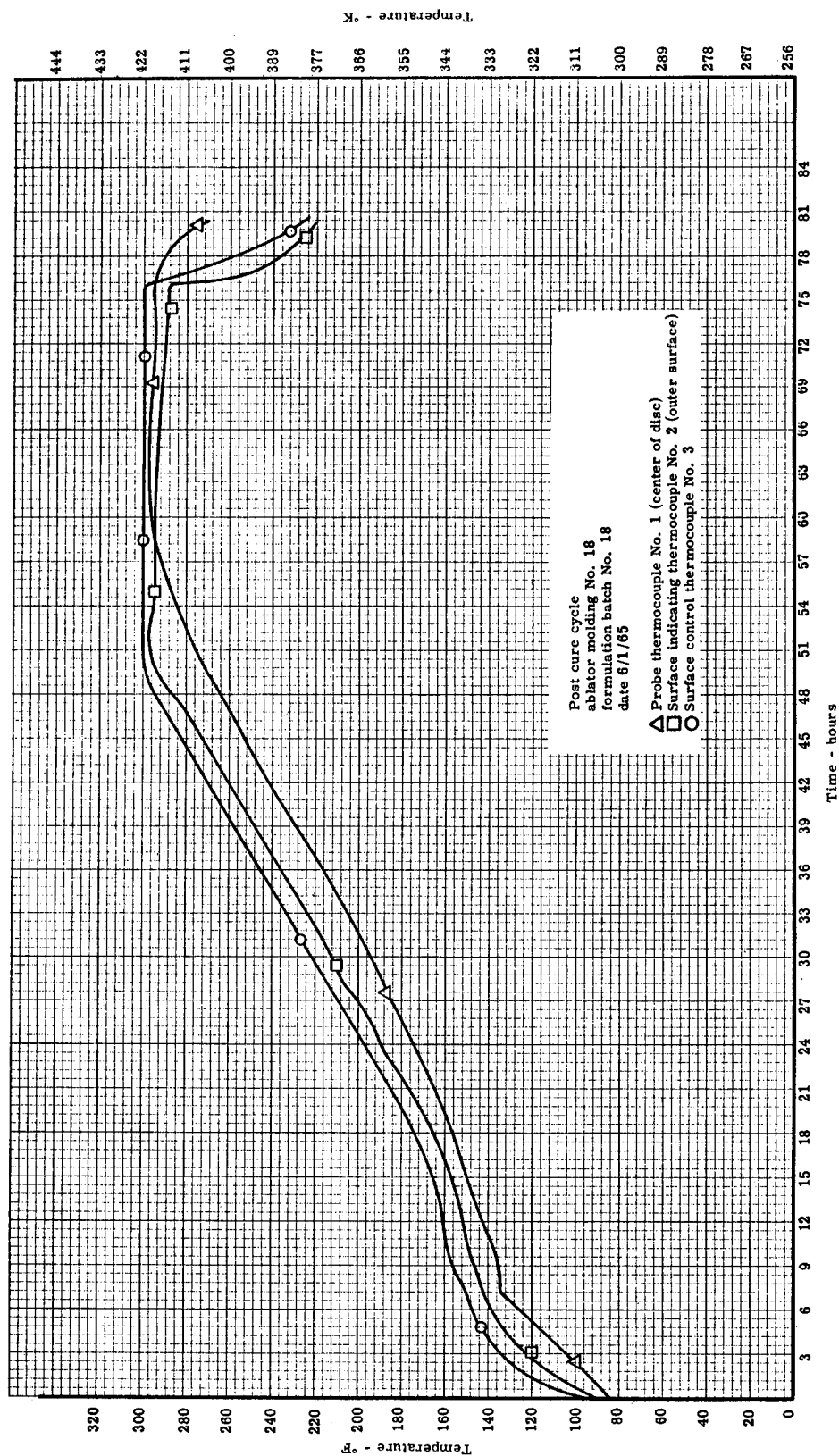
Figure 2. Post cure of low-density phenolic-nylon (data supplied by NASA, Langley Research Center)

23
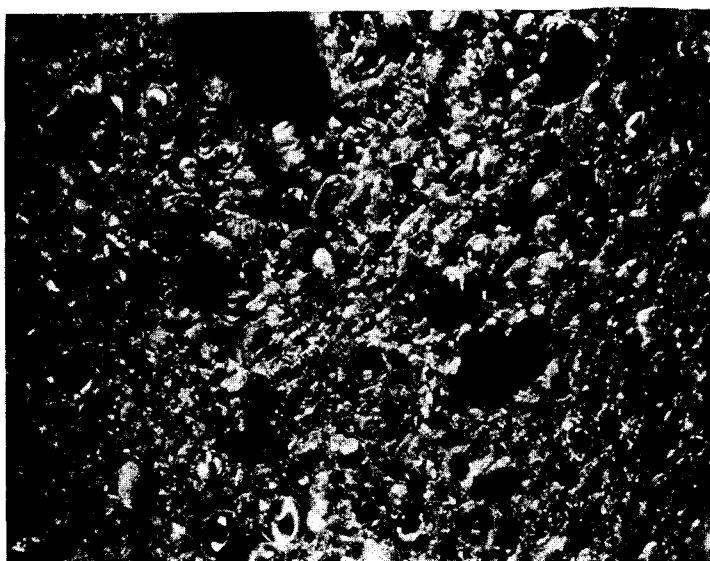
Figure 3. Photomicrograph of typical pore structure of the low-density phenolic-nylon char (100X)
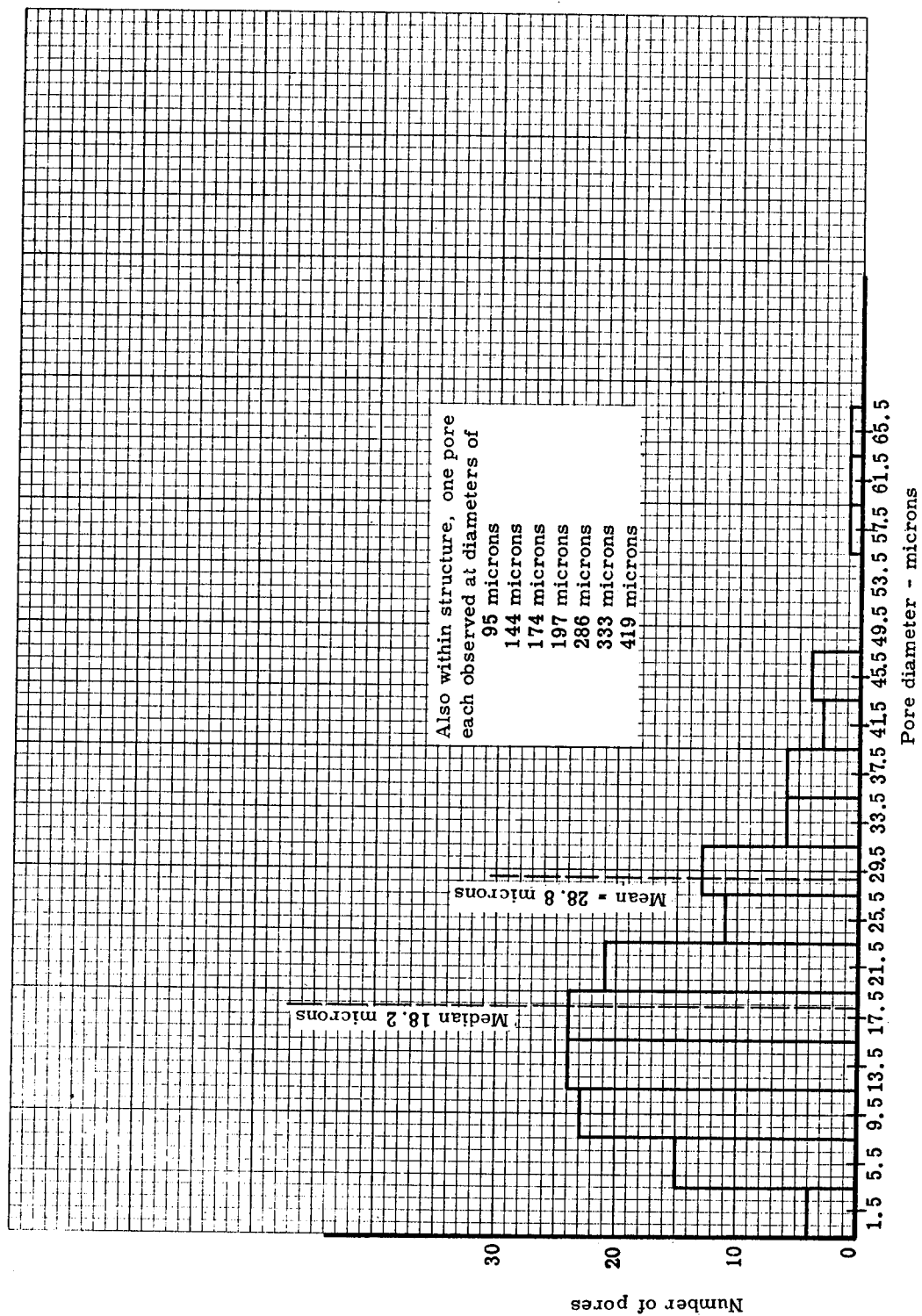
Figure 4. Histogram of pore diameters in the low-density phenolic-nylon char

Also within structure, one pore
each observed at diameters of
95 microns
144 microns
174 microns
197 microns
286 microns
333 microns
419 microns

Mean = 28.8 microns

Median 18.2 microns

Pore diameter – microns

Number of pores

25
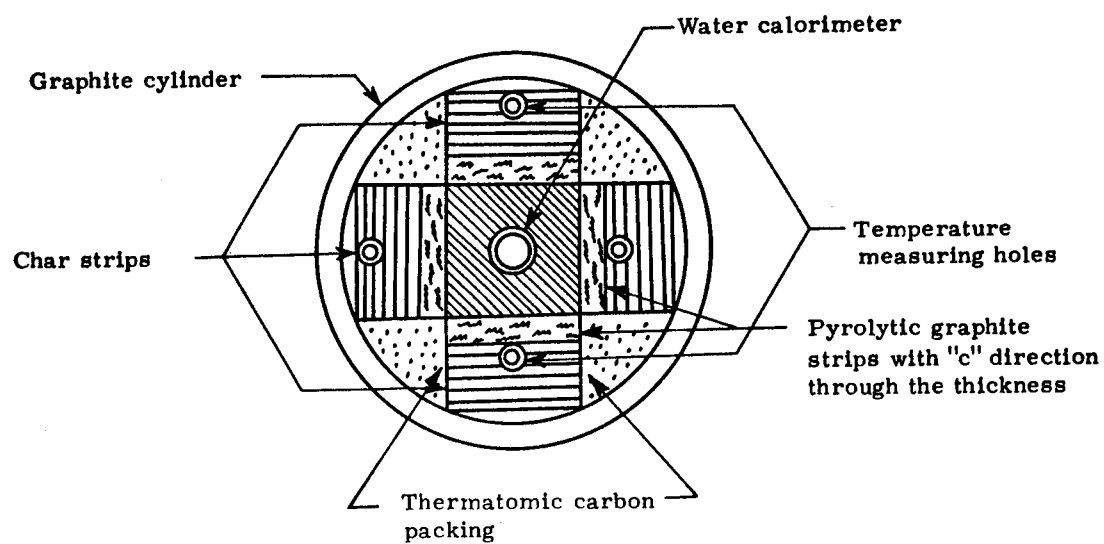
Figure 5. Strip specimen configuration for thermal conductivity
evaluation in the radial inflow apparatus

26
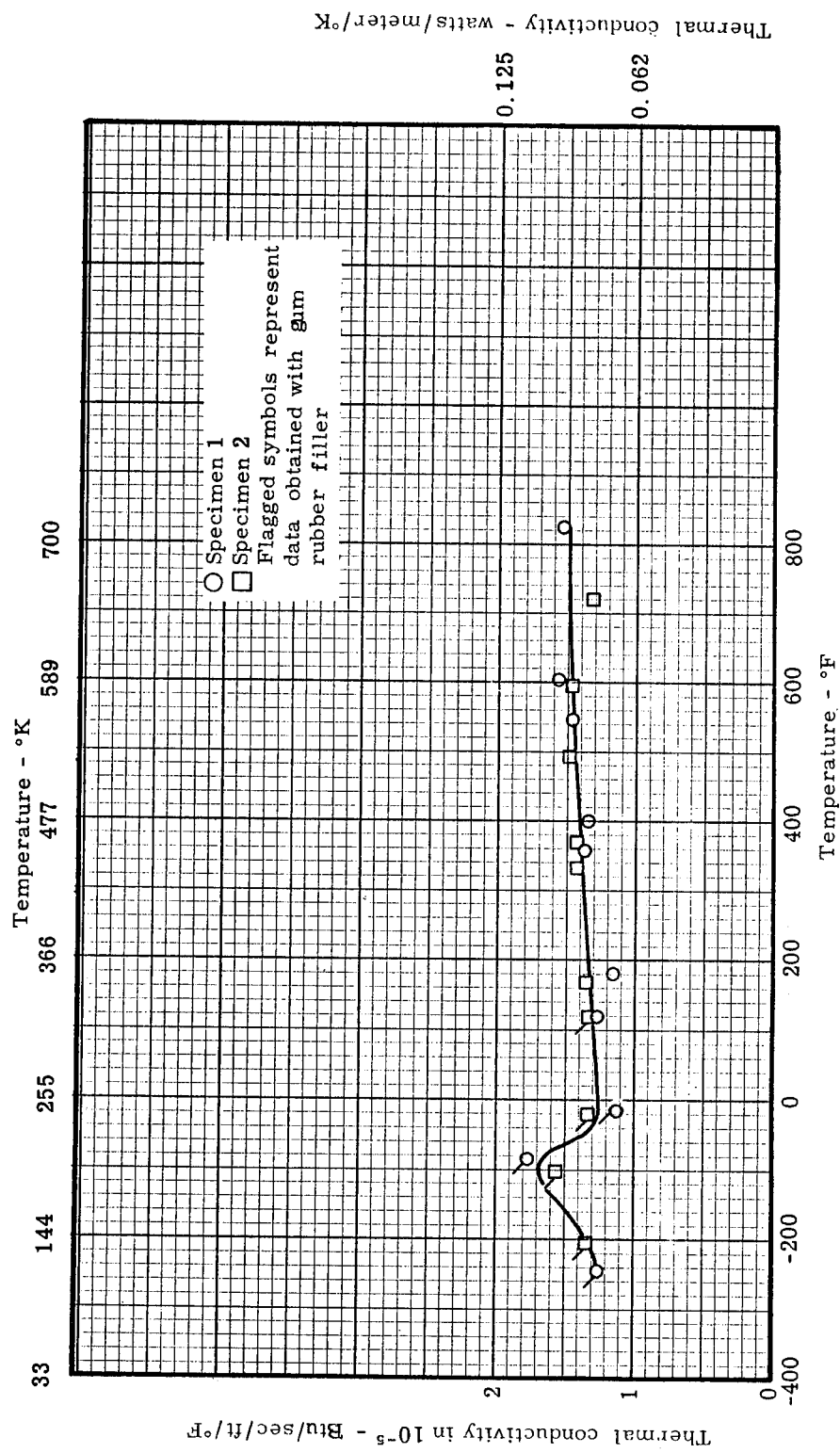
Figure 6. Thermal conductivity of the virgin low-density phenolic-nylon

27
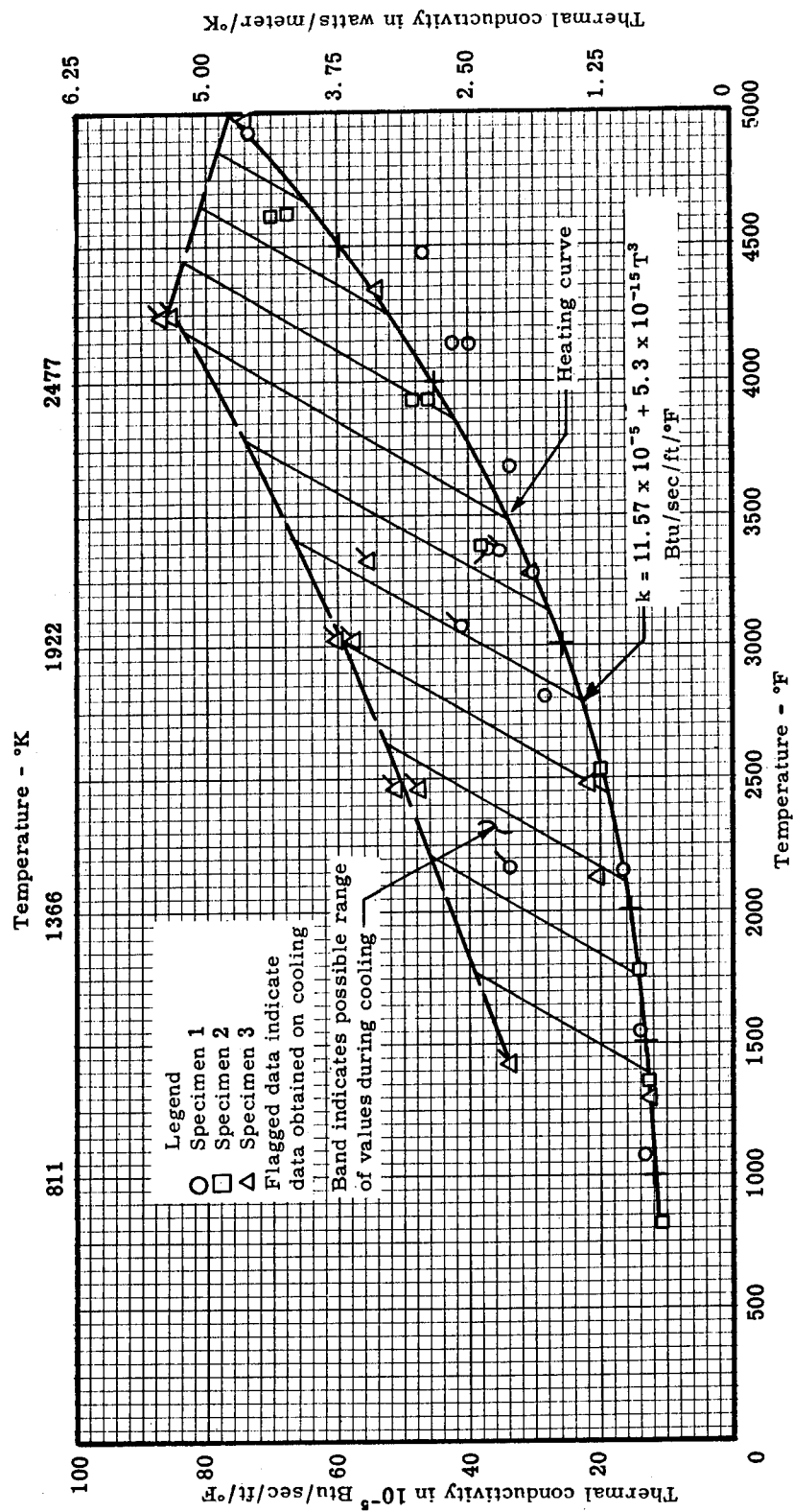
Figure 7. Thermal conductivity of low-density phenolic-nylon char

28
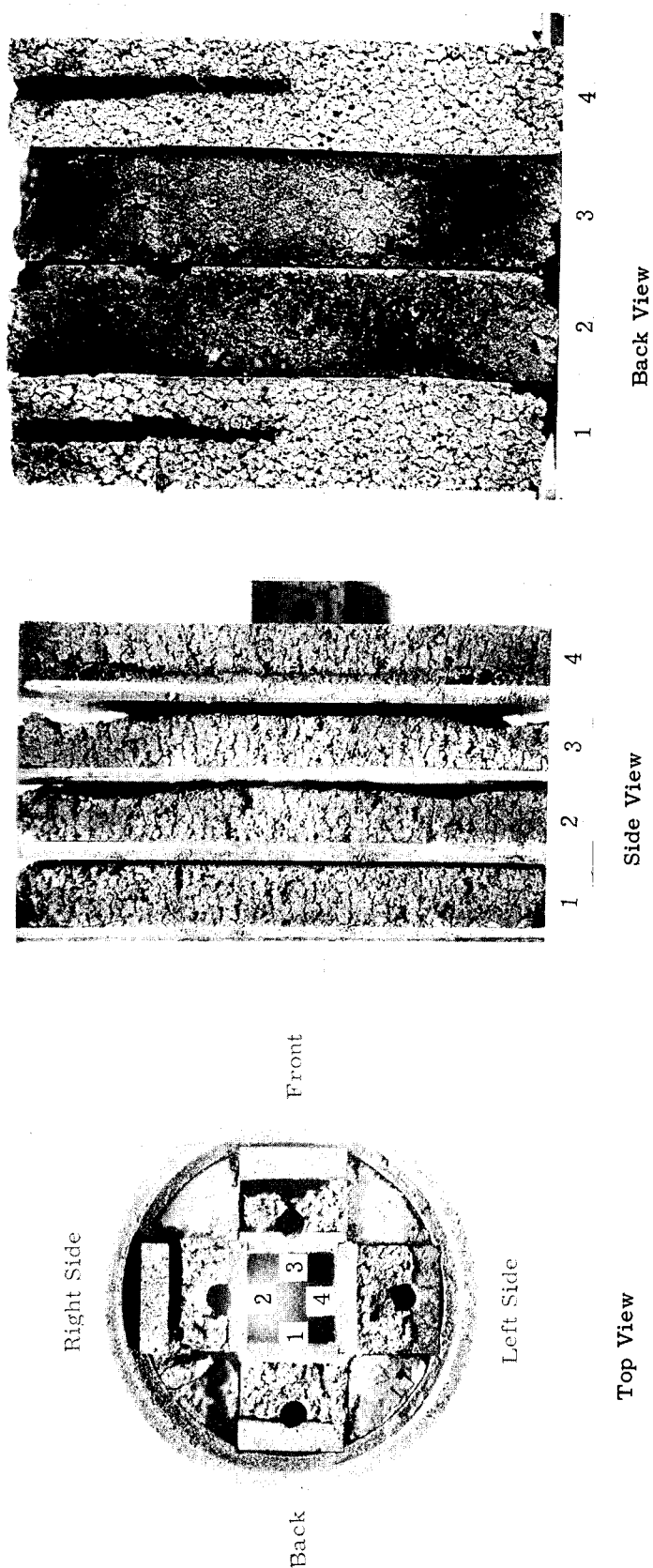
Figure 8. Photographs of low-density phenolic-nylon char, thermal conductivity Specimen 3, after exposure to 5000°F in radial inflow apparatus

Temperature - °K

33 144 255 366 477 589 700

Heat capacity - Btu/lb/°F

0.60
0.40
0.20
0.00

2511
1674
837
0

Heat capacity - Joules/kg/°K

Heat capacity
— Best fit from graphical and mathematical solution
O Graphical solution
+ Mathematical curve fit (from -50°F to 600°F)
$HC = 0.15 + 4.3 \times 10^{-4} T - 1114 T^{-2}$
(T in degrees R)

Low density phenolic nylon evaluated under contract NAS 1-2978, Task Order 1

-400 -200 0 200 400 600 800

Temperature - °F

Temperature - °K

33 144 255 366 477 589 700

Enthalpy - Btu/lb (85°F reference)

300
200
100
0
-100

698
465
233
0
-233

Enthalpy in 10³ Joules/kg

Enthalpy
O Specimen 1
□ Specimen 2
△ Specimen 3
◇ Specimen 4
▽ Specimen 5
▽ Specimen 6
◁ Specimen 7
▽ Specimen 8
◇ Specimen 9
◁ Specimen 10
+ Least squares curve fit (from -50°F to 600°F)
$h_{85} = 0.15T + 2.1 \times 10^{-4} T^2 + 3897T^{-1} + 148$
(T in degrees R)

Excessive charring

85°F reference

-400 -200 0 200 400 600 800

Temperature - °F

Figure 9. Enthalpy and heat capacity of the virgin low-density phenolic-nylon

30
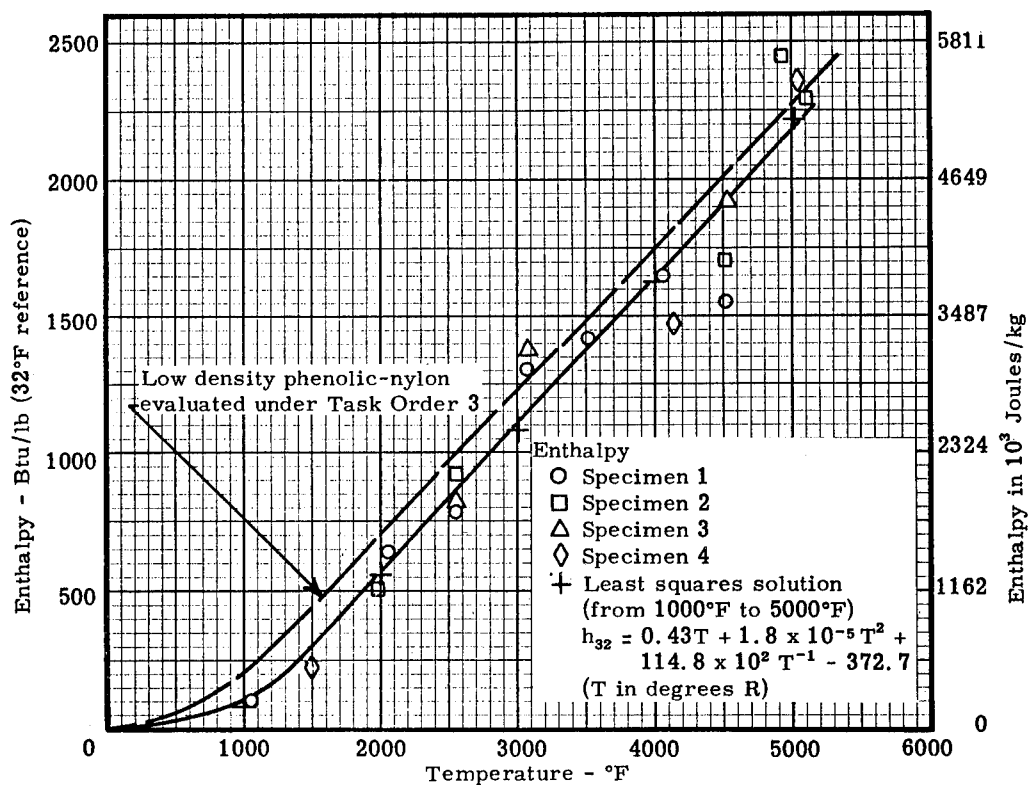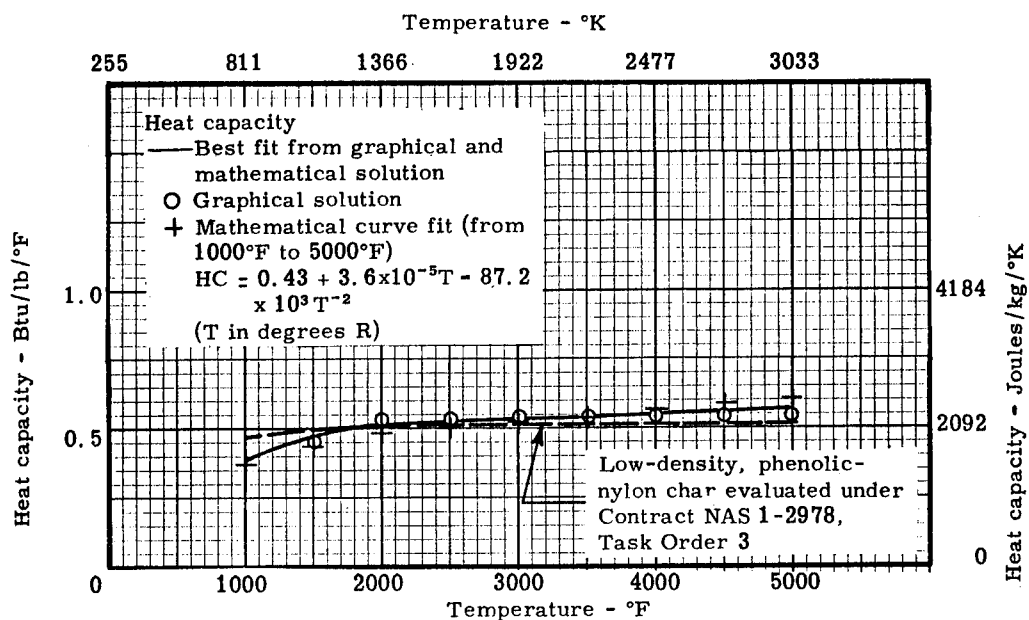
Figure 10. Enthalpy and heat capacity of the low-density phenolic-nylon char
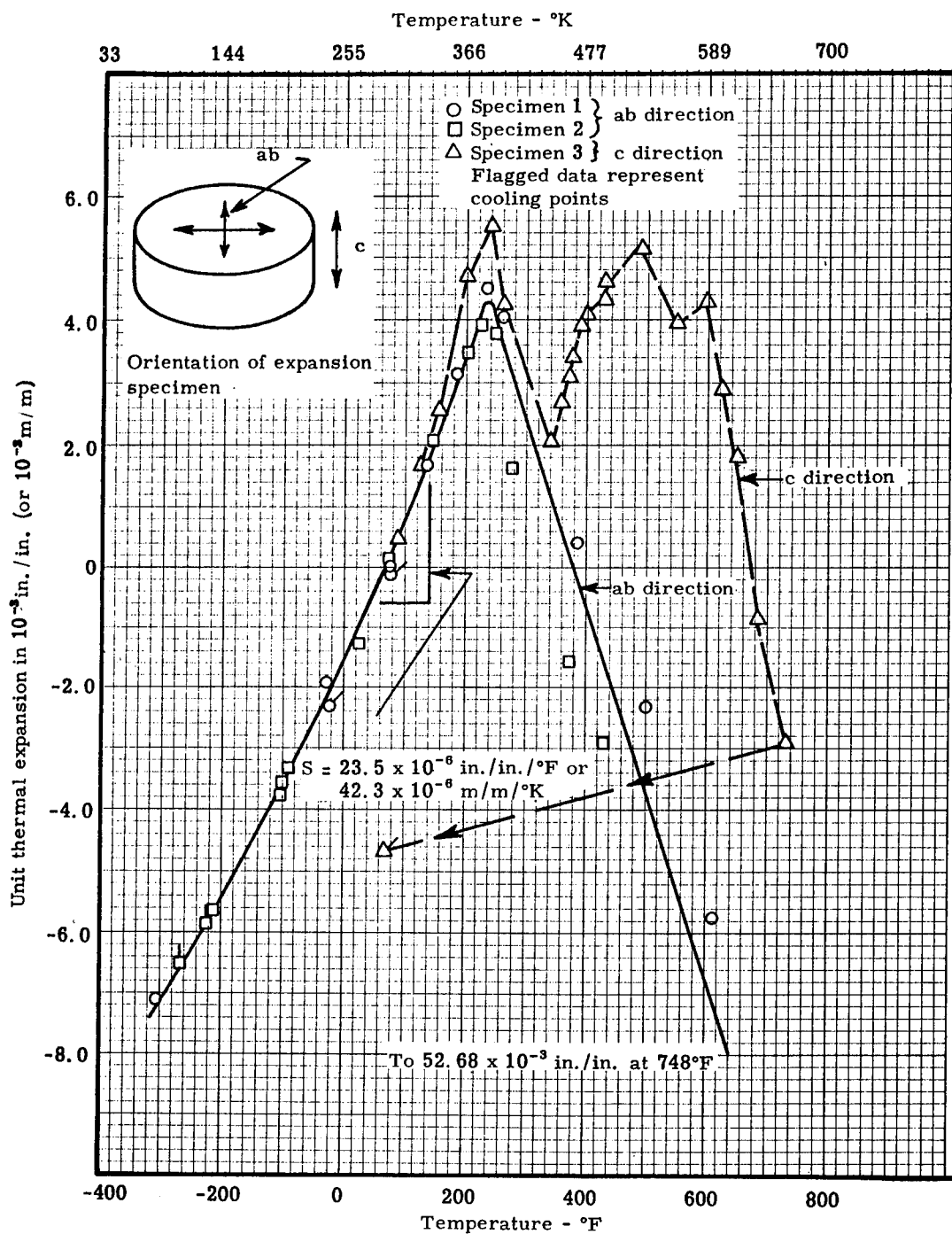
Figure 11. Thermal expansion of the virgin low-density phenolic-nylon
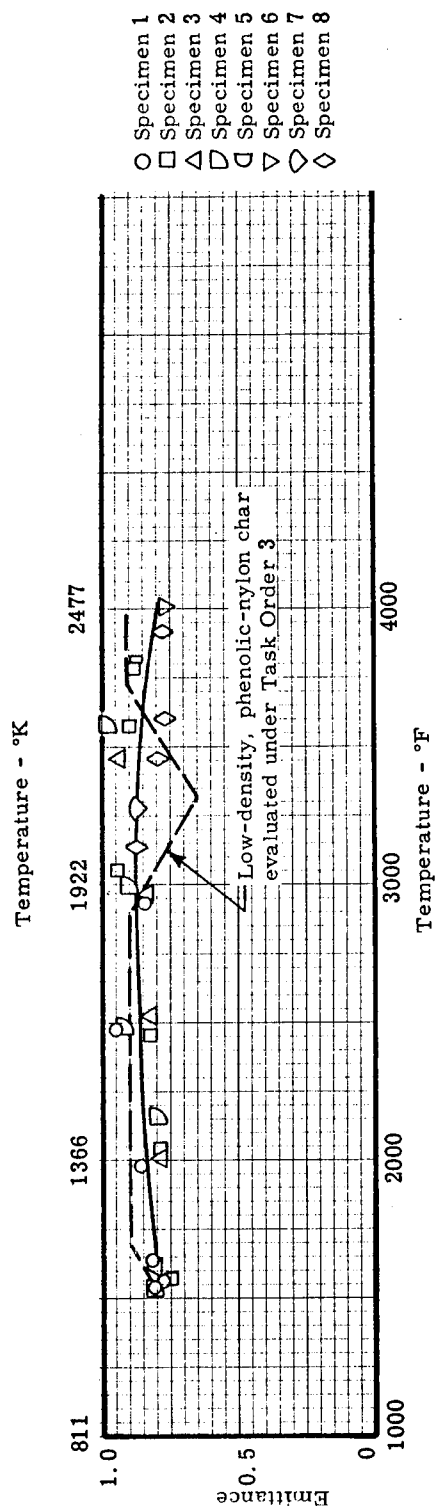
Figure 12. Total normal emittance of a low-density phenolic-nylon char

33
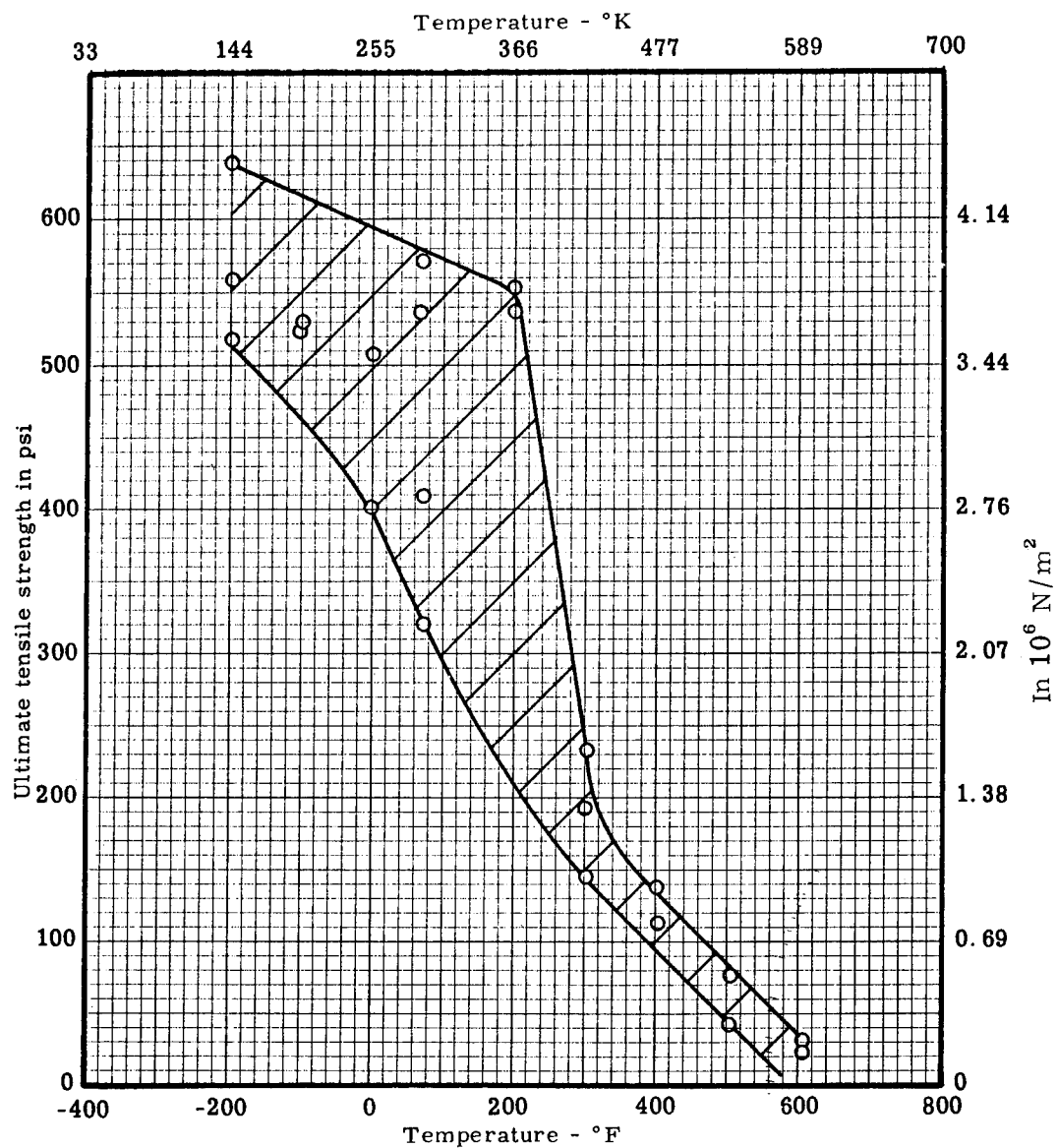
Figure 13. Ultimate tensile strength versus temperature for
the virgin low-density phenolic nylon
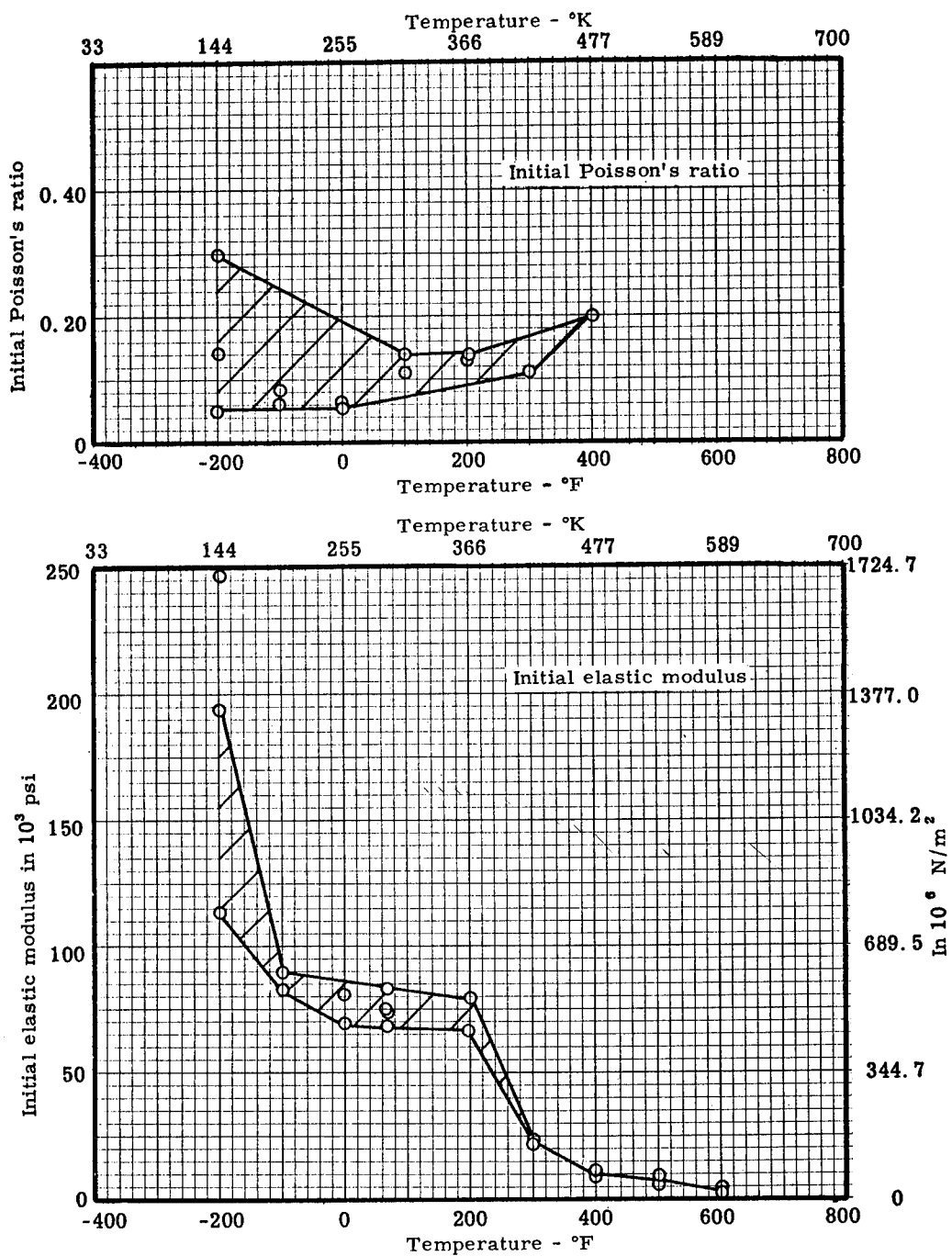
Figure 14. Initial elastic modulus and initial Poisson's ratio loaded in tension versus temperature for the virgin low-density phenolic-nylon
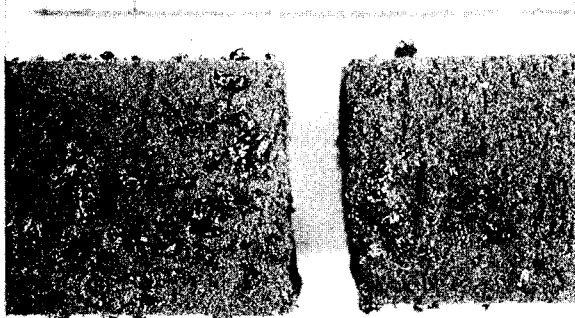
a. Specimen for Run T-11   b. Specimen for Run T-13   c. Specimen for Run T-14
        400°F   600°F   700°F

Figure 15. Photographs (about 3X) of virgin low-density phenolic-nylon tensile specimens' gage areas showing fracture and thermal degradation of material at 400°F, 600°F, and 700°F
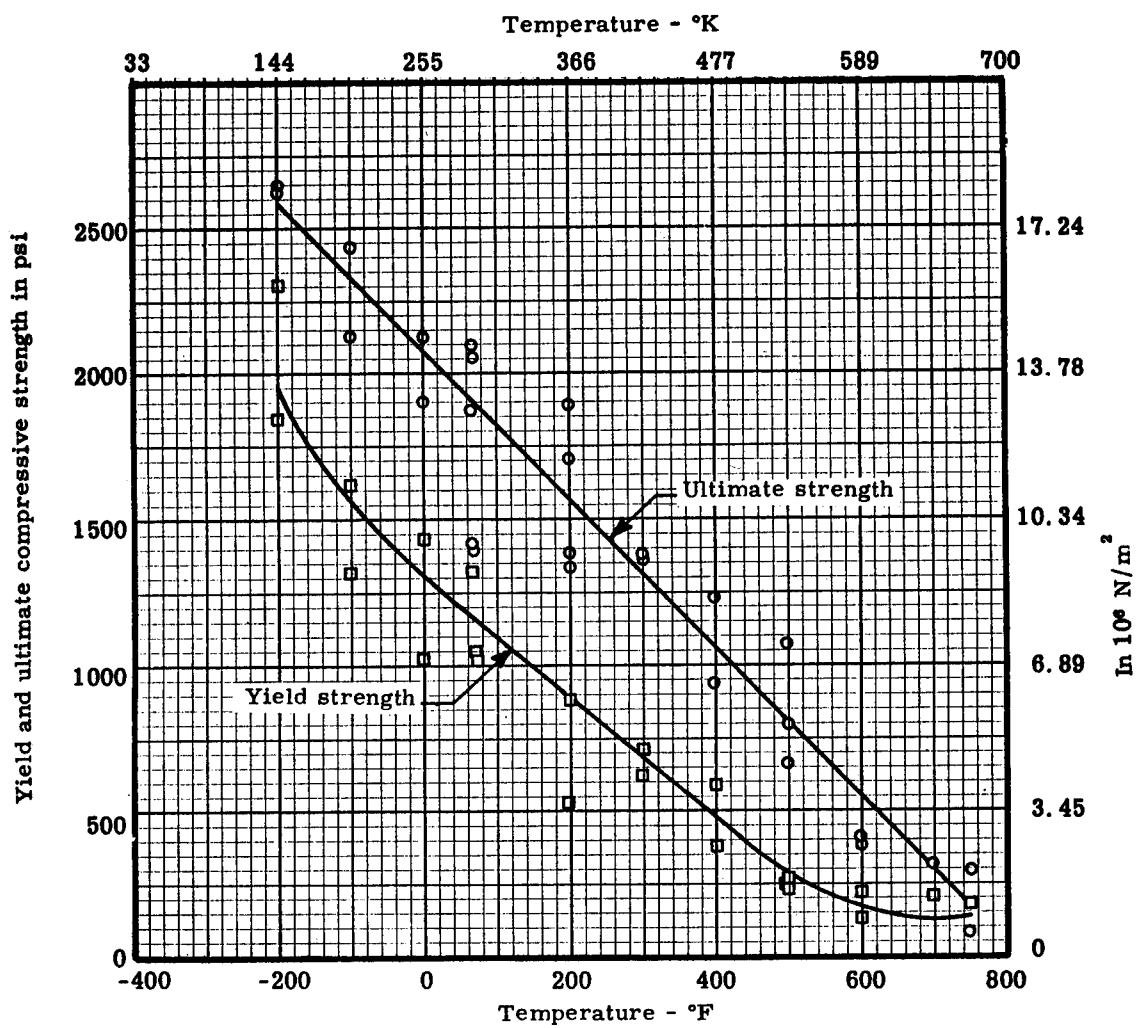
Figure 16. Yield and ultimate compressive strength versus temperature for the virgin low-density phenolic-nylon
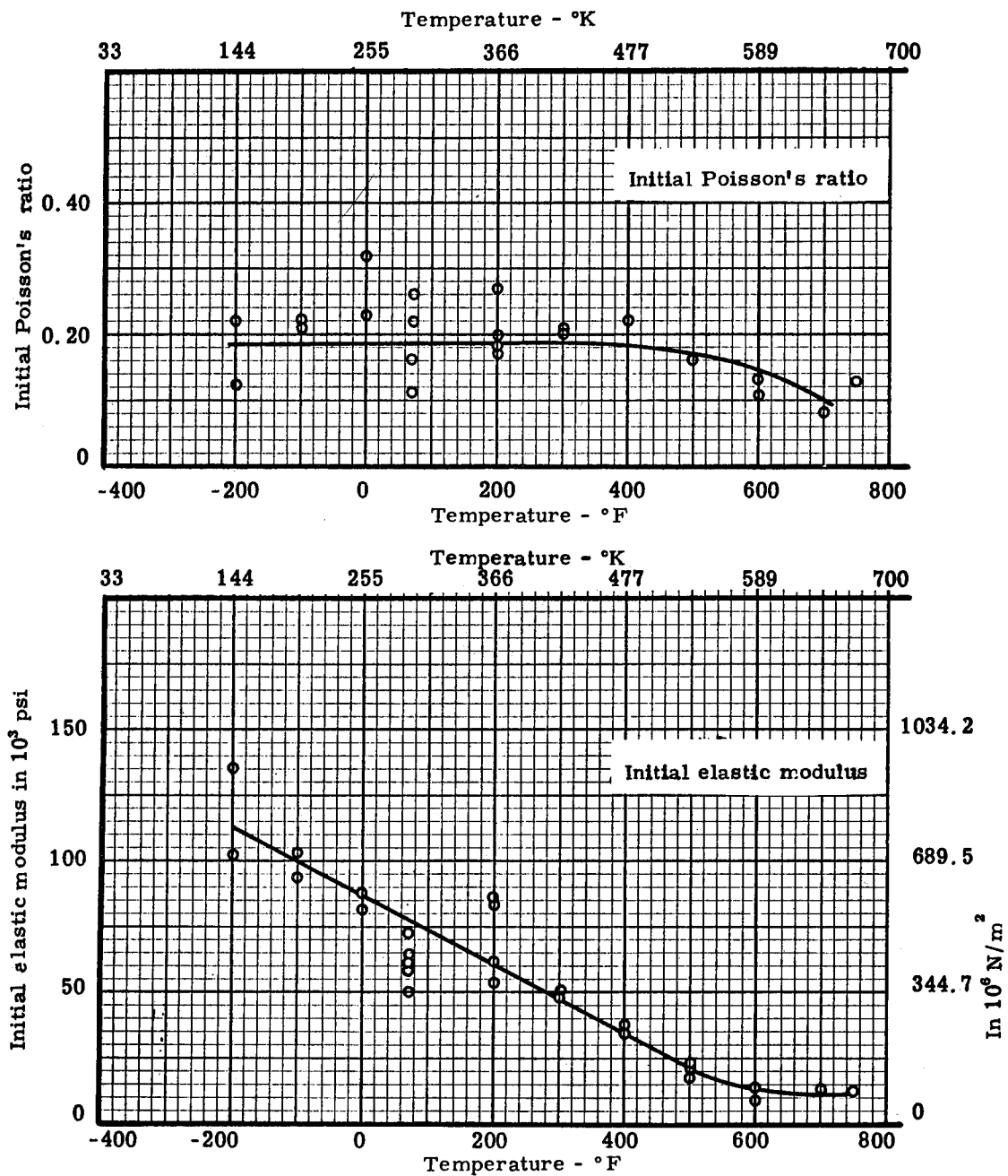
Figure 17. Initial elastic modulus and initial Poisson's ratio loaded in compression versus temperature for the virgin low-density phenolic-nylon
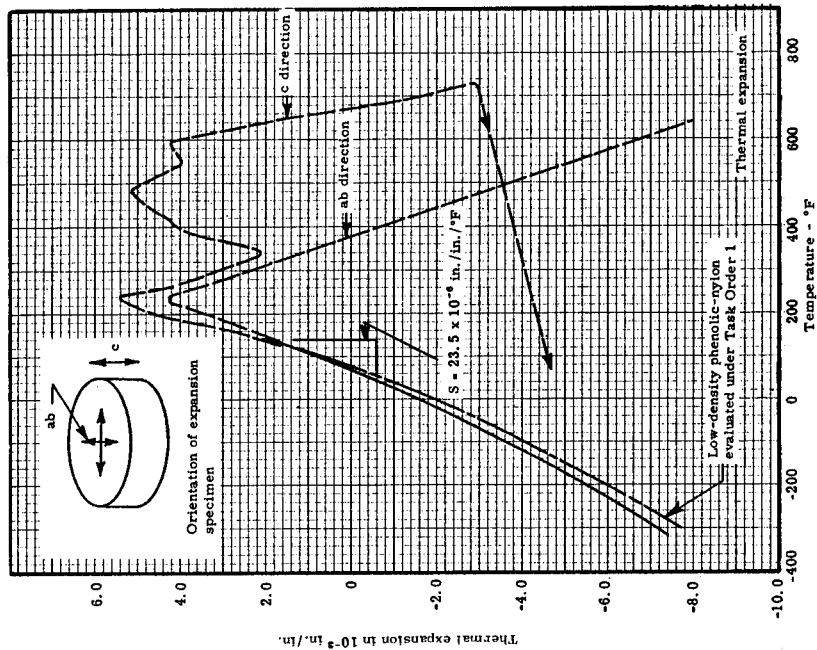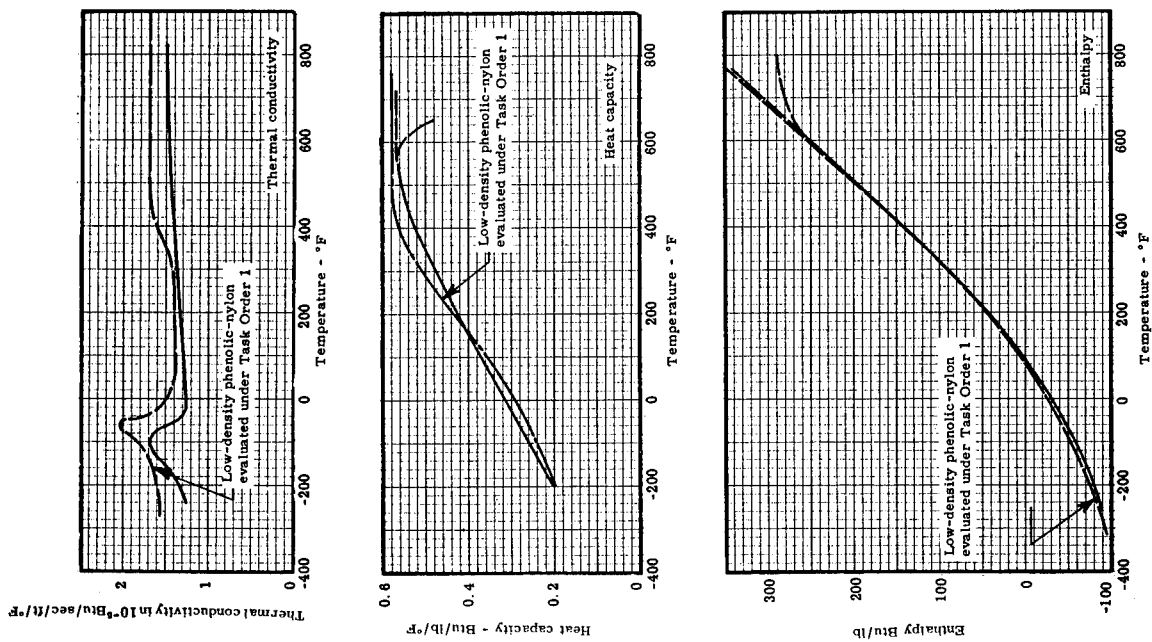
Figure 18. Composite plot of the thermal properties of nondegraded low-density phenolic-nylon

39
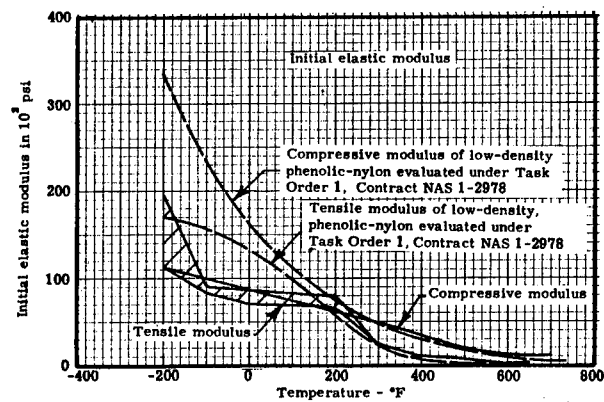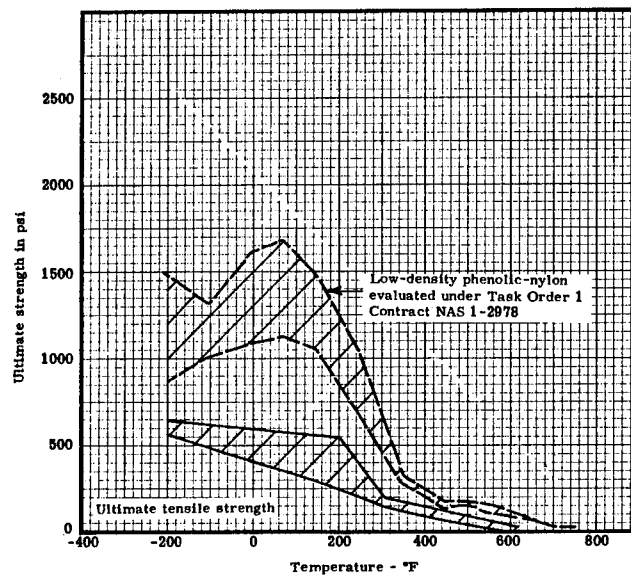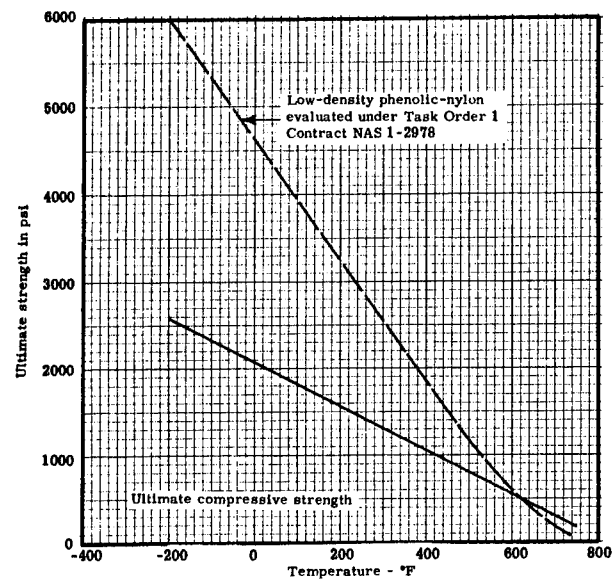
Figure 19. Composite plot of mechanical properties of nondegraded low-density phenolic-nylon
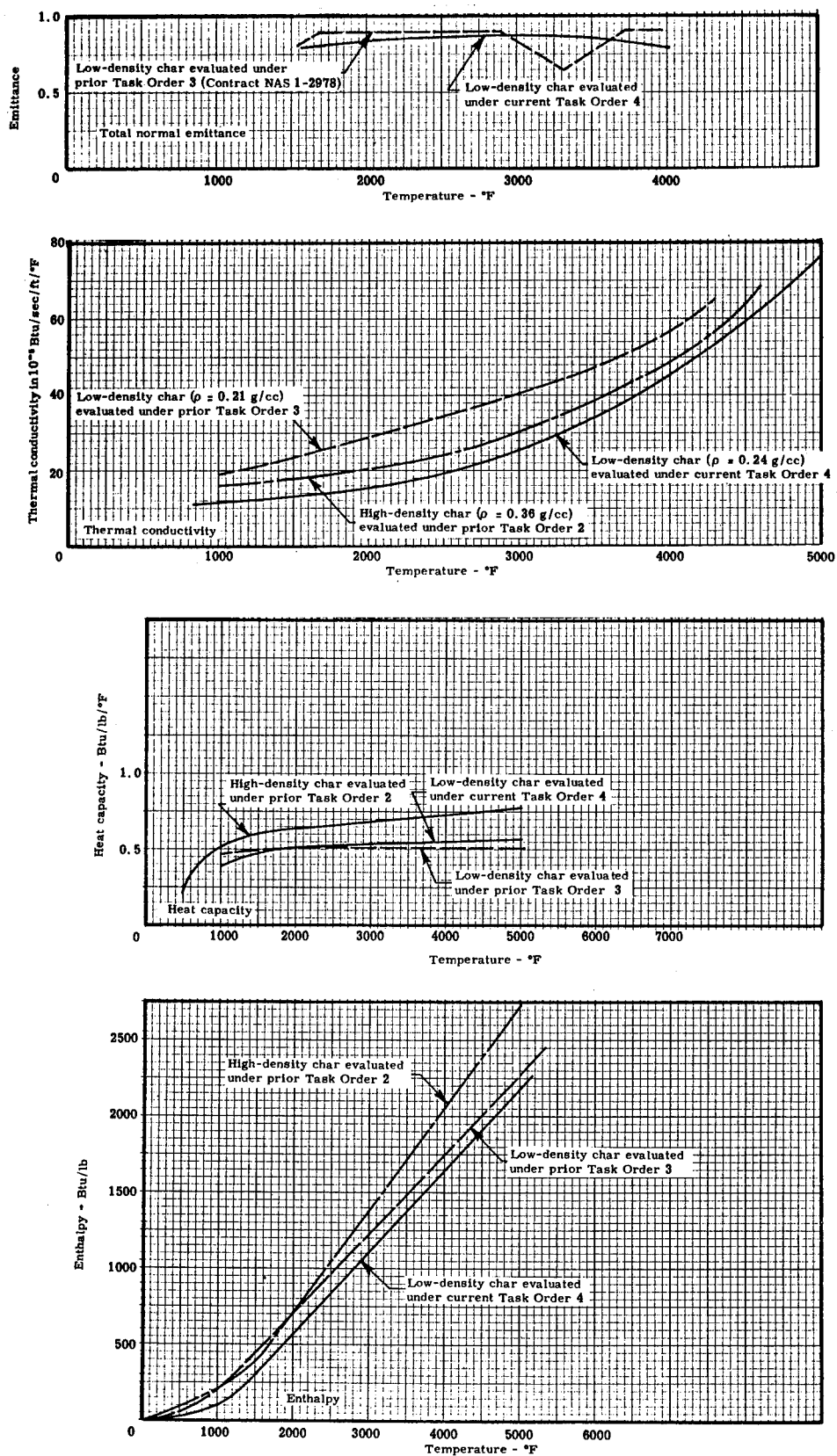
Figure 20. Composite plots of the thermal properties of the low-density phenolic-nylon chars
showing comparison with prior chars

TABLE 1

DENSITY VARIATION WITH TEMPERATURE OF THE
VIRGIN LOW-DENSITY PHENOLIC-NYLON*

Temperature		Density	
°F	°K	kg/m³	lb/ft³
-200	144	596	37.2
-100	200	592	36.9
0	255	589	36.8
75	297	586	36.6
100	311	585	36.5
200	366	579	36.1

*Calculated from density values measured at room temperature and
measured coefficients of thermal expansion.

· TABLE 2

THERMAL CONDUCTIVITY OF THE VIRGIN LOW-DENSITY PHENOLIC-NYLON

Average specimen mean temperature - °F	Total heat input watts	Average specimen ΔT °F	Specimen thermal conductivity in 10^{-5} Btu/sec/ft/°F	Specimen thermal conductivity W/m/°K	Time at temperature hour
Specimen No. 1 Gum Rubber Filler					
-241.6	4.82	43.6	1.25	0.078	5.0
-87.6	6.95	44.0	1.78	0.111	5.0
-13.5	9.21	93.1	1.12	0.069	5.0
118.3	5.20	45.9	1.28	0.080	5.0
Fiberfrax- Gum Rubber Filler					
182.3	9.08	87.2	1.17	0.073	4.0
359.4	27.80	230.6	1.36	0.085	4.5
398.8	16.25	136.7	1.34	0.084	5.5
547.0	25.17	195.2	1.45	0.091	4.8
606.0	30.45	223.0	1.54	0.096	14.0
821.8	44.78	293.5	1.53	0.095	6.5
Specimen No. 2 Gum Rubber Filler					
-202.2	4.70	39.9	1.35	0.084	6.0
-101.6	6.52	48.1	1.55	0.097	5.3
-20.1	5.86	80.7	1.35	0.084	4.5
117.0	5.42	46.2	1.34	0.084	18.0
Fiberfrax - Gum Rubber Filler					
168.5	9.07	76.2	1.36	0.085	6.0
324.8	26.23	201.8	1.43	0.089	18.5
362.7	16.73	129.3	1.42	0.088	6.5
490.7	24.48	170.0	1.49	0.093	16.0
592.4	30.63	209.3	1.47	0.092	7.5
594.8	30.52	211.7	1.45	0.090	22.7
714.8	37.28	259.5	1.31	0.082	8.3

Central diameter = 4.0 inches
Specimen thickness
    Specimen 1 = 0.2493 inch prior to run 0.2216 inch after run
    Specimen 2 = 0.2529 inch prior to run (no change observed to 325°F)
             = 0.2439 inch at 324.8°F + 3% ⎫
             = 0.2421 inch at 362.7°F + 3% ⎪ Thickness estimated from monitoring thickness
             = 0.2289 inch at 490.7°F + 7% ⎬ change by measuring the gap spacing between
             = 0.2221 inch at 592.4°F + 8% ⎪ the hot and cold face of the specimen.
             = 0.2217 inch at 594.8°F + 8% ⎭
             = 0.2015 inch at 714.8°F - measured after run with micrometer.

TABLE 3

THE THERMAL CONDUCTIVITY OF LOW-DENSITY
PHENOLIC-NYLON CHAR USING THE RADIAL INFLOW APPARATUS

SRI run number	Time	Specimen outer face temperature °F	ΔT across gage length °F	Total heat removed by $\frac{1}{2}$" calorimeter gage length Btu/hr	Mean temperature of specimen °F	Specimen thermal conductivity Btu/hr/ft²/°F/in.	in 10^{-5} Btu/sec/ft/°F	Watts/meter/°K	Notes
Run 1 on Specimen 1 (5-12-66) Cal. A-5	On 7:45	-	710	130	1069	5.66	13.1	0.816	1
	9:00	-	710	136	1067	5.91	13.7	0.852	1
		-	712	135	1068	5.87	13.6	0.846	1
		-	714	135	1070	5.82	13.5	0.839	1
	Up 9:10	2110	951	188	1540	6.12	14.2	0.882	1
	9:50	2110	956	192	1545	6.21	14.4	0.895	1
		2110	958	182	1545	5.86	13.5	0.845	1
		2110	961	187	1546	5.99	13.9	0.864	1
	Up 10:15	2800	1107	258	2115	7.19	16.6	1.036	1
	11:00	2800	1107	250	2115	6.99	16.2	1.008	1
		2800	1107	253	2115	7.06	16.3	1.018	1
	Up 11:45	3425	834	342	2805	11.7	28.1	1.687	3,4
	12:30	3425	834	336	2805	11.5	26.6	1.658	3,4
		3425	834	339	2805	11.6	26.2	1.673	3,4
	Up 1:30	3970	934	428	3275	13.0	30.1	1.875	3,4
	1:45	3970	934	429	3275	13.1	30.3	1.889	3,4
		3970	934	421	3275	12.8	29.6	1.846	3,4
	Up 2:10	4390	968	502	3670	14.7	34.0	2.120	3,4
	2:45	4390	968	493	3670	14.5	33.6	2.091	3,4
		4390	968	493	3670	14.5	33.6	2.091	3,4

TABLE 3 - Continued

THE THERMAL CONDUCTIVITY OF LOW-DENSITY
PHENOLIC-NYLON CHAR USING THE RADIAL INFLOW APPARATUS

SRI run number	Time	Specimen outer face temperature °F	ΔT across gage length °F	Total heat removed by $\frac{1}{2}''$ calorimeter gage length Btu/hr	Mean temperature of specimen °F	Specimen thermal conductivity			Notes
						Btu/hr/ft^2/°F/in.	in 10^{-6} Btu/sec/ft/°F	Watts/meter/°K	
Run 1 on Specimen 1 (continued)	Up 3:05	4795	878	568	4140	18.4	42.6	2.653	3, 4
	3:55	4795	878	573	4140	18.6	43.0	2.682	3, 4
		4795	878	529	4140	17.2	39.8	2.480	3, 4
	Up 4:25	5110	852	607	4475	20.2	46.7	2.912	3, 4
	5:10	5110	852	614	4475	20.5	47.4	2.956	3, 4
		5110	852	612	4475	20.4	47.1	2.942	3, 4
	Up 5:35 6:00	5355	580	672	4925	32.9	73.7	4.744	3, 4, 5
	Down 6:50	3930	770	428	3360	15.8	38.6	2.278	3, 4
		3930	770	438	3360	16.2	37.4	2.??	3, 4
		3930	770	420	3360	15.5	35.8		3, 4
		3930	770	430	3360	15.9	36.8	2.235	3, 4
	Down 7:17	3525	599	365	3080	17.3	40.0	2.495	3, 4
	7:45	3525	599	374	3080	17.7	40.9	2.552	3, 4
		3525	599	378	3080	17.9	41.4	2.581	3, 4
		3525	599	381	3080	18.1	41.9	2.610	3, 4
	Down 8:09	--	547	282	2163	14.7	34.0	2.120	3, 4
	9:20	--	547	284	2161	14.8	34.2	2.134	3, 4
		--	547	276	2156	14.4	33.3	2.076	3, 4

45

TABLE 3 - Continued

THE THERMAL CONDUCTIVITY OF LOW-DENSITY
PHENOLIC-NYLON CHAR USING THE RADIAL INFLOW APPARATUS

SRI run number	Time	Specimen outer face temperature °F	ΔT across gage length °F	Total heat removed by 1" calorimeter gage length Btu/hr	Mean temperature of specimen °F	Specimen thermal conductivity			Notes
						Btu/hr/ft²/°F/in.	in 10^{-6} Btu/sec/ft/°F	Watts/meter/°K	
Run 1 on Specimen 2 (5-10-66) Cal. A-5	On 10:00	—	585	97.9	814	4.69	10.9	0.676	1
	11:20	—	586	99.7	814	4.77	11.0	0.688	1
		—	587	97.5	816	4.66	10.8	0.672	1
		—	589	95.8	818	4.56	10.6	0.658	1
	Up 11:30	1890	856	169	1347	5.54	12.8	0.799	1
	12:20	1890	856	168	1341	5.48	12.7	0.790	1
		1890	850	168	1353	5.42	12.5	0.782	2
		1890	853	163	1356	5.24	12.1	0.756	2
	Up 12:45	2475	1035	231	1776	6.24	14.4	0.900	1
	1:30	2475	1035	229	1781	6.21	14.4	0.895	1
		2475	1036	232	1785	6.28	14.5	0.906	1
		2475	1038	232	1788	6.28	14.5	0.906	1
	Up 1:45	3250	1000	320	2515	8.80	20.4	1.269	3, 4
	2:45	3250	1000	315	2515	8.72	20.2	1.257	3, 4
		3250	1000	315	2515	8.64	20.0	1.246	3, 4
		3290	1000	316	2555	8.72	20.2	1.257	3, 4
	Up 2:50	3850	650	390	3375	16.5	38.2	2.379	3, 4
	3:30	3850	650	388	3375	16.4	38.0	2.365	3, 4
		3850	650	384	3375	16.2	37.5	2.336	3, 4
		3850	650	385	3375	16.2	37.5	2.336	3, 4

TABLE 3 - Continued

THE THERMAL CONDUCTIVITY OF LOW-DENSITY
PHENOLIC-NYLON CHAR USING THE RADIAL INFLOW APPARATUS

SRI run number	Time	Specimen outer face temperature °F	ΔT across gage length °F	Total heat removed by 1" calorimeter gage length Btu/hr	Mean temperature of specimen °F	Specimen thermal conductivity $Btu/hr/ft^2/°F/in.$	in 10^{-5} $Btu/sec/ft/°F$	Watts/meter/°K	Notes
Run 1 on Specimen 2 (continued)	Up 4:00 4:55	4385 4385 4385 4385	616 616 616 616	472 469 470 474	3935 3935 3935 3935	21.0 20.9 20.0 21.1	48.6 48.4 46.3 48.8	3.028 3.014 2.884 3.043	3,4 3,4 3,4 3,4
	7:05	5040 5040 5040 5040	588 588 588 588	629 629 611 652	4610 4610 4610 4610	29.3 29.3 28.5 30.4	67.8 67.8 66.0 70.4	4.225 4.225 4.110 4.384	3,4 3,4 3,4 3,4
Run 1 on Specimen 3 (5-25-66) Cal. A-5	On 7:50 9:35	1800 1800 1800	832 831 834	153 155 156	1289 1289 1292	5.58 5.66 5.69	12.9 13.1 13.2	0.805 0.816 0.820	1 1 1
	Up 9:50 11:00	2760 2760 2760	900 900 900	268 262 264	2120 2120 2120	8.88 8.66 8.73	20.6 20.0 20.2	1.280 1.249 1.259	3,4 3,4 3,4
	Up 11:40 12:45	3140 3140 3140	942 942 942	298 298 304	2470 2470 2470	9.41 9.43 9.60	21.8 21.8 22.2	1.357 1.360 1.384	3,4 3,4 3,4

TABLE 3 - Continued

THE THERMAL CONDUCTIVITY OF LOW-DENSITY
PHENOLIC-NYLON CHAR USING THE RADIAL INFLOW APPARATUS

SRI run number	Time	Specimen outer face temperature °F	ΔT across gage length °F	Total heat removed by $\frac{1}{4}$" calorimeter gage length Btu/hr	Mean temperature of specimen °F	Specimen thermal conductivity			Notes
						Btu/hr/ft^2/°F/in.	in 10^{-5} Btu/sec/ft/°F	Watts/meter/°K	
Run 1 on Specimen 3 (continued)	Up 1:00	3920	912	405	3270	13.2	30.6	1.903	3, 4
	1:45	3920	912	404	3270	13.2	30.6	1.903	3, 4
		3920	912	403	3270	13.2	30.6	1.903	3, 4
	Up 2:45	4795	657	518	4330	23.5	54.4	3.389	3, 4
	3:20	4795	657	512	4330	23.2	53.7	3.345	3, 4
		4795	657	516	4330	23.4	54.2	3.374	3, 4
	Up 4:02	5405	615	656	4970	31.8	73.6	4.586	3, 4
	4:15	5405	615	660	4970	32.0	74.1	4.614	3, 4
		5405	615	656	4970	31.7	73.4	4.571	3, 4
		5405	615	664	4970	32.1	74.3	4.629	3, 4
	Down 4:30	4535	405	512	4245	37.6	87.0	5.422	3, 4
	5:26	4535	405	498	4245	36.6	84.7	5.278	3, 4
		4535	405	505	4245	37.2	86.1	5.364	3, 4
		4535	405	507	4245	37.2	86.1	5.364	3, 4
	Down 5:56	3655	466	373	3325	23.9	55.3	3.446	3, 4
	6:50	3655	466	377	3325	24.0	55.6	3.461	3, 4
		3655	466	378	3325	24.1	55.8	3.475	3, 4
		3655	466	374	3325	23.9	55.3	3.446	3, 4

48

TABLE 3 - Concluded

THE THERMAL CONDUCTIVITY OF LOW-DENSITY
PHENOLIC-NYLON CHAR USING THE RADIAL INFLOW APPARATUS

SRI run number	Time	Specimen outer face temperature °F	ΔT across gage length °F	Total heat removed by 1" calorimeter gage length Btu/hr	Mean temperature of specimen °F	Specimen thermal conductivity			Notes
						Btu/hr/ft²/°F/in.	in 10⁻⁵ Btu/sec/ft/°F	Watts/meter/°K	
Run 1 on Specimen 3 (continued)	Down 7:05								
	8:00	3300	390	324	3025	24.8	57.4	3.576	3, 4
		3300	390	330	3025	25.2	58.3	3.634	3, 4
		3300	390	339	3025	25.9	60.0	3.735	3, 4
		3300	390	330	3025	25.2	58.3	3.634	3, 4
	Down 8:25								
	9:00	2710	359	261	2455	21.6	50.0	3.115	3, 4
		2710	359	248	2455	20.5	47.5	2.956	3, 4
		2710	359	259	2455	21.5	49.8	3.100	3, 4
		2710	359	266	2455	22.1	51.2	3.187	3, 4
	Down 9:18								
	10:00	1770	318	159	1422	15.0	34.7	2.163	2
		1770	318	157	1422	14.6	33.8	2.105	2
		1770	318	159	1422	15.0	34.7	2.163	2
		1770	318	158	1422	14.7	34.0	2.120	2
	Off 10:17								

Notes:

1. ΔT measured with thermocouples, in front and back holes.
2. ΔT measured with thermocouples, in left and right side holes.
3. ΔT measured with optical pyrometer, using left and right side holes. Average of several ΔT readings used.
4. Mean temperature calculated as follows:

   Specimen 1, $T_{mean} = T_{of} - 0.744\ \Delta T$ (°F)

   Specimen 2, $T_{mean} = T_{of} - 0.734\ \Delta T$ (°F)

   Specimen 3, $T_{mean} = T_{of} - 0.710\ \Delta T$ (°F)

5. Only one ΔT measured before heater element failed.
6. No cooling data taken with specimen 2. Heater element failed.
7. Conductivity calculated from the following:

   $$K = \text{Factor} \times \frac{q}{\Delta T}$$

8. Factors were the following: (for calculation in Btu/hr/ft/°F/in.)

	Front to Back	Side to Side
Specimen 1	30.91	28.42
Specimen 2	28.03	27.46
Specimen 3	30.34	29.76

49

TABLE 4

ENTHALPY OF THE VIRGIN LOW-DENSITY PHENOLIC-NYLON

Specimen number and run number	Initial cup temperature °F	Final cup temperature °F	Change in cup temperature °F	Initial sample temperature °F	Heating time to temperature min	Initial wt. of sample gm	Final wt. of sample gm	Enthalpy $h = \frac{K}{W_s}(t_2 - t_1)$ Btu/lb	Enthalpy above 85°F reference Btu/lb
Specimen 1									
Run 1	76.08	78.60	2.52	274	125	4.0201	3.9390	77.02	74.49
3	92.43	99.17	6.74	533	35	3.8568	3.7900	214.09	221.07
4	88.91	95.87	6.96	628	40	3.7900	3.2331	259.16	264.44
5	77.77	83.09	5.32	722	75	3.2331	2.3043	277.94	277.13
Specimen 2									
Run 1	74.90	75.95	1.05	171	85	3.6863	3.6146	35.97	31.63
2	78.56	81.87	3.31	340	45	3.6146	3.5746	111.47	110.13
3	87.95	94.00	6.05	542	60	3.5746	3.5640	204.36	208.45
4	92.26	98.04	5.78	562	35	3.5640	3.1762	219.08	225.23
5	83.00	87.17	4.17	790	48	3.1762	1.7240	291.19	292.09
Specimen 3									
Run 1	76.26	77.36	1.10	182	55	3.2346	3.1770	41.68	38.63
2	77.32	79.04	1.72	250	43	3.1770	3.1592	65.54	59.80
3	78.87	82.56	3.69	376	29	3.1592	3.1448	141.26	140.08
4	81.87	86.30	4.43	448	47	3.1448	3.0760	173.38	173.98
5	84.78	89.39	4.61	495	55	3.0760	2.9064	190.95	193.01
6	97.48	102.87	5.39	629	35	2.9064	2.5250	256.98	265.69
7	85.65	90.56	4.91	780	100	2.5250	1.7790	332.26	334.92
Specimen 4									
Run 1	88.95	87.39	-1.56	-72	40	3.4870	3.4985	-53.68	-52.88
2	74.64	73.30	-1.34	-80	43	3.4985	3.5312	-45.68	-49.15
3	73.30	72.45	-0.85	-21	73	3.5312	3.5400	-28.91	-32.80
Specimen 5									
Run 1	72.90	72.77	-0.18	-1	60	2.3259	2.3381	-9.27	-10.81
Specimen 6									
Run 1	74.54	78.30	3.76	512	90	2.3647	2.1381	211.71	208.45
Specimen 7									
Run 1	82.82	86.39	3.57	716	31	2.3471	1.4977	286.96	287.50
Specimen 8									
Run 1	80.04	86.56	6.52	787	30	4.3460	2.3138	339.23	339.98
Specimen 9									
Run 1	81.09	88.22	7.13	789	37	4.9902	2.7425	312.98	314.39
Specimen 10									
Run 1	77.14	75.39	-1.75	-197	20	3.0953	3.0784	-68.44	-70.85
2	93.70	91.17	-2.53	-223	19	3.0784	3.0569	-99.64	-97.67
3	89.39	87.13	-2.26	-262	20	3.0569	3.0560	-89.03	-88.48

50

TABLE 5

ENTHALPY OF THE LOW-DENSITY PHENOLIC-NYLON CHAR

Specimen number and run number	Drop temperature °F	Initial weight grams	Final weight grams	Enthalpy from drop temperature to 32°F Btu/lb
Specimen 1				
Run 3	1025	1.165	1.095	101.5
6	2050	1.245	1.235	642.8
7	2550	1.290	1.275	784.5
8	3075	1.310	1.240	1305.9
9	3505	1.245	1.245	1415.5
10	4075	1.240	1.235	1645.4
11	4555	1.275	1.250	1549.5
Specimen 2				
Run 5	1985	1.280	1.265	502.0
6	2540	1.205	1.195	916.7
8	3500	1.250	1.230	1316.5
11	4920	1.290	1.230	2452.4
12	5055	1.220	1.210	2296.1
Specimen 3				
Run 2	2520	1.230	1.215	823.2
3	3055	1.255	1.230	1381.1
4	4520	1.265	1.230	1923.2
Specimen 4				
Run 1	1497	1.235	1.255	227.7
4	3020	1.195	1.185	1018.2
5	4140	1.180	1.185	1473.7
6	5025	1.230	1.205	2358.3

TABLE 6

THERMAL EXPANSION IN THE "ab" (PERPENDICULAR TO THE THICKNESS)
DIRECTION OF THE VIRGIN LOW-DENSITY PHENOLIC-NYLON

Specimen	Time	Temperature No. 1 °F	Temperature No. 2 °F	Temperature No. 3 °F	Average temperature °F	Observed total elongation 10^{-3} in.	Observed unit elongation 10^{-3} in./in.	Unit elongation correction for dilatometer motion 10^{-3} in./in.	Corrected specimen unit elongation 10^{-3} in./in.
Specimen 1									
Initial length 2.9976	9:00	73.5	73.5	73.5	73.5	0.0	0.00	0.0	0.00
	9:20	-35.0	-35.0	-21.0	-30.3	-5.7	-1.90	0.0	-1.90
Final length 2.8731	9:30	-89.5	-89.5	-82.0	-87.0	-6.0	-2.00	0.0	-2.00
	9:45	-331.8	-325.6	-247.5	-301.6	-21.1	-7.04	0.0	-7.04
	10:00	-8.0	-8.0	-60.0	-25.3	-7.1	-2.37	0.0	-2.37
	10:22	73.5	73.5	73.5	73.5	-0.4	-0.13	0.0	-0.13
	11:00	139.5	139.5	139.5	139.5	4.0	1.63	0.02	1.65
	11:15	182.7	182.7	182.7	182.7	9.4	3.14	0.03	3.17
	11:35	234.5	234.5	234.5	234.5	13.5	4.50	0.04	4.54
	11:42	255.0	255.0	255.0	255.0	11.9	3.97	0.05	4.02
	12:20	388.6	388.7	388.7	388.7	1.0	0.33	0.10	0.43
	12:50	504.0	504.0	504.0	504.0	-7.5	-2.50	0.13	-2.37
	1:15	616.5	616.5	616.5	616.5	-17.7	-5.90	0.16	-5.74
	2:00	Reached bottom of scale							
Specimen 2									
Initial length 3.0070	12:25	78.0	78.0	78.0	78.0	0.0	0.00	0.0	0.00
	12:40	-213.0	-231.0	-231.0	-225.0	-17.5	-5.82	0.0	-5.82
Final length specimen broke	12:45	-253.0	-266.0	-266.0	-261.7	-18.8	-6.25	0.0	-6.25
	12:48	-266.0	-266.0	-266.0	-266.0	-18.8	-6.25	0.0	-6.25
	1:00	-213.0	-219.0	-219.0	-217.0	-16.9	-5.62	0.0	-5.62
	1:15	-92.0	-107.5	-111.0	-103.5	-11.4	-3.79	0.0	-3.79
	1:30	-88.5	-86.5	-94.5	-89.8	-10.0	-3.33	0.0	-3.33
	1:33	-99.5	-99.5	-105.0	-101.3	-10.7	-3.56	0.0	-3.56
	1:41	30.5	22.7	20.5	-24.6	-3.7	-1.23	0.0	-1.23
	5:00 pm	75.5	75.5	75.5	75.5	0.4	0.13	0.0	0.13
	11:30 am	78.4	78.4	78.4	78.4	1.6	0.53	0.0	0.53
	12:20	148.3	148.0	148.0	148.1	6.3	2.10	0.02	2.12
	1:05	203.4	203.7	203.3	203.5	10.5	3.49	0.04	3.53
	1:20	226.8	227.3	226.8	227.0	11.8	3.92	0.04	3.96
	1:30	243.6	244.0	242.6	243.5	11.4	3.79	0.05	3.84
	1:45	275.2	275.0	274.7	275.0	4.7	1.56	0.06	1.62
	2:15	376.0	381.2	380.7	379.3	-4.8	-1.60	0.09	-1.51
	2:40	426.0	430.8	430.5	429.1	-9.0	-2.99	0.11	-2.88
	3:20	660.0	658.0	656.0	658.0	-31.9	-10.61	0.17	-10.44
	3:22	664.3	679.8	677.3	673.8	-38.0	-12.64	0.18	-12.46
	3:33	692.3	719.2	728.9	713.5	-95.0	-31.59	0.19	-31.40
	3:40	722.5	759.3	765.0	748.9	-159.0	-52.88	0.20	-52.68

TABLE 7

THERMAL EXPANSION IN THE "c" OR THICKNESS DIRECTION OF THE VIRGIN LOW-DENSITY PHENOLIC-NYLON

Specimen	Time	Temperature No. 1 °F	Temperature No. 2 °F	Temperature No. 3 °F	Average temperature °F	Observed total elongation 10⁻³ in.	Observed unit elongation 10⁻³ in./in.	Unit Elongation correction for dilatometer motion 10⁻³ in./in.	Corrected specimen unit elongation 10⁻³ in./in.
Specimen 1 Initial length 3.0117 Final length 2.8684	3:05	75.0	75.0	75.0	75.0	0.0	0.00	0.00	0.00
	3:24	92.0	92.7	92.3	92.3	1.6	0.53	0.00	0.53
	3:40	125.5	126.5	125.5	126.0	5.0	1.66	0.01	1.67
	3:56	149.5	149.0	148.5	149.0	7.7	2.56	0.02	2.58
	4:40	203.0	201.3	203.0	202.4	14.4	4.78	0.04	4.82
	4:55	236.5	234.0	236.5	235.7	16.3	5.41	0.05	5.46
	5:05	258.0	256.0	257.5	257.2	12.5	4.15	0.05	4.20
	5:23	341.0	Not Obtained	Not Obtained	341.0	6.0	1.99	0.07	2.06
	5:24	352.5			352.5	7.9	2.62	0.08	2.70
	5:26	368.0			368.0	9.1	3.02	0.09	3.11
	5:27	375.7			375.7	10.0	3.32	0.09	3.41
	5:29	390.5			390.5	11.5	3.82	0.10	3.92
	5:30	400.5	398.5	401.0	400.0	12.0	3.98	0.10	4.08
	5:37	429.0	422.0	427.0	426.0	12.6	4.18	0.11	4.29
	5:45	461.0	461.0	462.0	430.6	14.0	4.65	0.11	4.76
	5:47	488.5	481.0	488.5	486.0	15.0	4.98	0.13	5.11
	5:52	549.7	549.0	544.5	547.7	10.9	3.62	0.14	3.76
	5:55	603.0	581.5	599.0	594.5	12.7	4.22	0.16	4.38
	5:58	628.0	610.5	626.5	621.7	8.4	2.79	0.17	2.96
	6:05	666.5	643.3	663.0	657.6	0.0	0.00	0.18	0.18
	6:11	692.7	672.0	677.7	680.8	-3.5	-1.16	0.20	-0.96
	6:18	750.0	711.5	743.5	735.0	-90.0	-29.88	0.20	-29.68
	8:00 am	75.0	75.0	75.0	75.0	-140.5	-46.65	0.00	-46.65

TABLE 8

PERMEABILITY OF VIRGIN LOW-DENSITY
PHENOLIC-NYLON AT ROOM TEMPERATURE

Specimen number and thickness	Purge gas	Pressure drop across specimen in. of water	Mean pressure of specimen in. of water	Flow rate of gas at bubble gage cm^3/sec	Admittance $K_{m\nu}$ cm^2/sec or $10^{-4} m^2/sec$	ft^2/sec
Specimen 1 0.263 inch	nitrogen	2.50	408.05	.1100	4.2078	.00453
		5.50	409.55	.2411	4.1922	.00451
		5.60	409.60	.2450	4.1839	.00450
		9.75	411.68	.4214	4.1333	.00445
		9.75	411.68	.4184	4.1038	.00442
	helium	2.50	408.05	.1062	4.0624	.00437
		2.80	408.20	.1210	4.1327	.00445
		5.60	409.60	.2465	4.2095	.00453
		5.30	409.60	.2381	4.2962	.00462
		9.60	411.60	.4077	4.0614	.00437
		9.60	411.60	.4120	4.1042	.00442
Specimen 2 0.4218 inch	helium	2.60	408.10	.0739	4.371	.00470
		2.70	408.15	.0782	4.454	.00479
		5.60	409.60	.1613	4.430	.00477
		5.60	409.60	.1647	4.523	.00487
		9.60	411.60	.2740	4.390	.00472
		9.70	411.65	.2809	4.454	.00479
	nitrogen	2.50	408.05	.0733	4.509	.00485
		2.70	408.15	.0703	4.004	.00431
		5.50	409.55	.1563	4.371	.00470
		5.60	409.60	.1468	4.032	.00434
		9.60	411.60	.2483	3.978	.00428
		9.60	411.60	.2475	3.965	.00427
Specimen 3 0.4334 inch	nitrogen	2.65	408.13	.0812	4.905	.00528
		2.70	408.15	.0851	5.045	.00543
		5.65	409.63	.1798	5.094	.00548
		5.75	409.68	.1808	5.033	.00542
		9.60	411.60	.3003	5.007	.00539
		9.70	411.65	.3086	5.093	.00548
	helium	2.50	408.05	.0805	5.154	.00555
		2.50	408.05	.0793	5.077	.00546
		5.75	409.68	.1852	5.166	.00555
		5.75	409.68	.1855	5.164	.00556
		9.40	411.50	.2907	4.950	.00533
		9.55	411.58	.3067	5.141	.00553

TABLE 8 - Concluded

PERMEABILITY OF VIRGIN LOW-DENSITY
PHENOLIC-NYLON AT ROOM TEMPERATURE

Specimen number and thickness	Purge gas	Pressure drop across specimen in. of water	Mean pressure of specimen in. of water	Flow rate of gas at bubble gage cm³/sec	Admittance $K_{m\nu}$ cm²/sec or 10^{-4} m²/sec	ft²/sec
Specimen 4 0.249 inch	helium	2.55	408.08	.1131	4.067	.00438
		2.80	408.20	.1223	4.017	.00432
		5.55	409.58	.2392	3.964	.00427
		5.55	409.58	.2392	3.964	.00427
		9.50	411.55	.4098	3.967	.00427
		9.65	411.63	.4098	3.905	.00420
	nitrogen	2.95	408.28	.1227	3.825	.00412
		3.00	408.30	.1240	3.801	.00409
		5.60	409.60	.2314	3.800	.00409
		5.75	409.68	.2380	3.807	.00410
		9.15	411.38	.3717	3.736	.00402
		9.55	411.58	.3831	3.689	.00397
Specimen 5 0.250 inch	nitrogen	2.65	408.13	.1190	4.065	.00437
		3.05	408.33	.1428	4.238	.00456
		5.45	409.53	.2433	4.041	.00435
		5.55	409.58	.2538	4.139	.00445
		9.45	411.53	.4255	4.076	.00439
		9.55	411.58	.4273	4.050	.00436
	helium	2.60	408.10	.1164	4.052	.00436
		2.65	408.13	.1176	4.017	.00432
		5.45	409.53	.2493	4.141	.00446
		5.50	409.55	.2557	4.208	.00453
		9.40	411.50	.4166	4.012	.00432
		9.40	411.50	.4255	4.097	.00441

Note:

Exposed area of specimen = 2.52 cm²

55

TABLE 9

PERMEABILITY OF THE LOW-DENSITY PHENOLIC-NYLON CHAR AT ROOM TEMPERATURE

Specimen number and thickness	Purge gas	Pressure drop across specimen inch of water	Mean pressure of specimen inch of water	Pressure at flowmeter inch of water	Flow rate of gas at flowmeter cm³/sec	Admittance $Km\nu$ cm²/sec or 10⁻⁴ m²/sec	Admittance $Km\nu$ ft²/sec
Specimen 1 0.250 inch	helium	1.50	401.25	400.3	122	12,219	13.2
		3.00	402.60	400.5	233	11,664	12.6
	nitrogen	1.50	401.50	400.4	101	10,150	11.0
		3.00	403.30	401.0	163	8,186	8.8
Specimen 2 0.250 inch	nitrogen	1.50	402.69	401.4	98	9,883	10.7
		1.50	402.59	401.4	98	9,881	10.7
		3.00	404.54	402.1	163	8,208	8.9
		3.00	404.44	402.1	161	8,086	8.7
	helium	1.50	402.24	401.4	115	11,552	12.5
		3.00	403.59	401.5	213	10,668	11.6

Note:

Exposed area of specimen = 1.69 cm²

TABLE 10

TOTAL NORMAL EMITTANCE OF LOW-DENSITY PHENOLIC-NYLON CHAR

Time	Observed temperature °F	Radiometer output millivolts	True temperature °F	Emittance	Remarks
Specimen 1					
3:53	1468	0.198	1551	0.77	Attempted to run at
3:58	1463	0.206	1540	0.81	higher temperature
4:05	1561	0.256	1649	0.82	(approx. 3200°F)
4:15	1865	0.482	1985	0.86	but radiometer sig-
4:24	2326	1.139	2485	0.95	nal became noisy.
4:38	2710	1.835	2940	0.85	White coating on
4:44	2720	1.818	2960	0.82	surface noted dur-
					ing disassembly.
Specimen 2					
9:21	1480	0.199	1566	0.75	
9:29	1910	0.490	2047	0.79	
9:35	2280	0.954	2460	0.82	
9:45	2840	2.336	3059	0.94	
9:53	3305	3.986	3591	0.90	
10:03	3480	4.763	3796	0.88	
Specimen 3					
1:13	1526	0.235	1611	0.81	
1:23	1875	0.461	2007	0.79	
1:32	2333	1.030	2521	0.82	
1:38	2720	1.810	2961	0.82	
1:45	3199	3.605	3463	0.93	
Specimen 4					
9:38	1448	0.199	1524	0.81	
9:44	2015	0.600	2164	0.80	
9:50	2286	1.043	2447	0.92	
10:00	2772	2.094	2991	0.91	
10:05	3330	4.339	3585	0.99	
Specimen 5					
10:18	3480	4.721	3802	0.87	
Specimen 6					
1:16	3605	4.954	4008	0.76	
Specimen 7					
9:45	3005	2.622	3286	0.87	
Specimen 8					
2:43	2895	2.396	3139	0.88	
2:48	3143	3.057	3451	0.80	
2:53	3262	3.441	3600	0.77	
3:06	3535	4.681	3913	0.78	

TABLE 11

TENSILE STRESS-STRAIN DATA FOR THE VIRGIN LOW-DENSITY PHENOLIC-NYLON

SRI run number	Temperature °F	Temperature rise rate °F/min	Crosshead rate in./min	Initial elastic modulus		Yield strength at 0.2% offset		Ultimate strength		Tensile elongation in percent	Load time to rupture min	Initial Poisson's ratio	Remarks
				in 10³ psi	in 10⁶ N/m²	in psi	in 10⁶ N/m²	in psi	in 10⁶ N/m²				
T-26	-200	-	0.03	194	1338	-	-	640	4.41	0.33	6	0.14	
T-27	-200	-	0.03	247	1703	-	-	559	3.85	0.27	6	0.30	
T-29	-200	-	0.03	114	788	-	-	519	3.58	0.40	6	0.05	
T-22	-100	-	0.04	90.0	620	-	-	530	3.65	0.68	4.2	0.08	
T-28	-100	-	0.03	83.7	577	-	-	526	3.63	0.66	5.3		
T-23	0	-	0.04	81.6	563	356	2.45	402	2.77	0.79	4	0.05	
T-24	0	-	0.04	69.0	476	492	3.39	510	3.52	0.95	5	0.06	
T-3	70	-	0.02	67.5	465	-	-	409	2.82	0.69	12.5	0.11	Loaded to ~45 psi and unloaded before final loading.
T-4	70	-	0.02	73.6	507	-	-	538	3.71	0.81	11	0.14	Loaded to ~49 and unloaded before final loading.
T-5	70	-	0.4	83.4	575	-	-	572	3.94	0.76	1	-	Lateral strain did not track.
T-20	70	-	0.03	74.1	511	279	1.92	320	2.21	0.73	3.5	-	Lateral strain did not track.
T-6	200	100	0.05	65.3	450	367	2.53	539	3.72	1.32	4.9	0.13	
T-7	200	100	0.05	79.2	546	513	3.54	553	3.81	0.96	3	0.14	
T-8	300	100	0.05	21.4	147	-	-	147	1.01	0.73	4	-	Loaded and unloaded before final load. Lateral strain did not track.
T-9	300	100	0.05	23.3	161	164	1.13	192	1.32	1.58	3	0.11	
T-19	300	100	0.05	21.6	149	-	-	234	1.61	1.37	3	0.50	
T-11	400	100	0.05	11.1	76.5	66.4	0.46	139	0.96	1.14	2.1	-	Lateral strain did not track.
T-16	400	100	0.03	9.45	65.2	-	-	113	0.78	2.42	6.3	0.20	Heated to 400°F twice.
T-12	500	100	0.05	5.9	41	-	-	76	0.52	1.32	8.1	-	Lateral strain not measured.
T-17	500	100	0.05	9.6	66	-	-	41	0.28	0.42	1.7	-	Lateral strain could not be measured due to charring of specimen.
T-13	600	100	0.03	3.6	25	-	-	30	0.21	0.87	2.4	-	Lateral strain not measured.
T-15	600	100	0.03	2.0	14	-	-	21	0.14	1.04	5.1	-	Lateral strain not measured.
T-14	700	100	-	-	-	-	-	-	-	-	-	-	Specimen burned.

Notes:
1. Yield strength at 0.2% offset not defined when ultimate and fracture occurred before this point.
2. Specimens held at temperature from 3-5 minutes.
3. Cooling rates not measured.

58

TABLE 12

COMPRESSIVE STRESS-STRAIN DATA FOR THE VIRGIN, LOW-DENSITY, PHENOLIC-NYLON

SRI run number	Temperature °F	Temperature rise rate °F/min[1]	Crosshead rate in./min.	Initial elastic modulus in 10³ psi	Initial elastic modulus in 10⁶ N/m²	Yield strength at 0.2% offset in psi	Yield strength at 0.2% offset in 10⁶ N/m²	Ultimate strength in psi	Ultimate strength in 10⁶ N/m²	Compressive deformation %	Load time to rupture min	Initial Poisson's ratio
C-17	-200	-237²	0.009	102	700	2310	15.93	2615	18.03	4.9	6	0.12
C-18	-200	-190²	0.009	136	937	1848	12.74	2640	18.20	3.5	5.5	0.22
C-19	-100	-125²	0.012	104	717	1615	11.14	2430	16.75	4.0	4.5	0.21
C-20	-100	-115²	0.012	94	645	1302	8.98	2120	14.62	4.5	4.5	0.22
C-21	0	-70²	0.013	88	610	1020	7.03	1900	13.10	4.0	4	0.32
C-22	0	-40³	0.013	81	559	1430	9.86	2120	14.62	4.6	5	0.23
C-1	70	-	0.015	50	344	1050	7.24	1405	9.69	5.0	-	0.22
C-2	70	-	0.015	59	407	1015	7.00	1392	9.50	4.9	-	0.26
C-3	200	100	0.020	84	576	876	6.04	1380	9.51	3.0	4	0.20
C-4	200	100	0.020	86	590	528	3.64	1330	9.17	5.8	4	0.27
C-5	300	100	0.020	48	334	703	4.85	1380	9.51	7.2	5.5	0.20
C-6	300	100	0.020	50	348	628	4.33	1365	9.41	7.6	4	0.21
C-7	400	100	0.030	34	232	591	4.07	1225	8.45	8.8	4	0.22
C-8	400	100	0.025	37	255	370	2.55	930	6.41	6.1	3.5	-
C-9	500	100	0.015	21	143	226	1.56	1060	7.31	21.7	14	-
C-10	500	100	0.030	17	117	237	1.63	655	4.52	12.5	5	0.16
C-11	500	100	0.030	23	158	277	1.91	795	5.48	14.7	5.5	0.16
C-12	600	100	0.030	14	97	204	1.41	381	2.63	9.0	3	0.13
C-13	600	100	0.024	9	61	138	0.95	418	2.88	14.6	6.5	0.11
C-14	750	100	0.030	12	86	186	1.28	290	2.00	13.1	6	0.13
C-15	750	100	0.020	-³	-³	-³	-³	80	0.55	8.2	4.5	-
C-16	700	100	0.025	13	89	210	1.45	306	2.11	5.4	2.5	0.08
C-24	70	-	0.015	62.3	430	1062	7.32	1870	12.89	4.5	4.5	-
C-25	70	-	-	72.7	501	1325	9.14	2090	14.41	6.2	10	0.11
C-26	70	-	-	62.8	433	1325	9.14	2057	14.18	5.6	7.8	0.16
C-27	200	100	-	53.5	369	523	3.61	1896	13.07	15.8	11.2	0.17
C-28	200	100	-	60.6	418	579	3.99	1705	11.76	8.9	4.8	0.18

Notes:
Soaked at temperature for 5 minutes.
1. This is an approximate cooling rate due to nonlinearity of the cooling.
2. Initial modulus and strength too low to accurately determine the modulus and yield strength on SRI Run No. C-15.
3. Initial modulus and strength too low to accurately determine the modulus and yield strength on SRI Run No. C-15.
4. This table supercedes Table 2 of the October 1965 progress report.

APPENDIX A

DETAILED MATERIAL DESCRIPTION

The following detailed description of each constituent within the low-density phenolic-nylon was supplied by the NASA Langley Research Center.

Union Carbide BRP-5549
Phenolic Resin

The properties of the resin as published by the manufacturer are shown in the table below

Property	Property value
Density	16. 8 to 19. 4 lb/ft^3 (270 to 310 kg/m^3)

Sieve Analysis
 (U.S. Std. Mesh)
    on 40 mesh 0. 0%
    on 100 mesh 0. 6%
    on 200 mesh 2. 0%
    through 200
      mesh   98. 0%
 Hexamethylene 8. 7 - 9. 5%
    tetramine
    content	

Measurements with a Coulter Counter (Coulter Electronics Industrial Division) at the Langley Research Center indicate that the range of diameters of the phenolic resin powder particles is 0. 0001 to 0. 0048 in. (2 to 120 μm) with about 80% by volume of the powder having diameters ranging from 0. 0003 to 0. 0023 in. (6 to 58 μm).

Phenolic Microballoons

The properties of the Microballoons as published by the manufacturer are given in the following table:

Property	Property value
Density (liquid displacement	15.6 lb/ft^3 (250 kg/m^3)
Density (air displacement)	18.7 lb/ft^3 (300 kg/m^3)
Flotation in toluene dupanol solution	Not less than 90% must float
Average particle size (dia)	0.0017 in. (43 μm)
Size range (dia)	0.002 to 0.0005 in. (13 to 51 μm)

Measurements with the Coulter Counter indicate that the range of diameters of the phenolic Microballoons is 0.0004 to 0.0100 in. (10 to 250 μm), with approximately 85% by volume of the Microballoons having diameters ranging from 0.0024 to 0.0080 in. (60 to 200 μm).

Nylon

Properties of the nylon powder as given by the manufacturer are listed in the table below:

Property	Property value
Specific Gravity	$1.3 - 1.15$
Melting Point	$482 - 500°$F ($523 - 533°$K)
Tensile Strength	$11,800$ psi (81.4 MN/m^2)
Coefficient of Linear Thermal Expansion	45.0×10^{-6} in./in. - °F (81.1×10^{-6} m/m - °K)
Thermal Conductivity	1.31×10^{-4} Btu-in./ft^2-sec-°F 0.068 W/m - °K
Specific Heat	$0.3 - 0.5$ Btu/lb - °F 1.25 to 2.09 kJ/kg - °K

Preliminary studies using a Coulter Counter indicate that about 85% by volume of the nylon powder lies in the range from about 0.0012 to 0.0157 in. (30 to 400 μm) in diameter, with about 5% below 30 μm and 10% above 400 μm.

APPENDIX B

APPARATUS FOR THE DETERMINATION OF PERMEABILITY

The flow of gas through a material can be of two different types, Knudsen (molecular) flow which is governed by the relation[1]

$$q = \frac{K_m \, (\Delta P) \, A \sqrt{RT}}{PL} \tag{1}$$

and Poiseuille (viscous) flow, which is described[1] by

$$q = \frac{K_\nu \, (\Delta P) \, \frac{1}{2} (P_2 + P_1) \, A}{PL \, \eta}$$

where

q	= volume flow rate measured at absolute pressure P
ΔP	= pressure drop across the specimen
A	= area of the specimen normal to the flow of gas
L	= length of the specimen parallel to the flow of gas
R	= gas constant of the gas
T	= absolute temperature
η	= viscosity of the gas
$\frac{1}{2} (P_2 + P_1)$	= average absolute pressure on the specimen
K_m	= molecular permeability coefficient
K_ν	= viscous permeability coefficient

For those cases where neither equation fully describes the gas flow, the flow is both molecular and viscous and the expressions for both types of flow are combined which yields:

$$q = \left(K_0 \sqrt{RT} + K_1 \frac{P_m}{\eta} \right) \frac{A \, \Delta P}{PL} \tag{3}$$

---

[1] Barrer, R. M., Diffusion In and Through Solids, Cambridge University Press, Cambridge, pp 60-61, 1951.

where K_0 and K_1 are permeability coefficients similar to K_m and K_ν, respectively, and $P_m = \frac{1}{2} (P_2 + P_1)$.

To evaluate the coefficients K_0 and K_1, let

$$K_{m\nu} = K_0 \sqrt{RT} + K_1 \frac{P_m}{\eta} \tag{4}$$

Equation (3) may then be written

$$q = K_{m\nu} \frac{A \Delta P}{PL} \tag{5}$$

or

$$K_{m\nu} = \frac{PLq}{A \Delta P} \tag{6}$$

$K_{m\nu}$, often called the admittance, can then be determined for the specimen at any pressure by measurement of the flow rate q at that pressure. Values of $K_{m\nu}$ for several different pressures can then be plotted versus P_m and, as seen from equation (4), the resulting line will have a slope of K_1/η and a zero intercept of $K_0 \sqrt{RT}$. Thus, K_1 and K_0 can be determined from the properties of the gas used.

If metric units are used throughout equation (3), K_0 will be in cm and K_1 in cm^2.

These coefficients should be dependent only on the structure of the material; that is, independent of specimen configuration, viscosity and molecular weight of the gas, temperature, pressure gradient, and the average pressure.

The data required to calculate the admittance ($K_{m\nu}$) are pressure at the flowmeter (P), indicated flow rate at the flowmeter (q), thickness of specimen (L), area (A), and pressure drop across the specimen (ΔP). For cases where the temperature of the specimen is at room temperature or the same temperature as the flowmeter, the product of Pq measured at the meter is equal to the product Pq at the specimen, since from continuity

$$W = \rho\, AV = \rho\, q = \text{constant} \tag{7}$$

For a perfect gas,

$$\rho = \frac{P}{RT} \tag{8}$$

Therefore, from (7), equating conditions at the specimen and the flowmeter

$$\rho_s\, q_s = \rho_m\, q_m \tag{9}$$

where the subscripts s and m refer to the specimen and meter, respectively.

Substituting from (8)

$$\frac{P_s}{RT_s}\, q_s = \frac{P_m}{RT_m}\, q_m \tag{10}$$

Therefore, for isothermal flow

$$P_s\, q_s = P_m\, q_m \tag{11}$$

If the temperatures at the specimen and meter are different, then the term $P_m\, q_m$ (Pq in equation 6) must be multiplied by the ratio $\dfrac{T_s}{T_m}$.

A schematic of the apparatus being used for the determinations of the permeability coefficients is shown in Figure 1. The primary side of the specimen is exposed to desired gage pressures which can be measured by a laboratory gage or a U tube manometer. Since the secondary side of the specimen is exposed to atmospheric pressure or a known pressure, the pressure drop across the specimen is readily obtained. The flow of gas is measured at the exit side of the specimen with either a bubble flowmeter, for which a stopwatch is employed to measure the displacement time of a soap bubble, or a wet test flowmeter. The bubble flowmeter operates at atmospheric pressure, and the wet test meter operates at a slightly higher pressure which is monitored.

For specimen materials that can be machined with good tolerance, the brass assembly containing the specimen is shown in Figure 2. The 1 inch diameter x $\frac{1}{2}$ inch thick specimen is placed on the $\frac{1}{64}$ inch shoulders and sealed by filling the annulus around the specimen with the sealer material. For porous and weaker structured materials, the specimens are mounted and sealed in the brass assembly shown in Figure 3. For this assembly, the specimens can be roughly machined in the form of a disc of approximately 1 inch diameter.

Several types of sealants were investigated for room temperature use with Dow Corning Silastic RTV 731 giving the best results. This material is viscous and can be applied easily. It wets the specimen well and provides an excellent seal after curing to a solid rubbery form. The system is thoroughly purged before securing the specimen assembly.
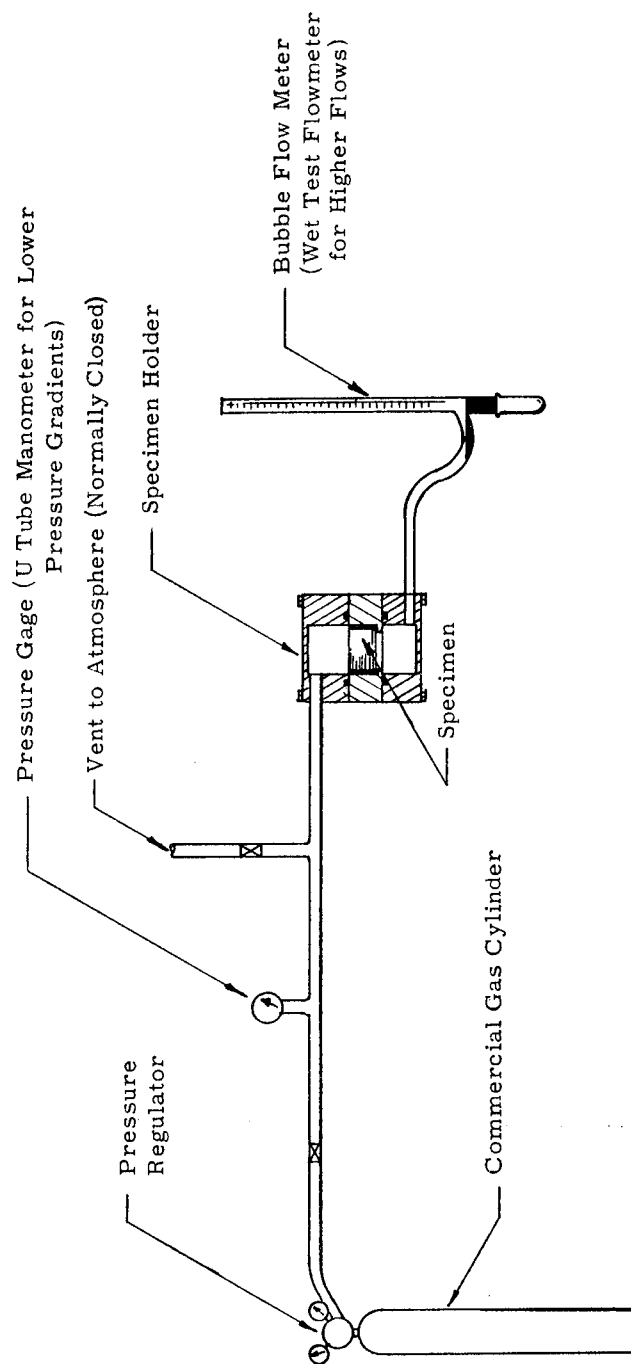
Figure B1. Schematic of the Permeability Apparatus

66
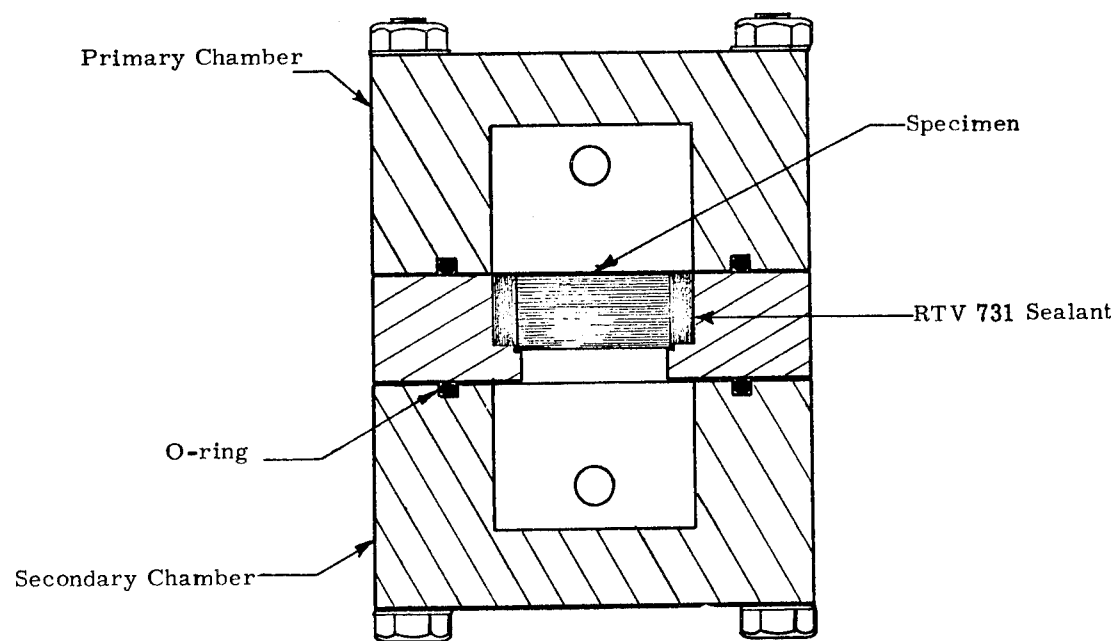
Figure B2.   Permeability Specimen Assembly

67
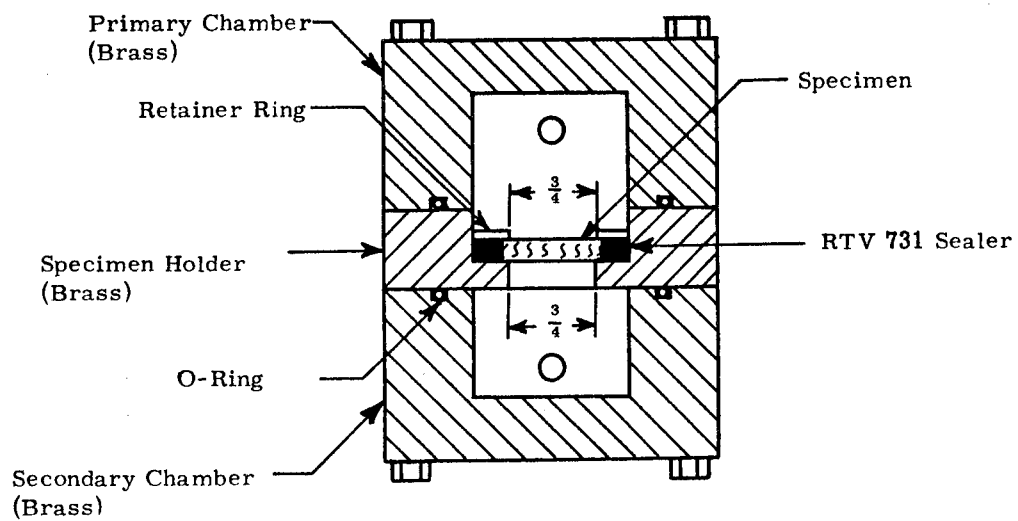
Figure B3. Permeability Specimen Assembly

- Primary Chamber (Brass)
- Retainer Ring
- Specimen Holder (Brass)
- O-Ring
- Secondary Chamber (Brass)
- Specimen
- RTV 731 Sealer

Dimensions: $\frac{3}{4}$, $\frac{3}{4}$

APPENDIX C

STRESS-STRAIN CURVES IN TENSION AND COMPRESSION
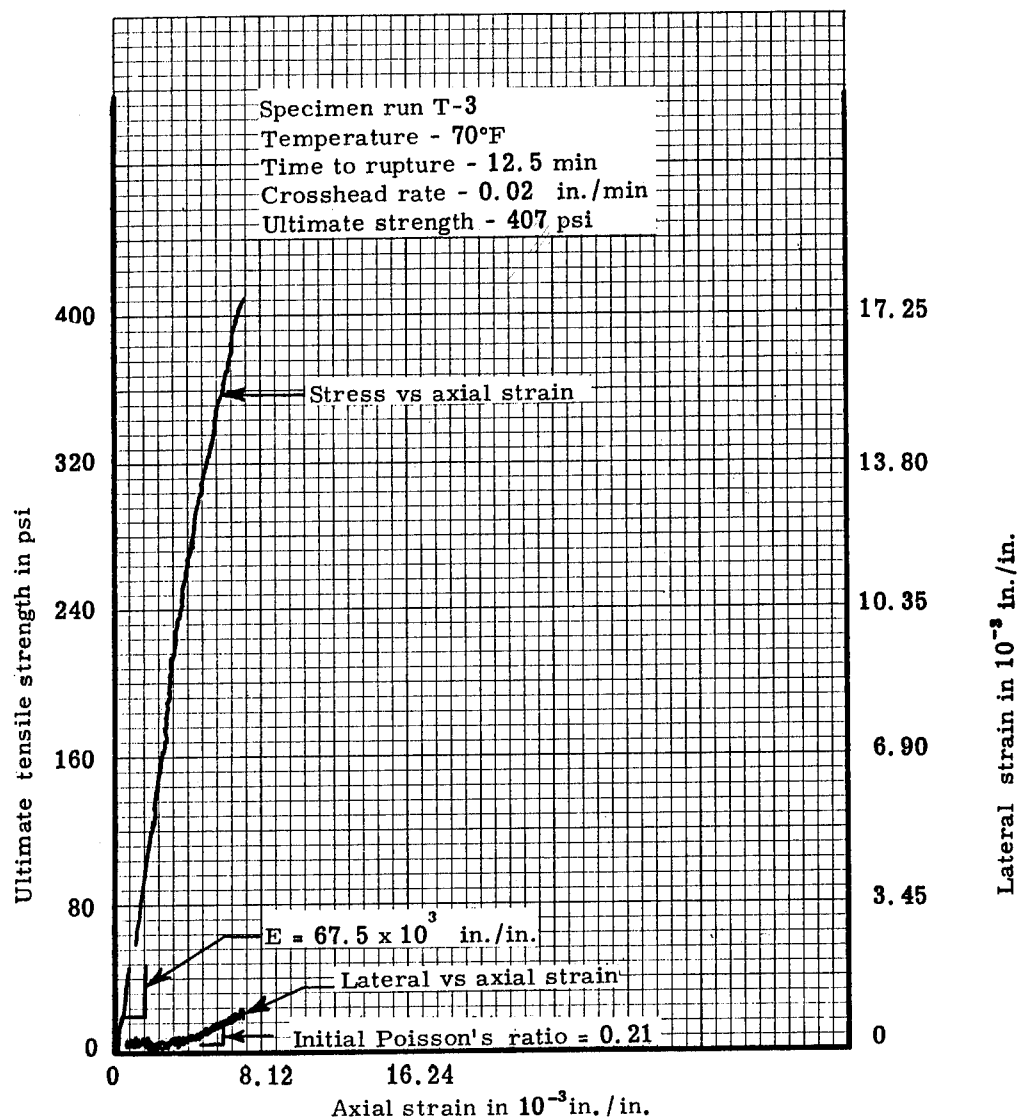
Figure C1. Axial tensile stress-strain and bi-directional strains at 70°F for a virgin low-density phenolic-nylon
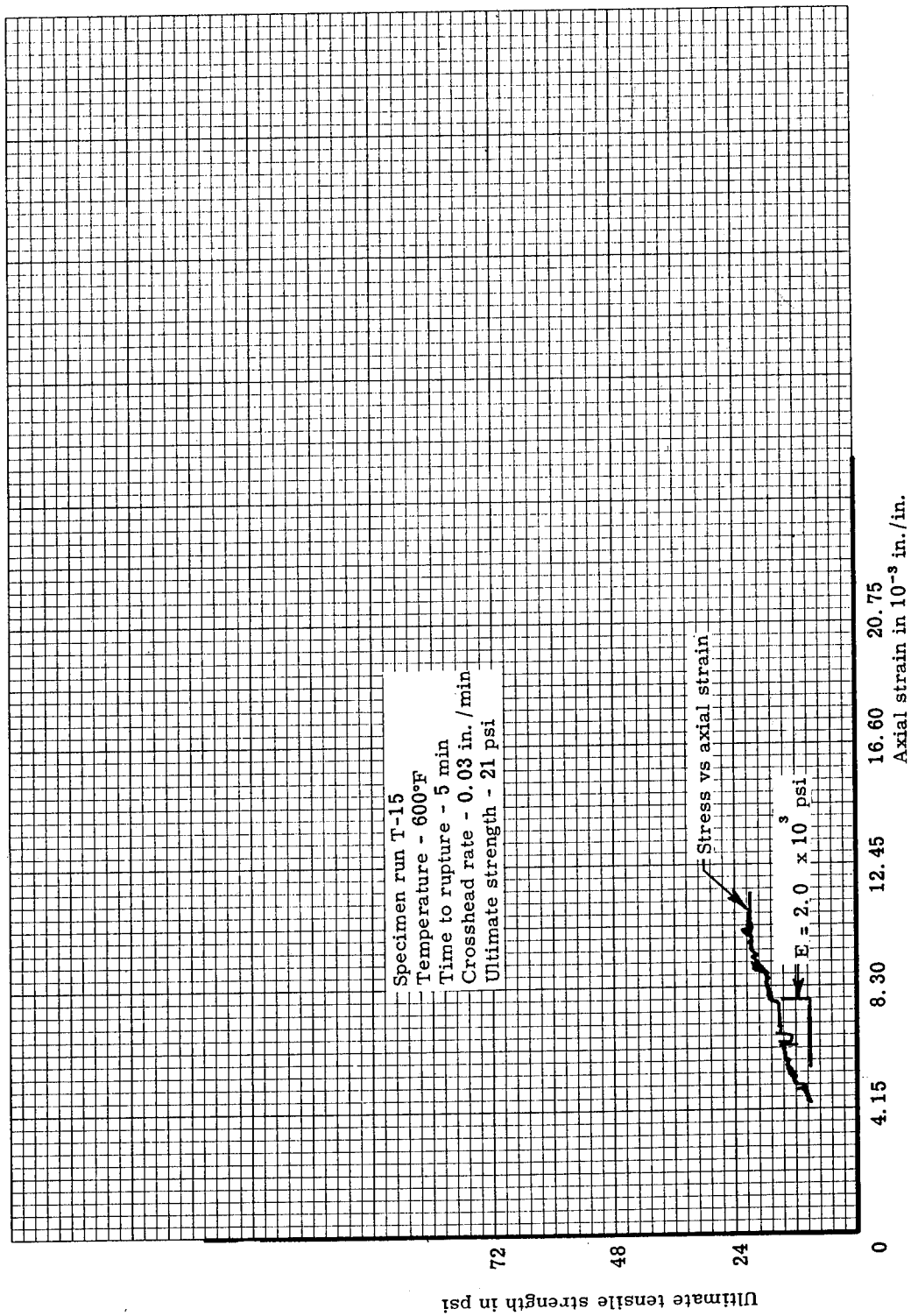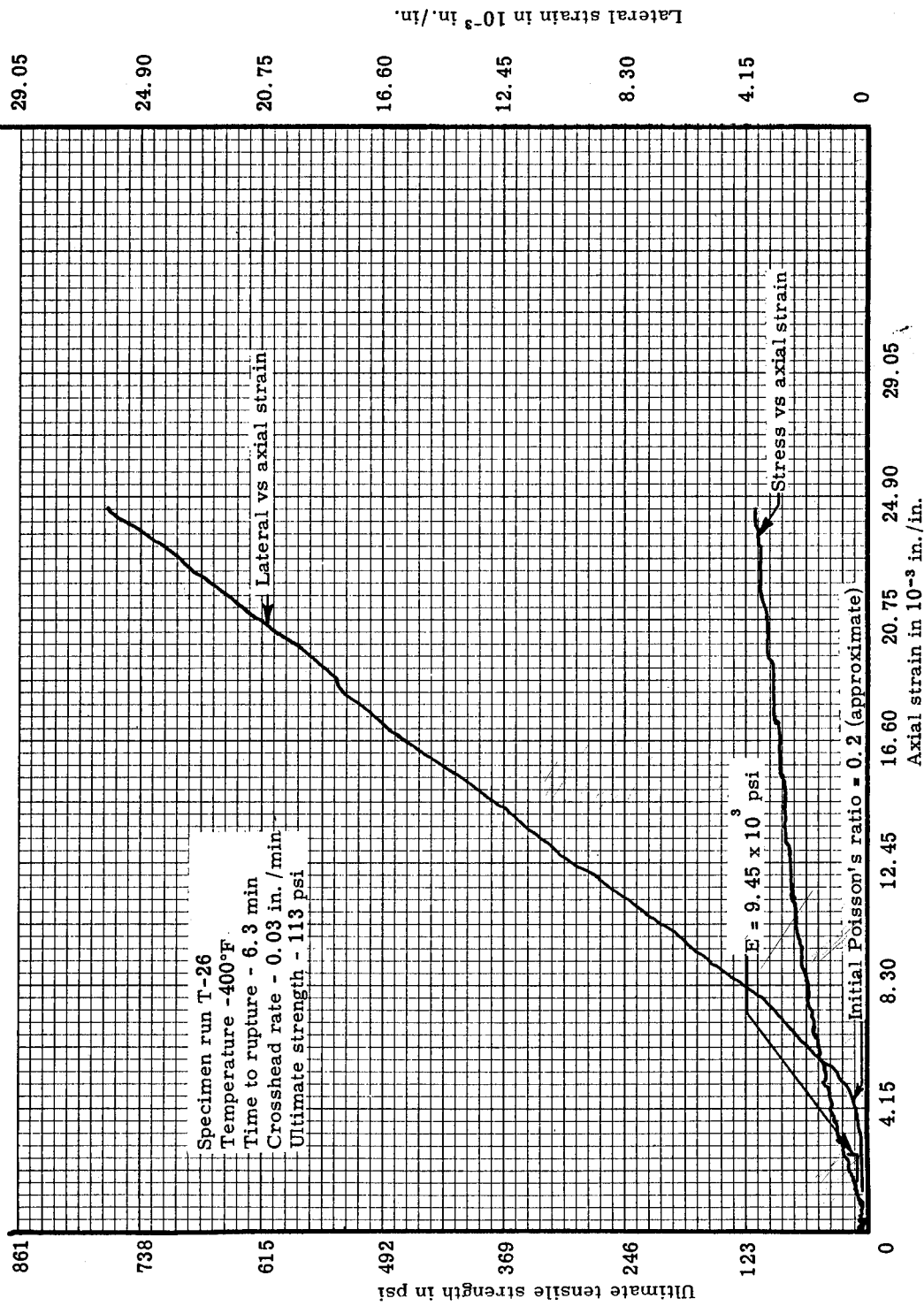
70
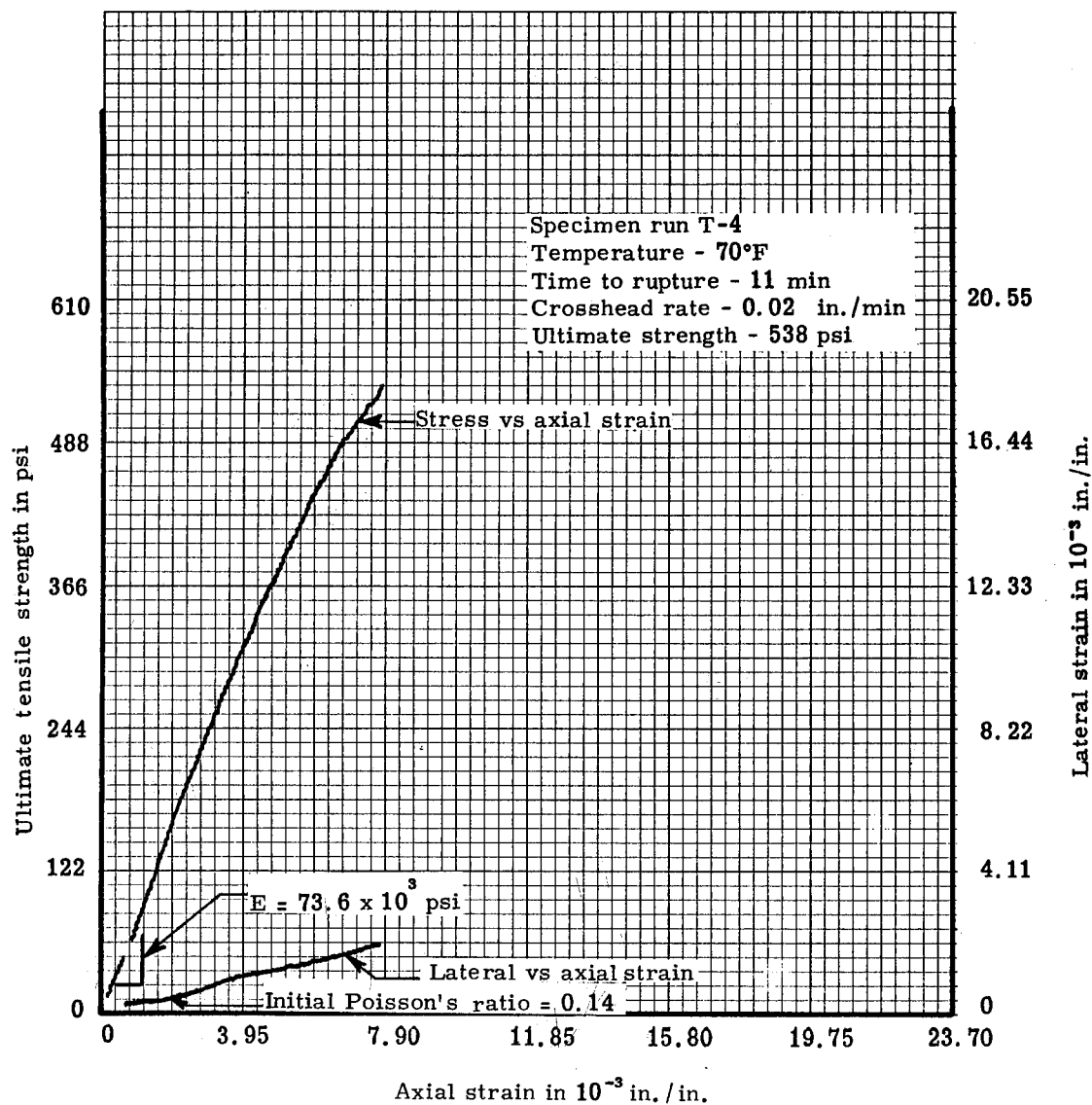
Figure C2. Axial tensile stress-strain and bi-directional strains at 70°F
for a virgin low-density phenolic-nylon
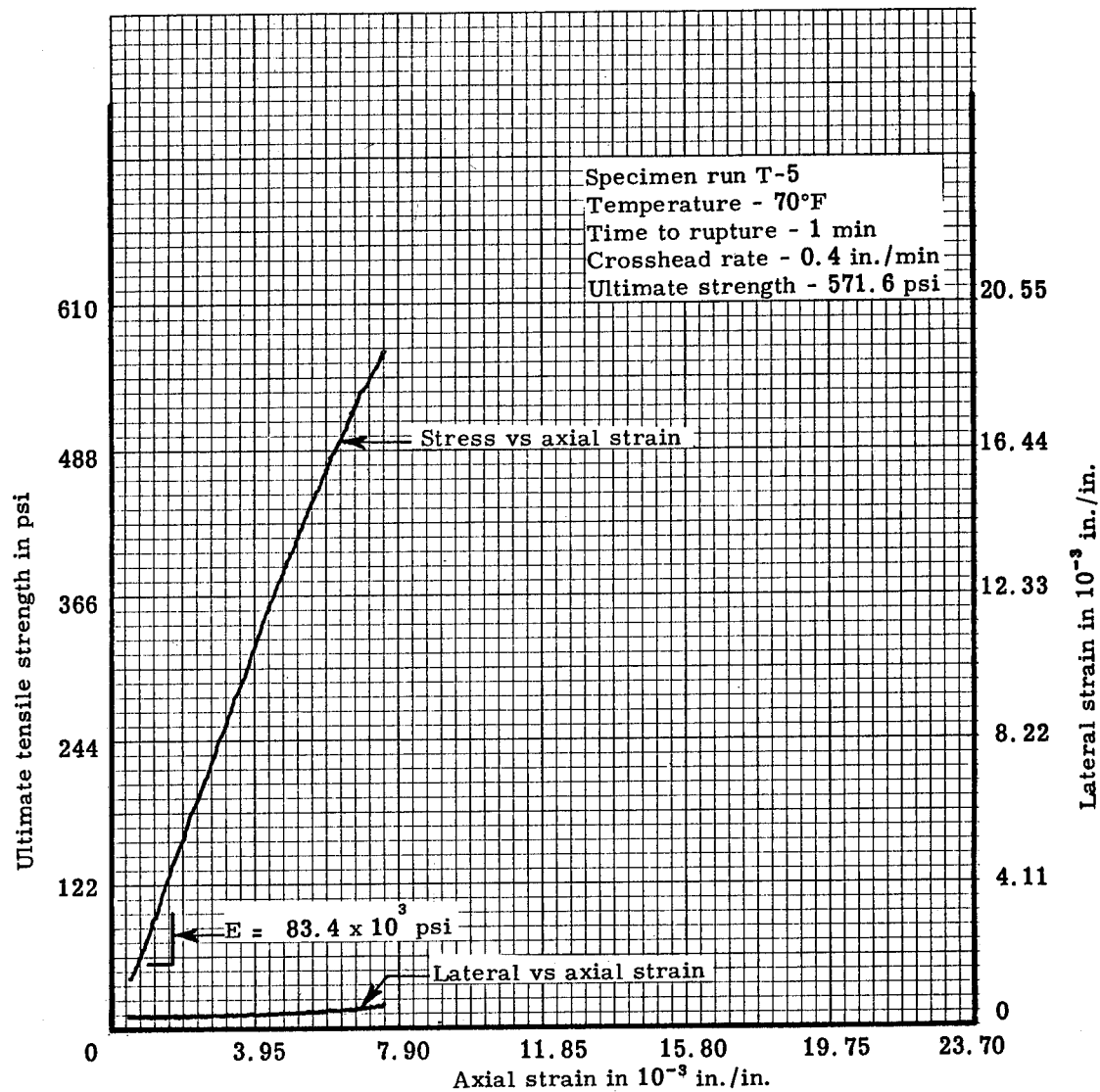
Figure C3. Axial tensile stress-strain and bi-directional strains at 70°F for a virgin low-density phenolic-nylon
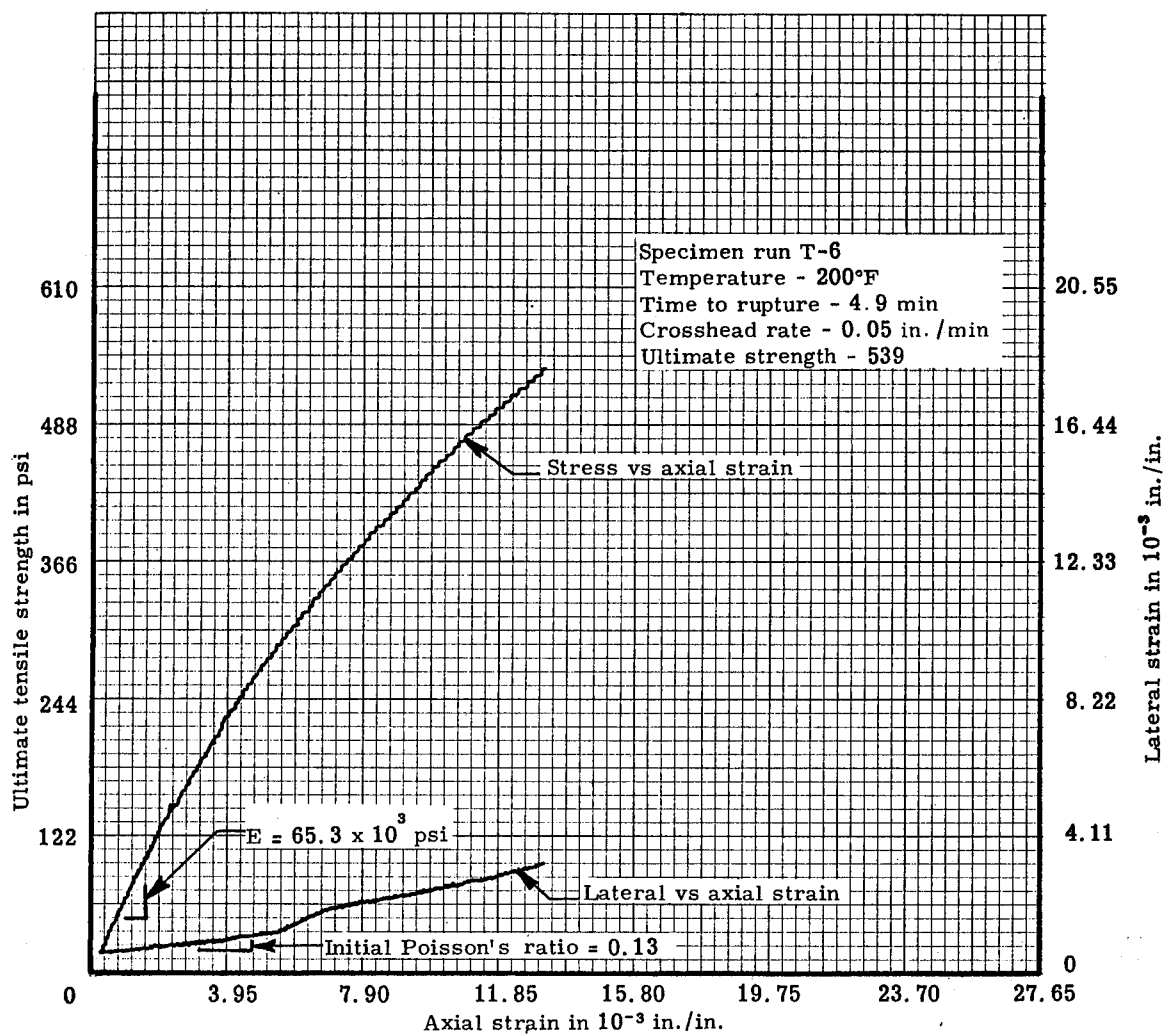
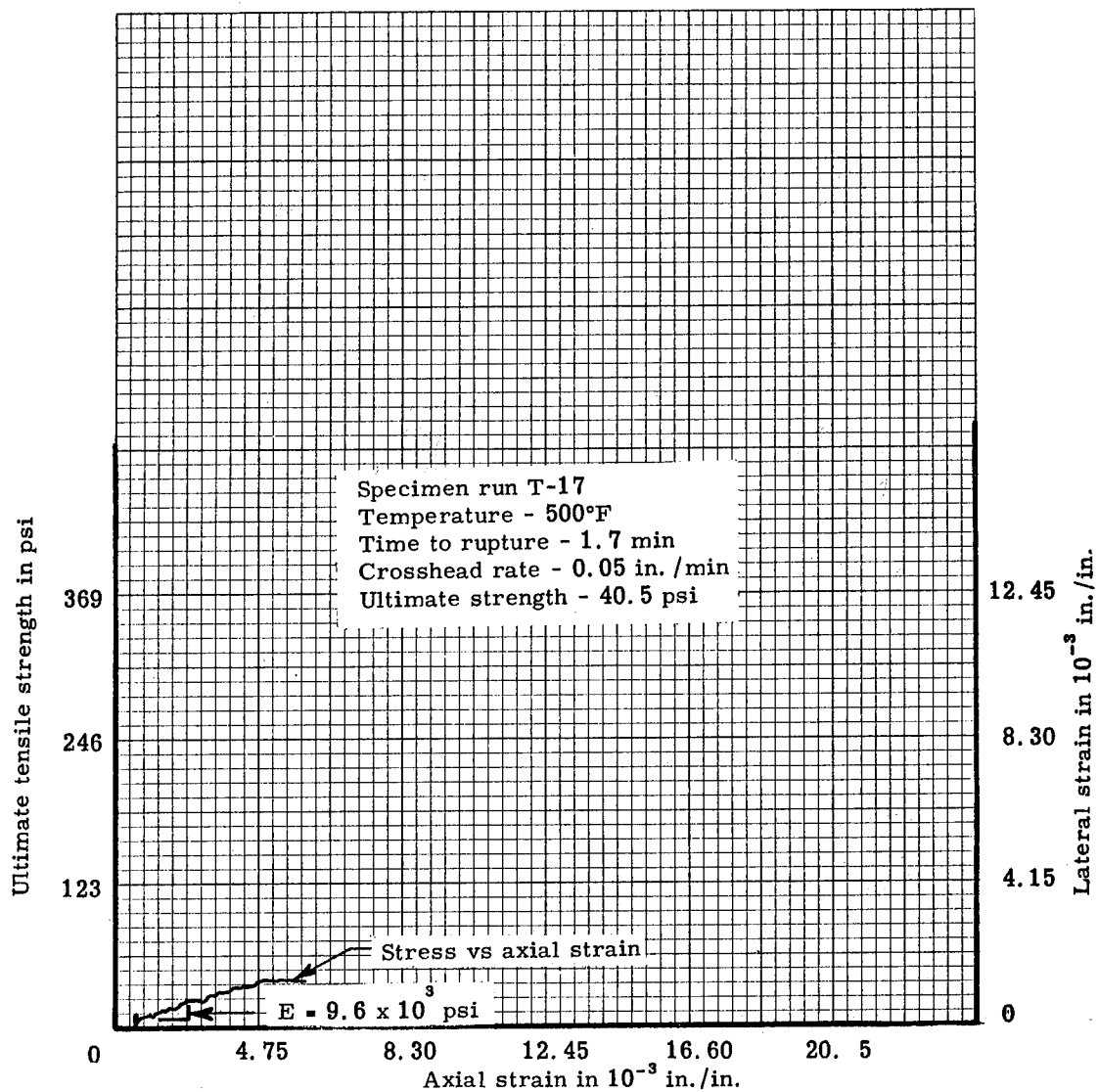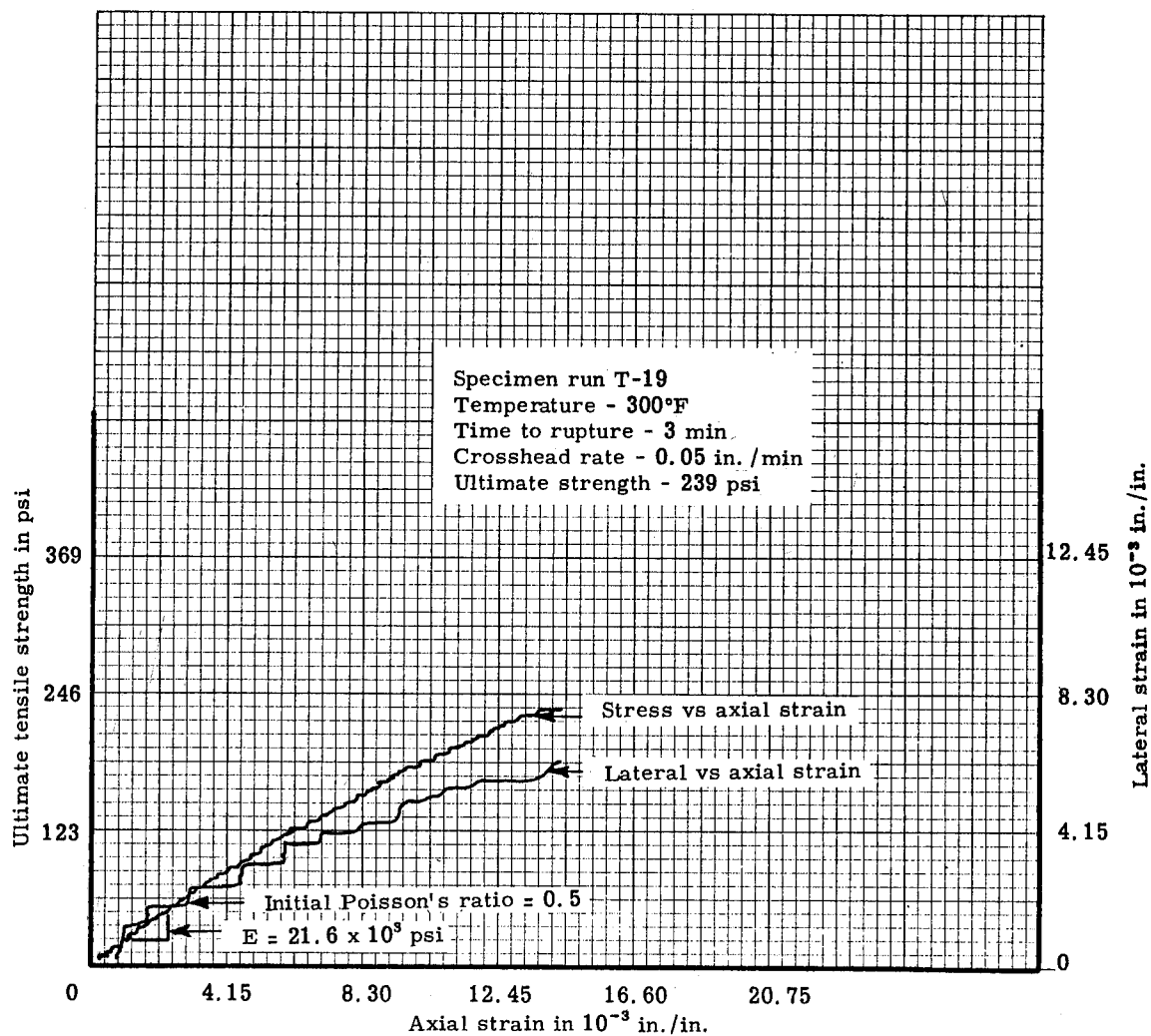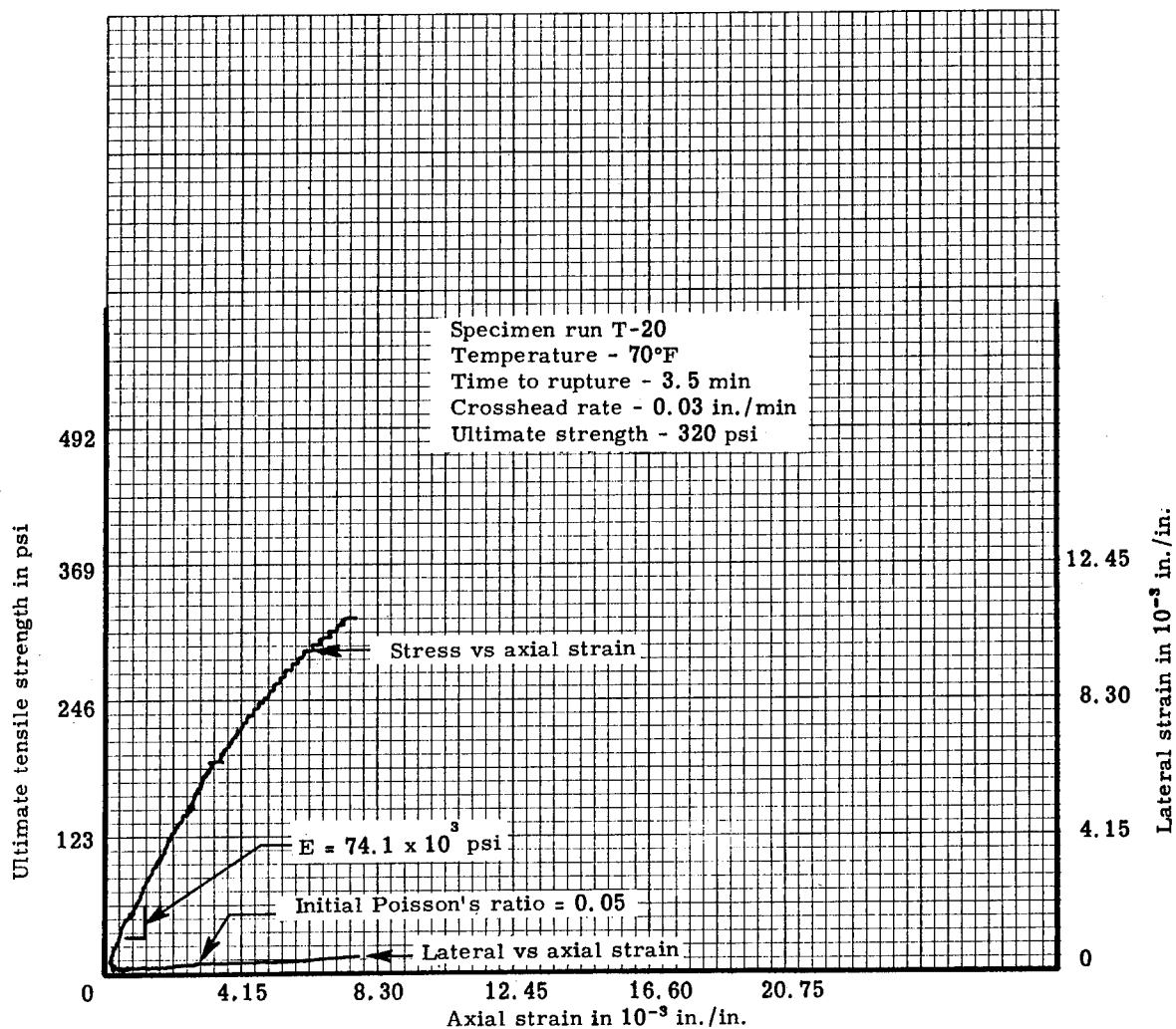Figure C4. Axial tensile stress-strain and bi-directional strains at 200°F for a virgin low-density phenolic-nylon

Specimen run T-7
Temperature - 200°F
Time to rupture - 3 min
Crosshead rate - 0.05 in./min
Ultimate strength - 553 psi

Stress vs axial strain

$E = 79.2 \times 10^3$ psi

Lateral vs axial strain

Initial Poisson's ratio = 0.14

Ultimate tensile strength in psi

610

488

366

244

122

0   3.95   7.90   11.85   15.80   19.75   23.70   27.65

Axial strain in 10^{-3} in./in.

Lateral strain in 10^{-3} in./in.

20.55

16.44

12.33

8.22

4.11

0
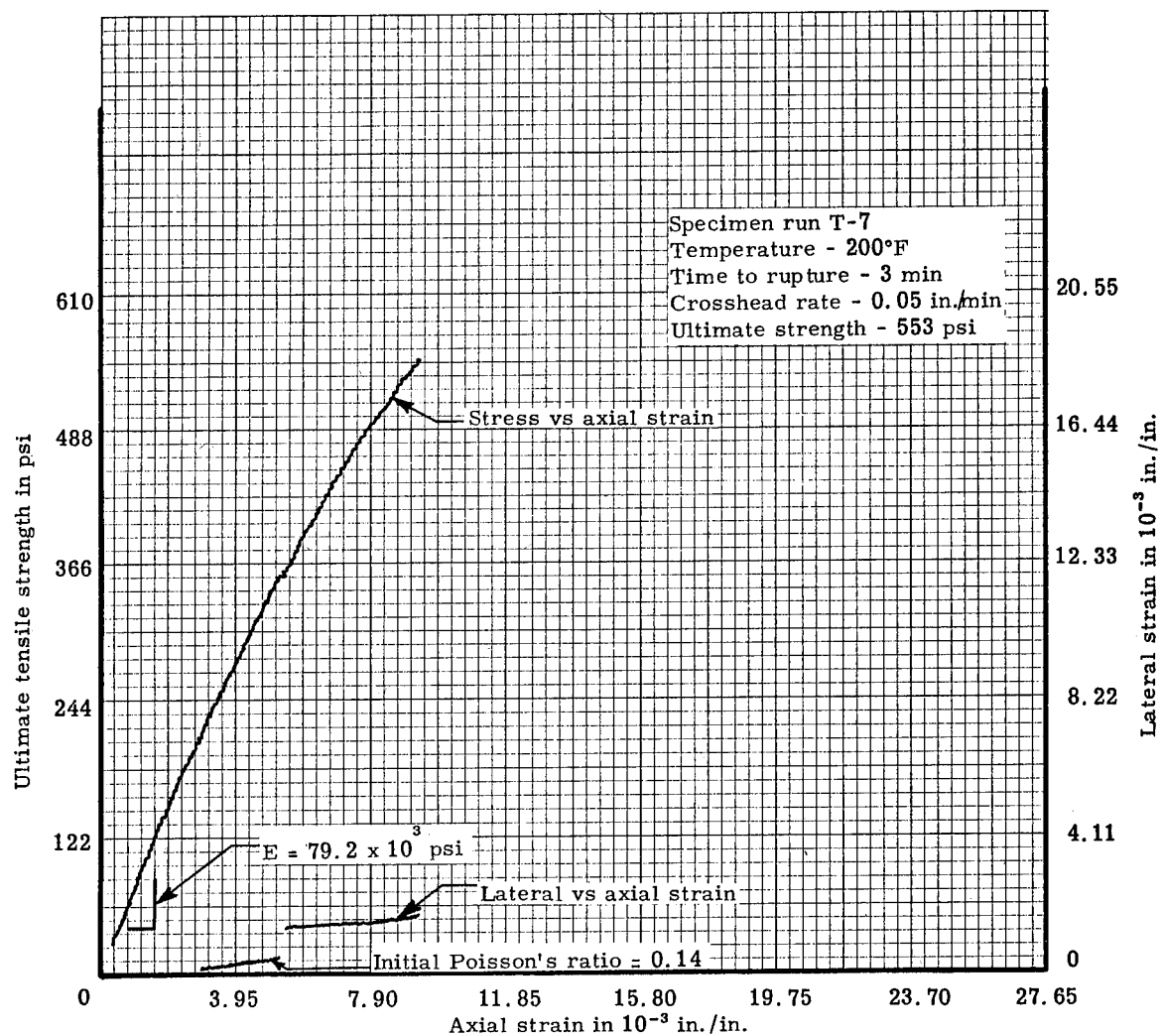
Figure C5. Axial tensile stress-strain and bi-directional strains at 200°F for a virgin low-density phenolic nylon

Specimen run T-8
Temperature - 300°F
Time to rupture - 4 min
Crosshead rate - 0.05 in./min
Ultimate strength - 147 psi

Stress vs axial strain

$E = 21.4 \times 10^3$ psi

Ultimate tensile strength in psi

366

244

122

0

3.95   7.90   11.85   15.80

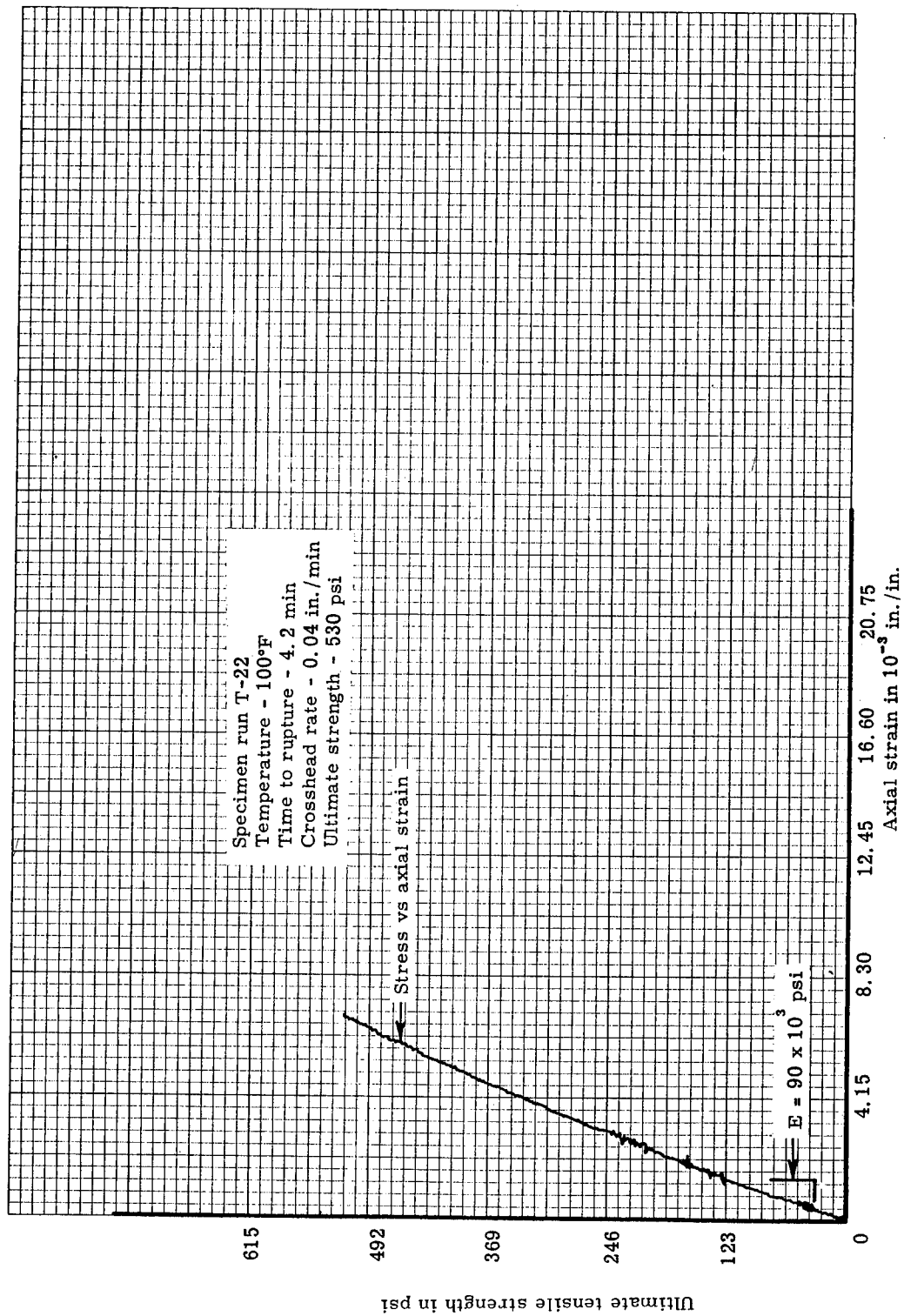Axial strain in 10^{-3} in./in.
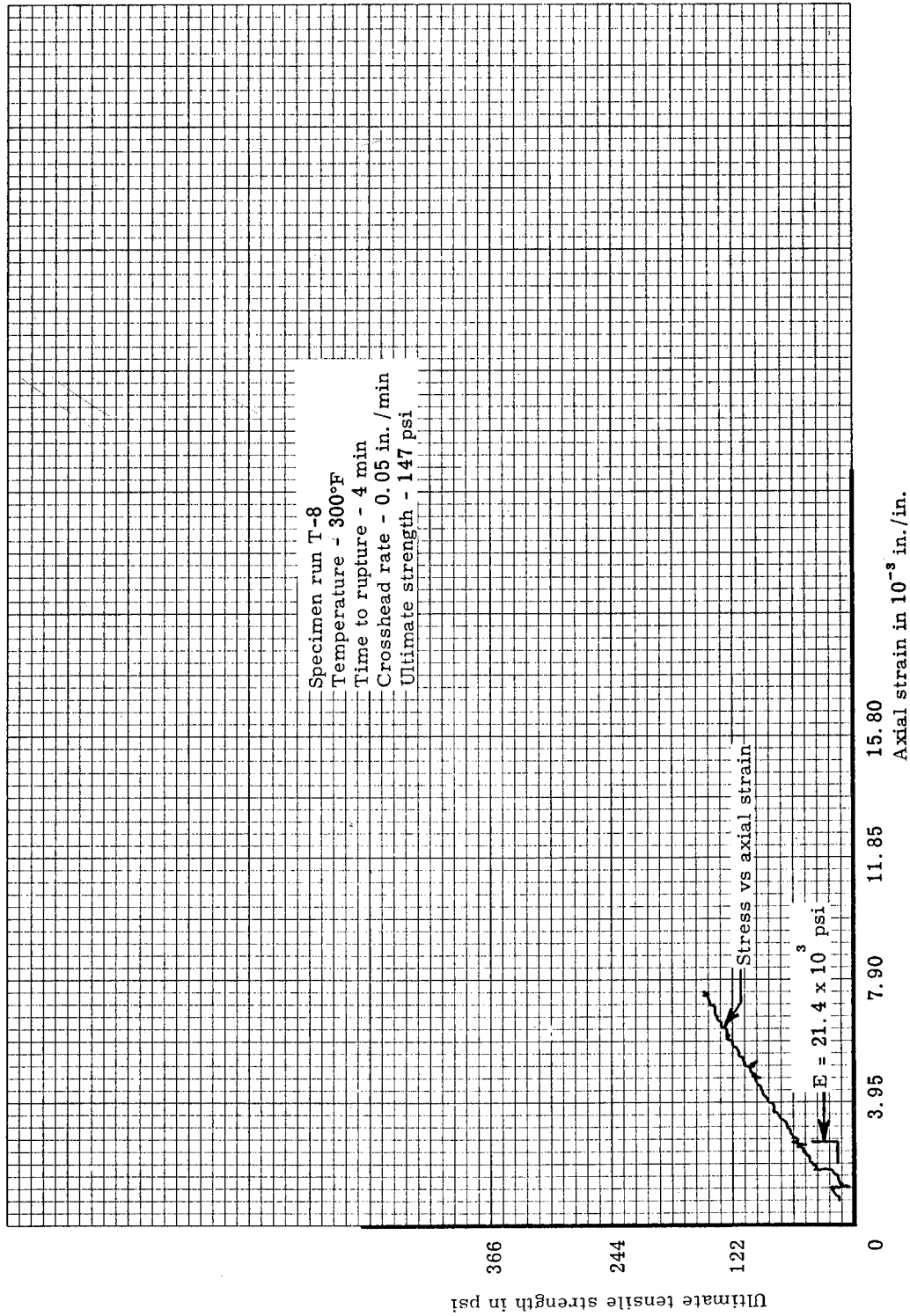
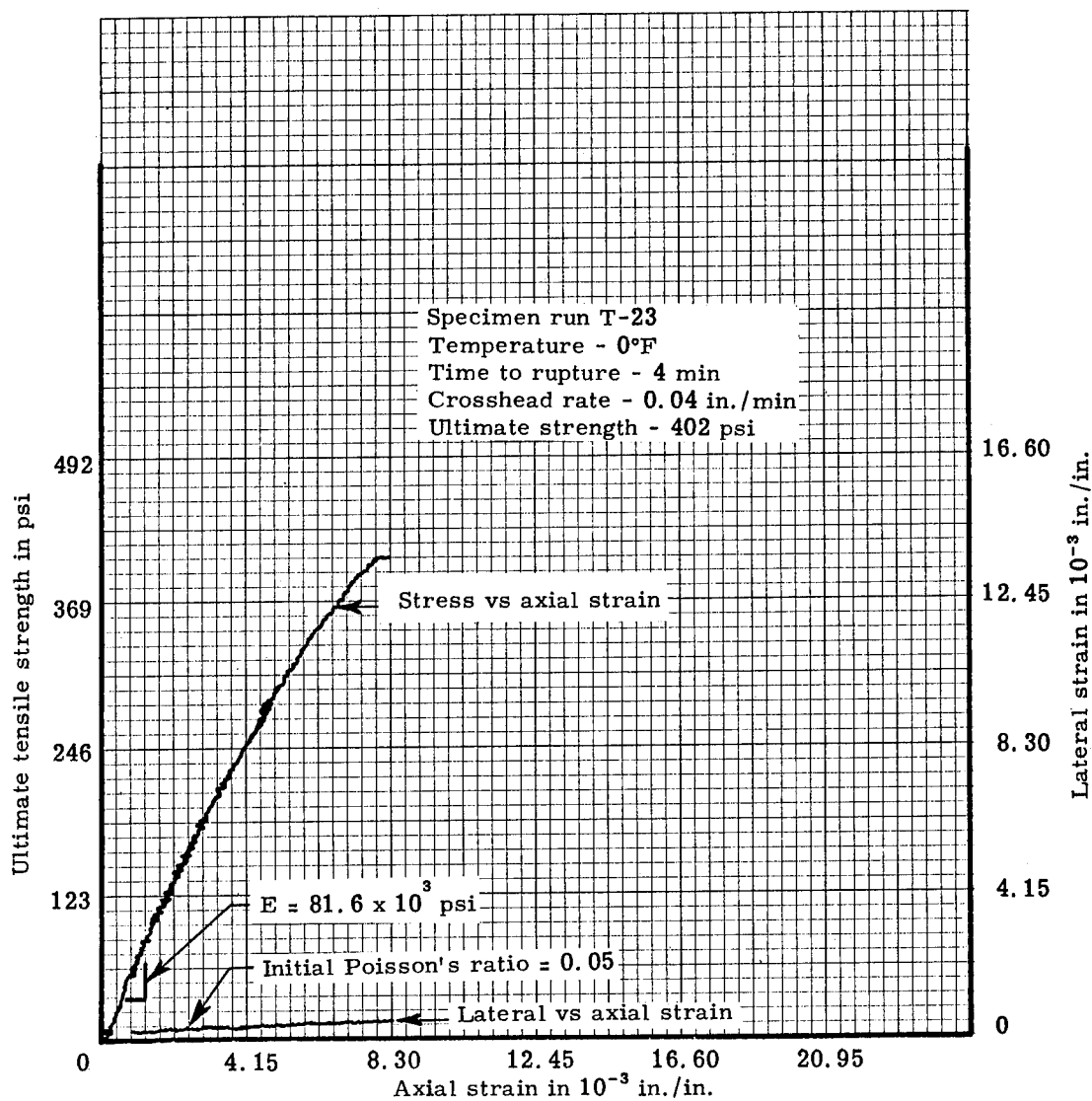Figure C6. Axial tensile stress-strain at 300°F for a virgin low-density phenolic-nylon

75
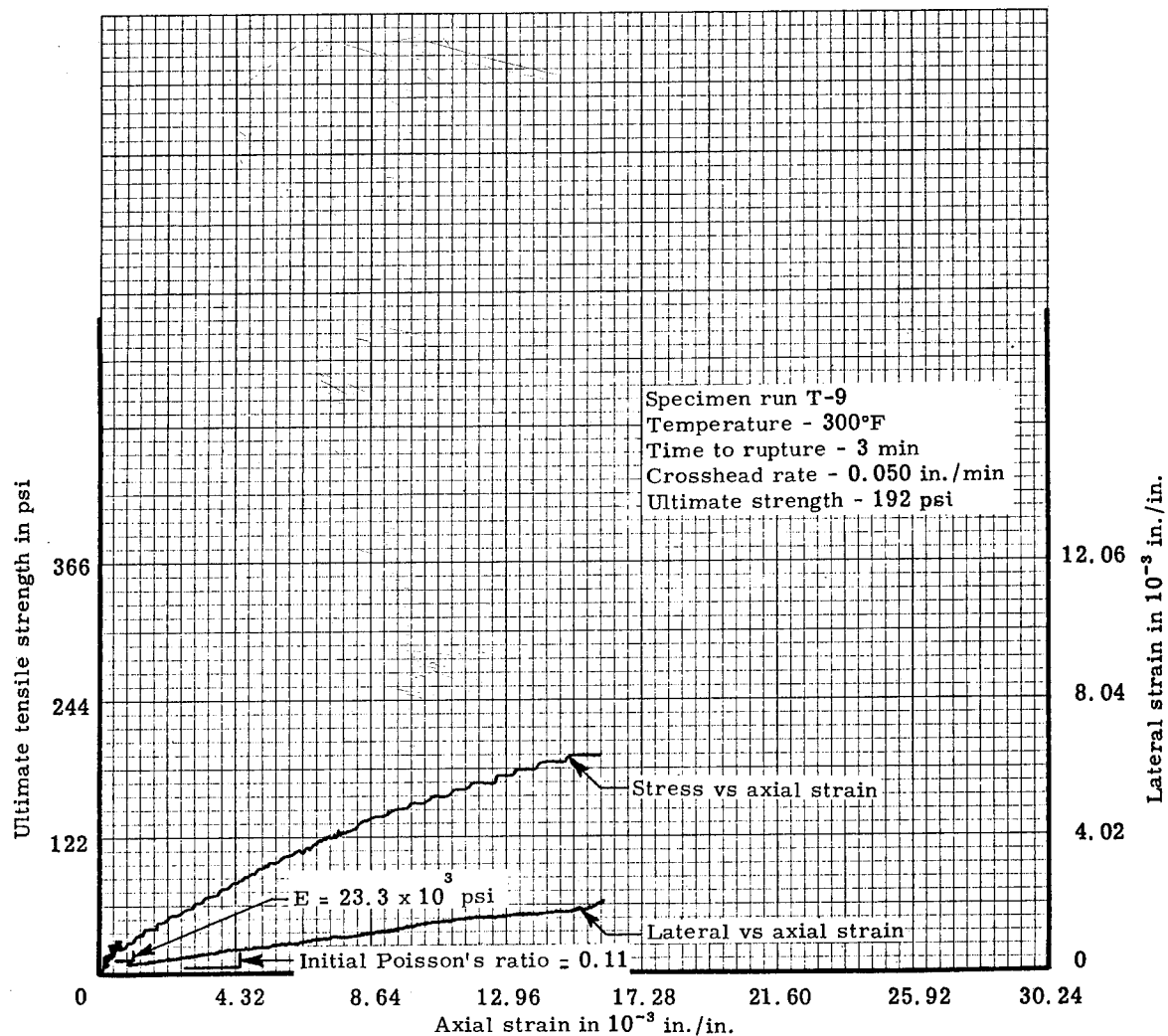
Figure C7. Axial tensile stress-strain and bi-directional strains at 300°F for a virgin low-density phenolic-nylon

Specimen run T-11
Temperature - 400°F
Time to rupture - 2.1 min
Crosshead rate - 0.05 in./min
Ultimate strength -139 psi

Stress vs axial strain

$E = 11.1 \times 10^3$ psi

Axial strain in 10^{-3} in./in.

Ultimate tensile strength in psi

246

123

0

4.15   8.30   12.45   16.60   20.75
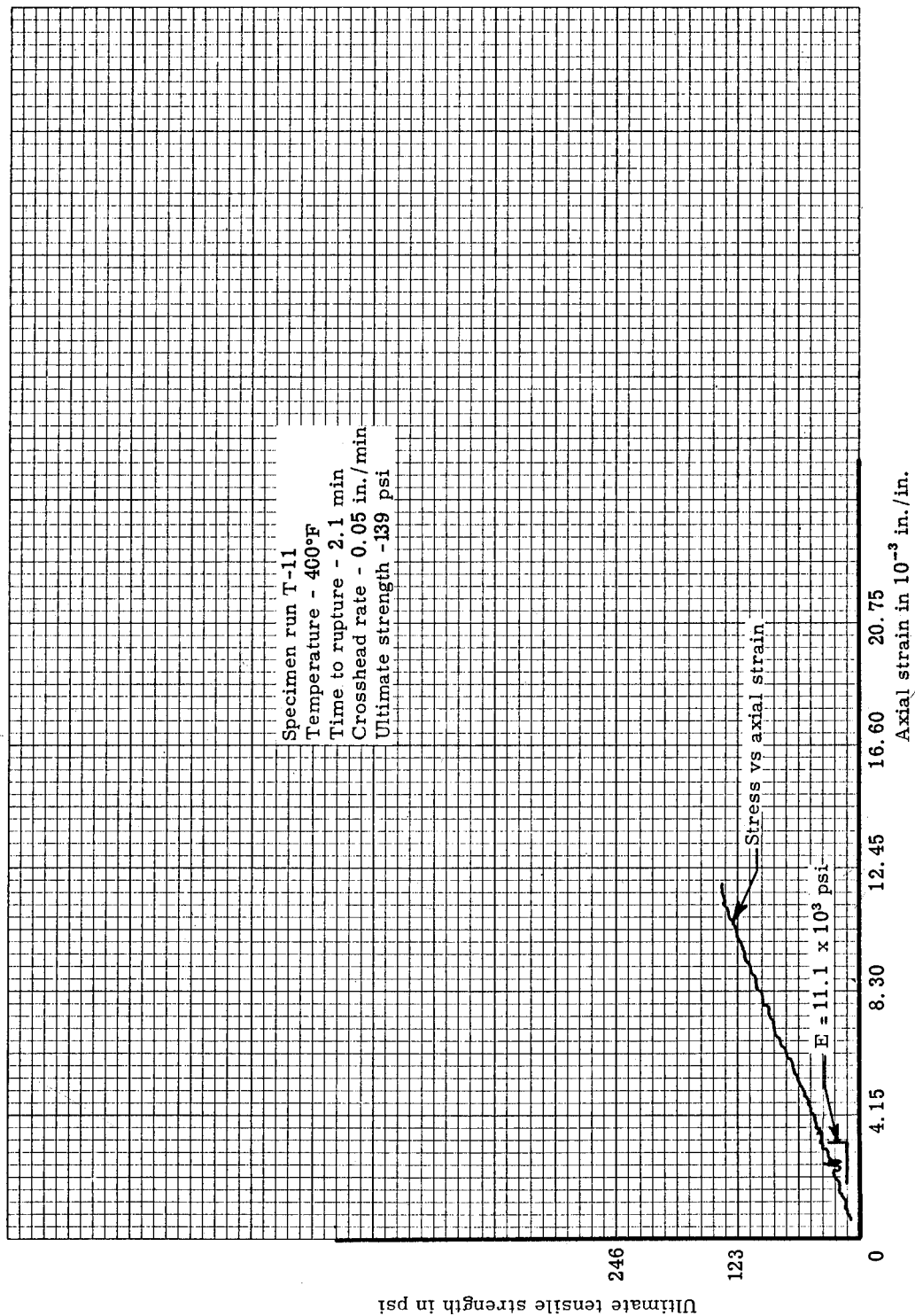
Figure C8.   Axial tensile stress-strain at 400°F for a virgin   low-density   phenolic-nylon

Specimen Run T-12
Temperature - 500°F
Time to rupture - 8.1 min
Crosshead rate - 0.05 in./min
Ultimate strength - 76 psi

Stress vs axial strain

E = 5.9 x 10³ psi

Ultimate tensile strength in psi

246

123

0

4.15   8.30   12.45   16.60   20.75

Axial strain in 10⁻³ in./in.
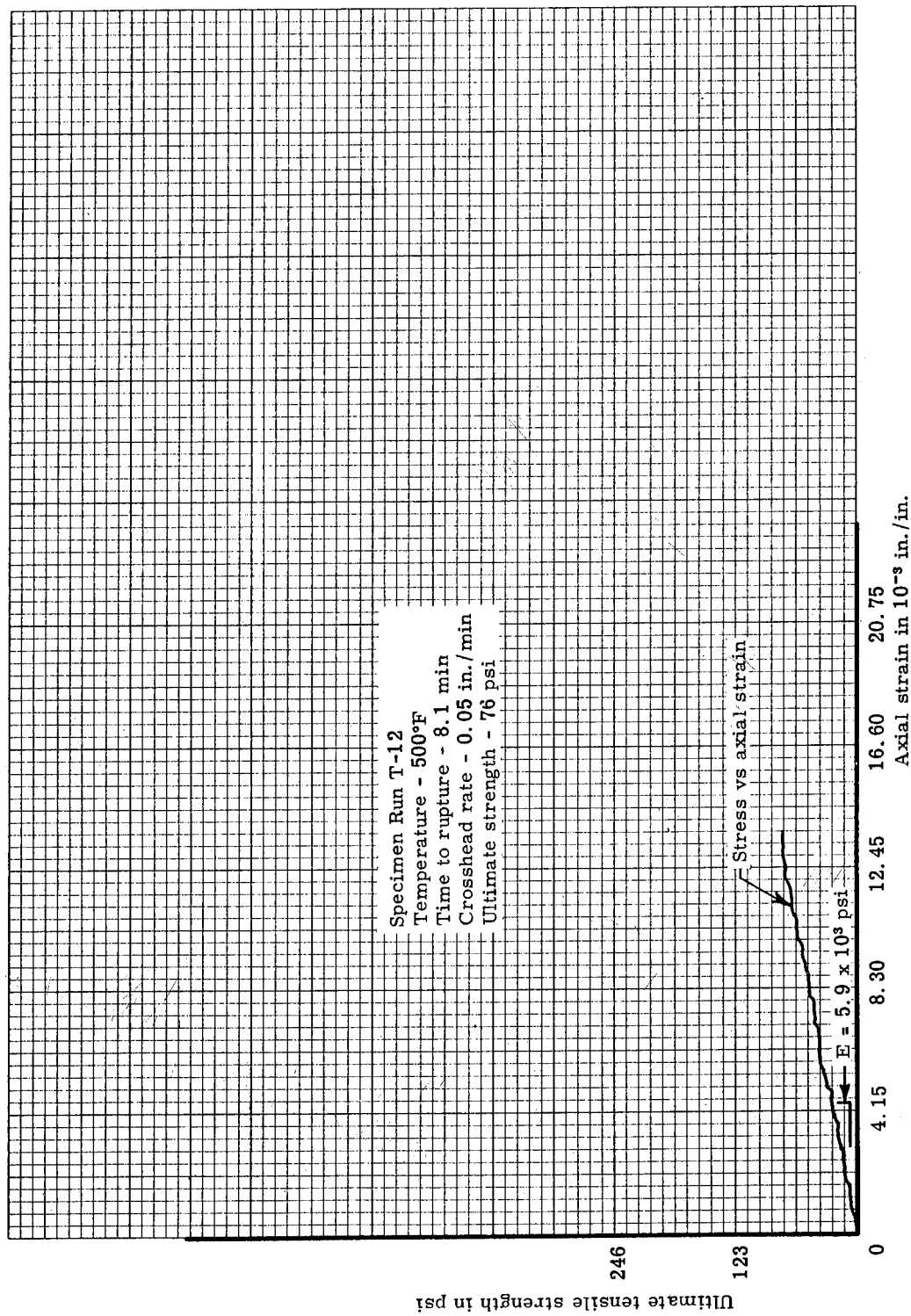
Figure C9. Axial tensile stress-strain at 500°F for a virgin low-density phenolic-nylon

Specimen run T-13
Temperature - 600°F
Time to rupture - 2.5 min
Crosshead rate - 0.03 in./min
Ultimate strength - 29.5 psi

Stress vs axial strain

$E = 3.55 \times 10^3$ psi

Ultimate tensile strength in psi

246

123

0   4.15   8.30   12.45   16.60   20.75

Axial strain in 10^{-3} in./in.
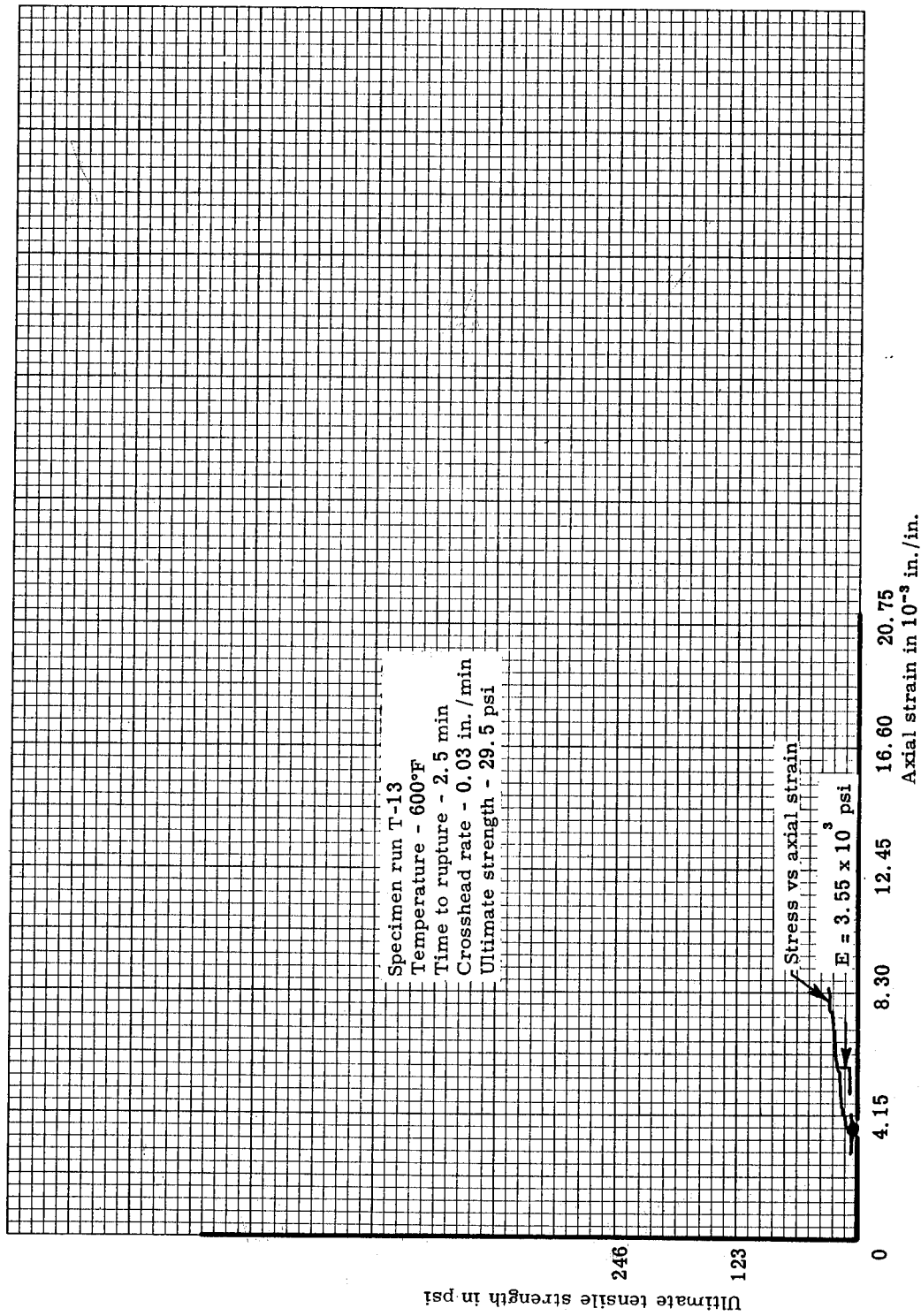
Figure C10. Axial tensile stress-strain at 600°F for a virgin low-density phenolic-nylon

79

Specimen run T-15
Temperature - 600°F
Time to rupture - 5 min
Crosshead rate - 0.03 in./min
Ultimate strength - 21 psi

Stress vs axial strain

$E = 2.0 \times 10^3$ psi

Ultimate tensile strength in psi

72   48   24   0

4.15   8.30   12.45   16.60   20.75

Axial strain in 10^{-3} in./in.

Figure C11. Axial tensile stress-strain at 600°F for a virgin low-density phenolic-nylon

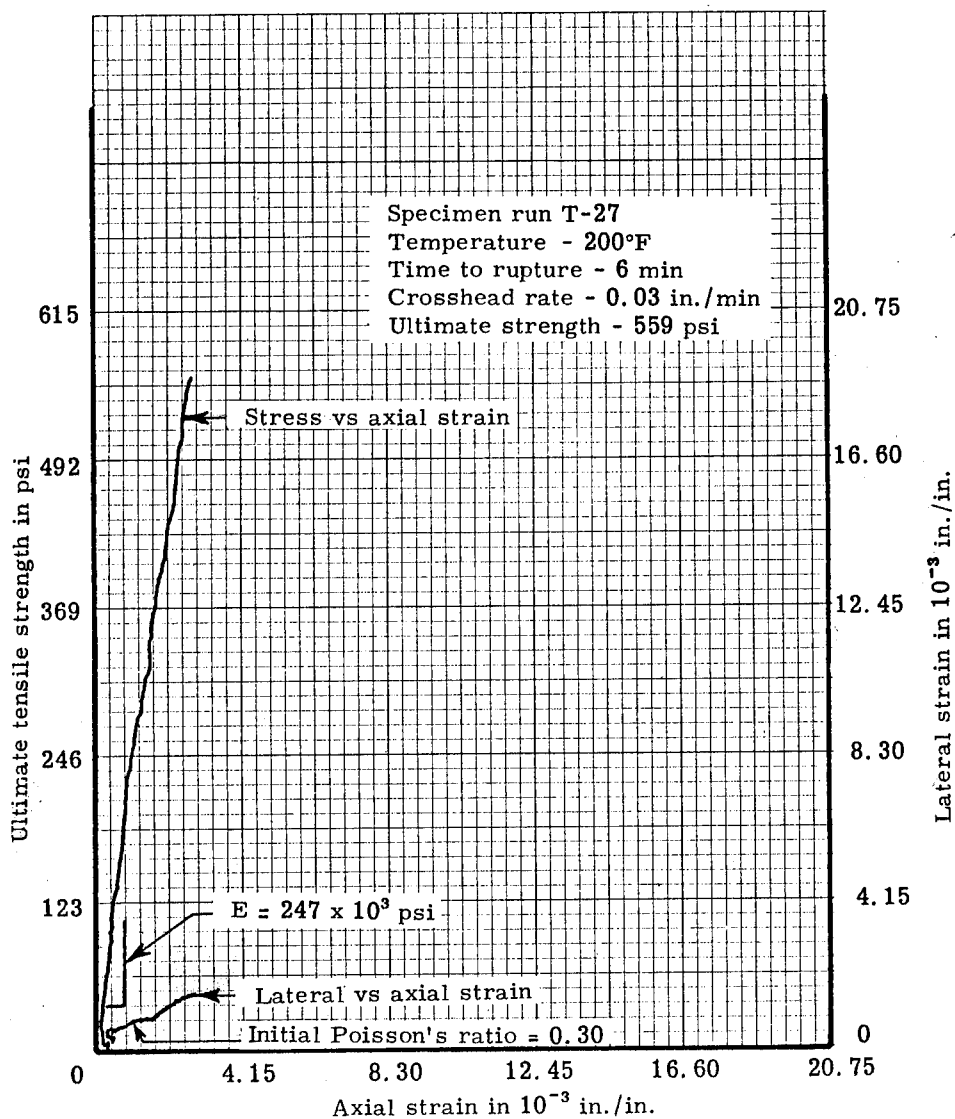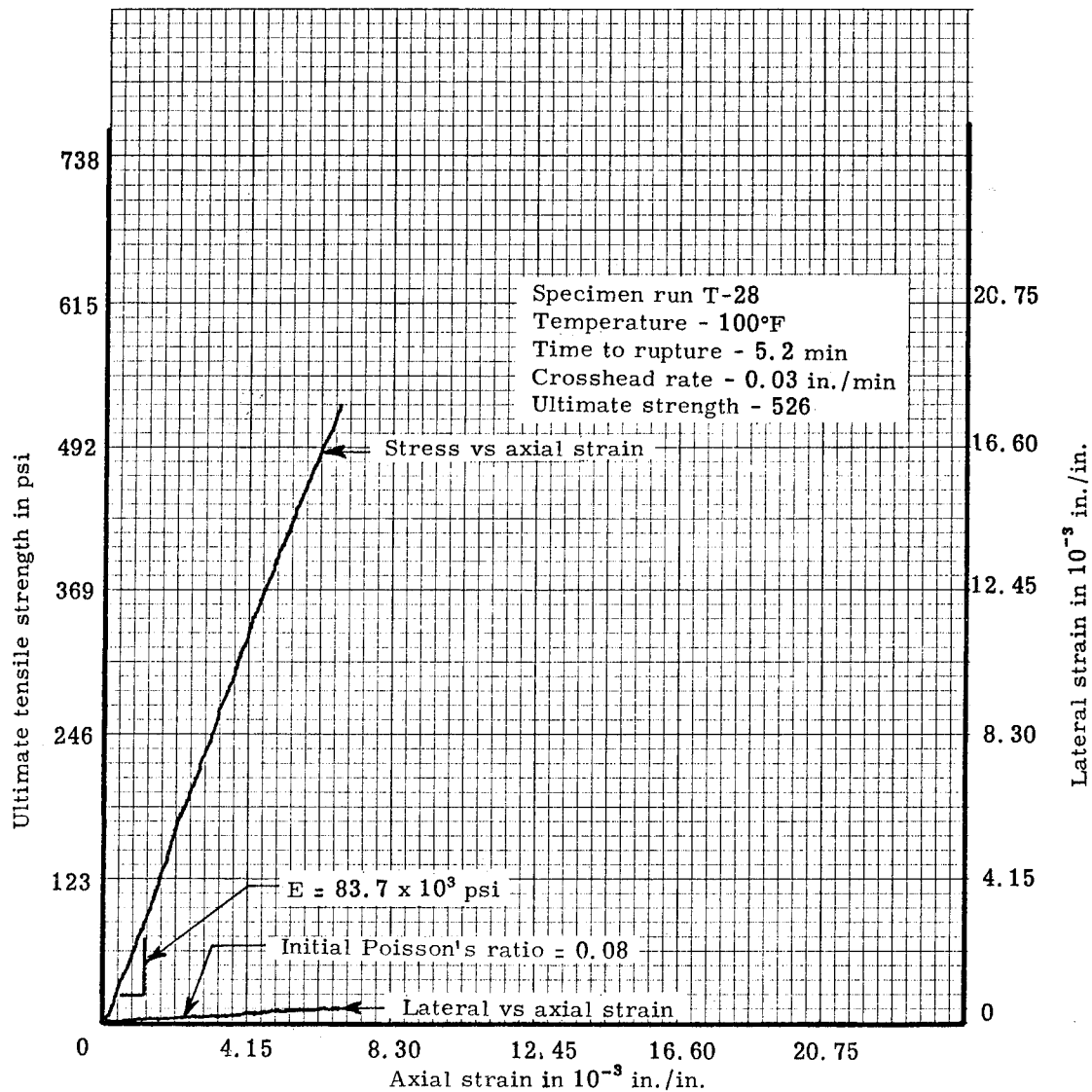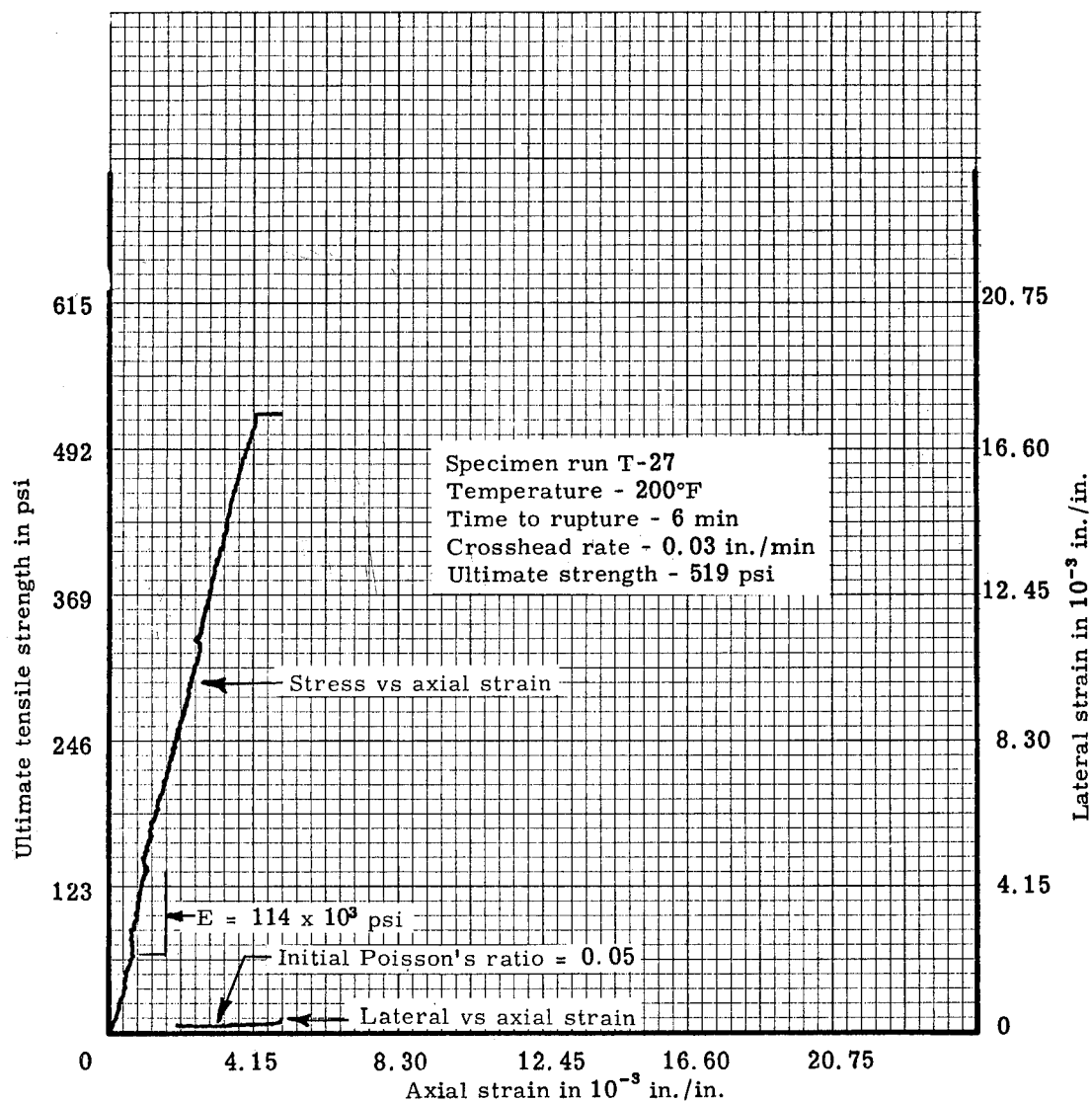Figure C12. Axial tensile stress-strain and bi-directional strains at 400°F for a virgin low-density phenolic-nylon

81

Figure C13. Axial tensile stress-strain at 500°F for a virgin low-density phenolic-nylon

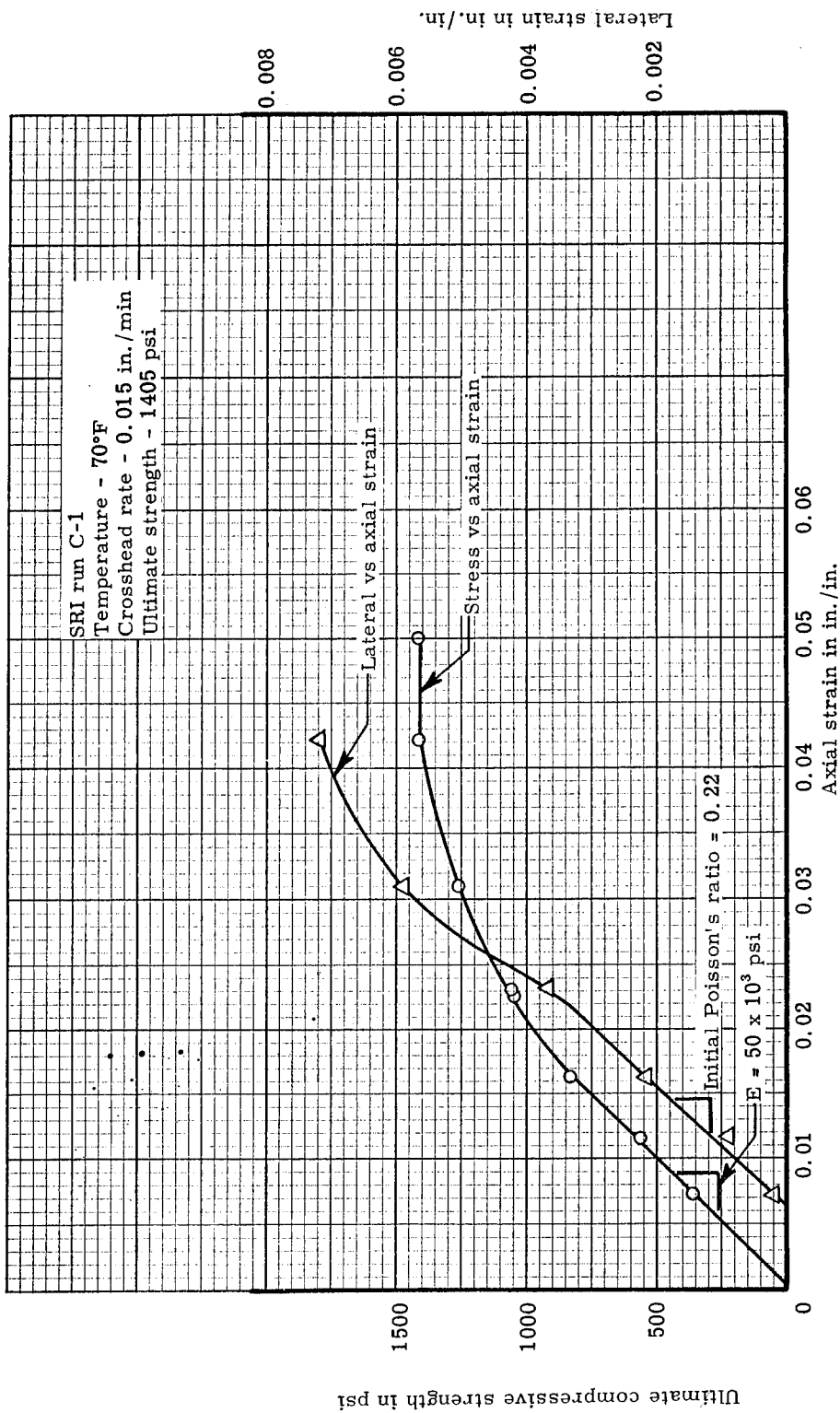Figure C14. Axial tensile stress-strain and bi-directional strains at 300°F for a virgin low-density phenolic-nylon

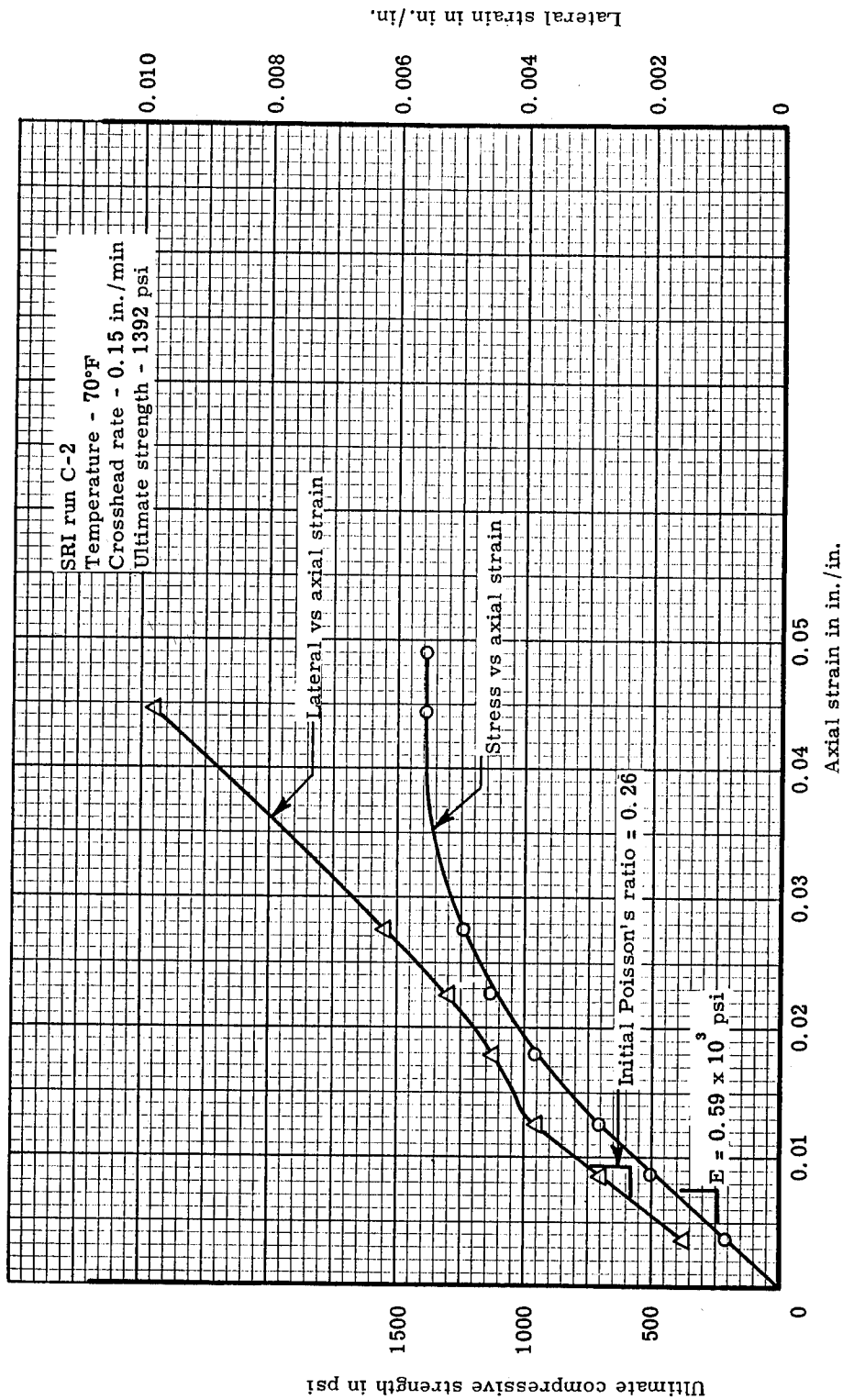Figure C15. Axial tensile stress-strain and bi-directional strains at 70°F for a virgin low-density phenolic-nylon

84

Figure C16. Axial tensile stress-strain at -100°F for a virgin low-density phenolic-nylon

Specimen run T-22
Temperature - 100°F
Time to rupture - 4.2 min
Crosshead rate - 0.04 in./min
Ultimate strength - 530 psi

Stress vs axial strain

$E = 90 \times 10^3$ psi

Axial strain in 10^{-3} in./in.

Ultimate tensile strength in psi

85

Figure C17. Axial tensile stress-strain and bi-directional strains at 0°F
for a virgin low-density phenolic-nylon
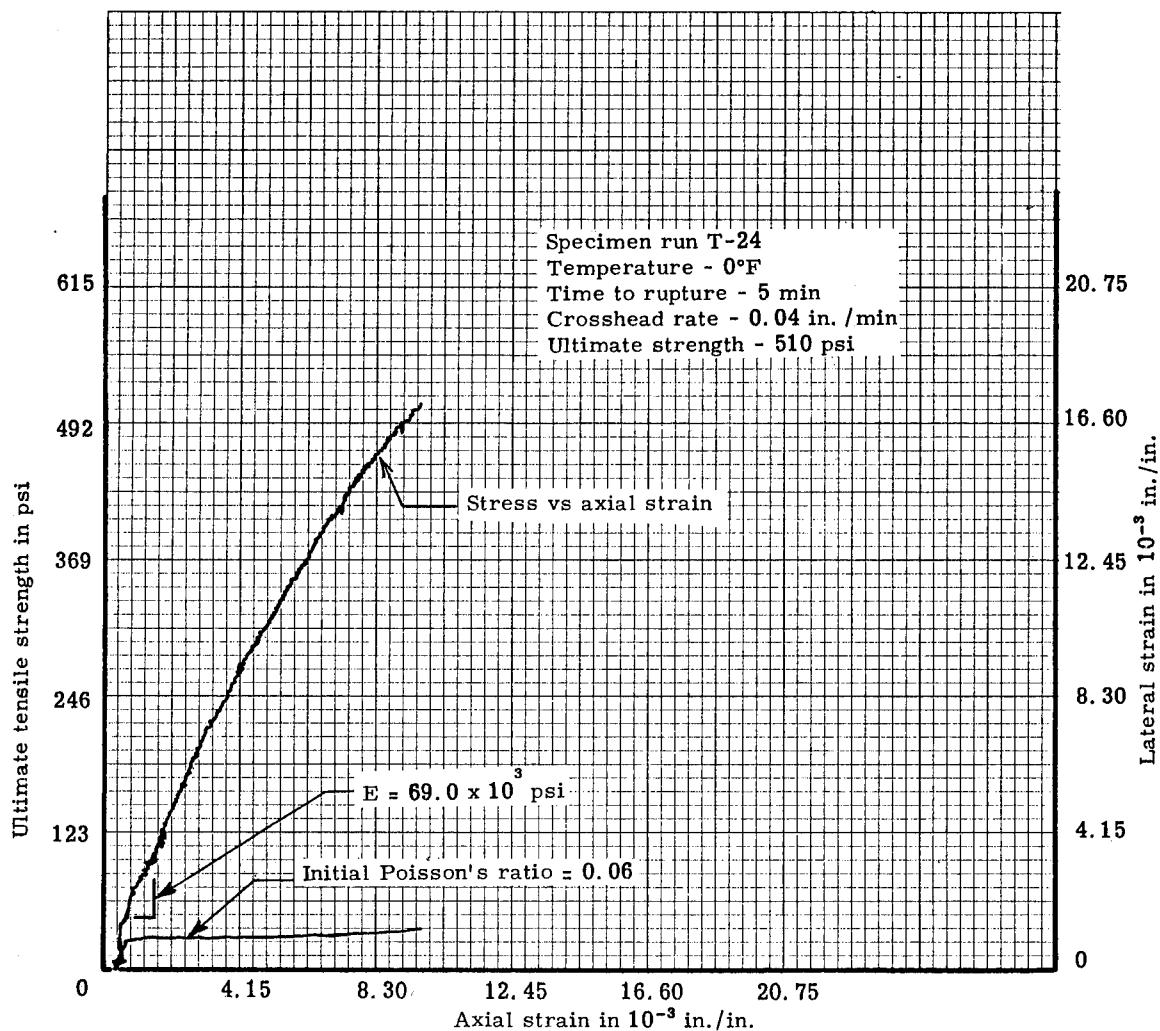
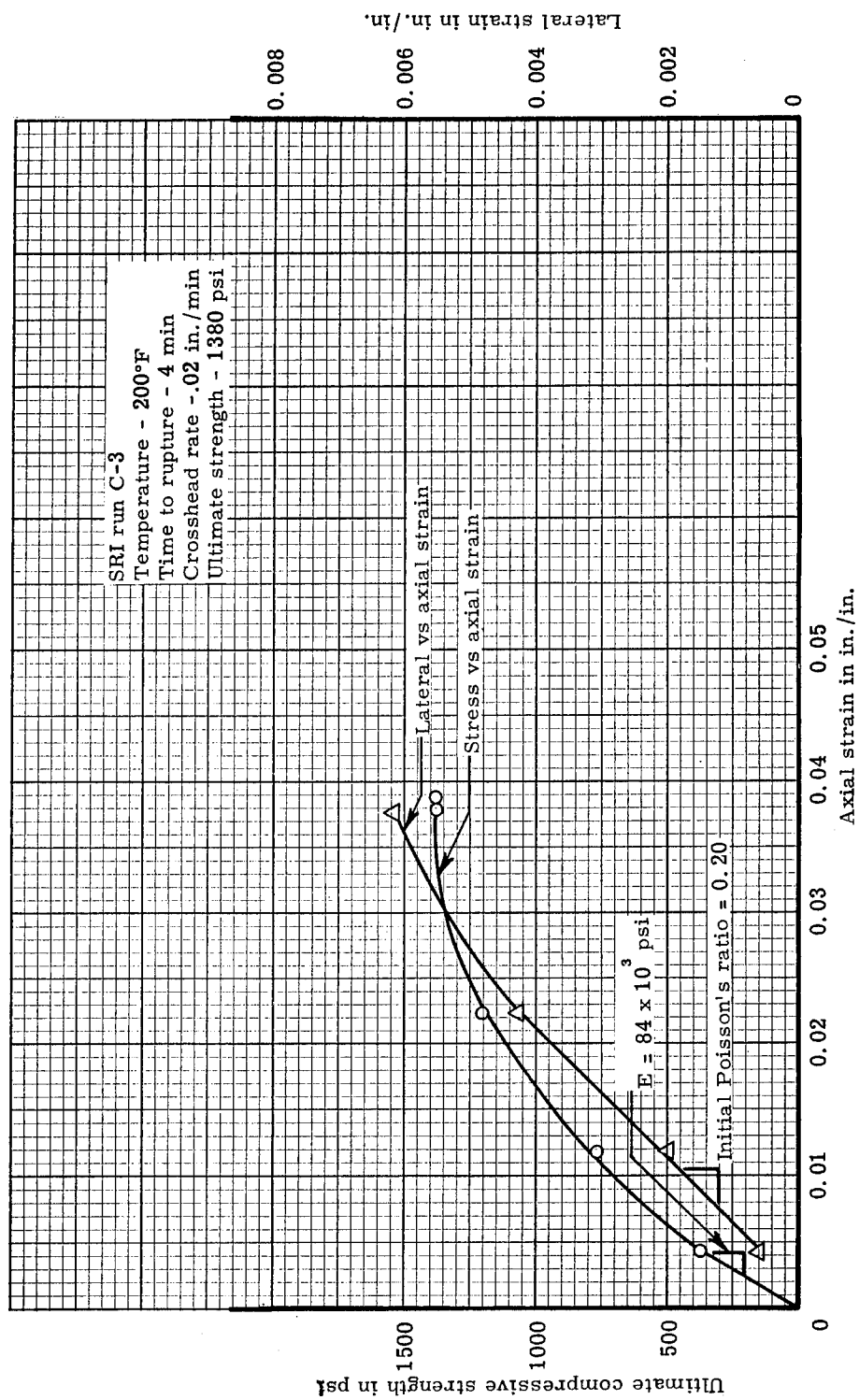Figure C18. Axial tensile stress-strain and bi-directional strains at 0°F for a virgin low-density phenolic-nylon
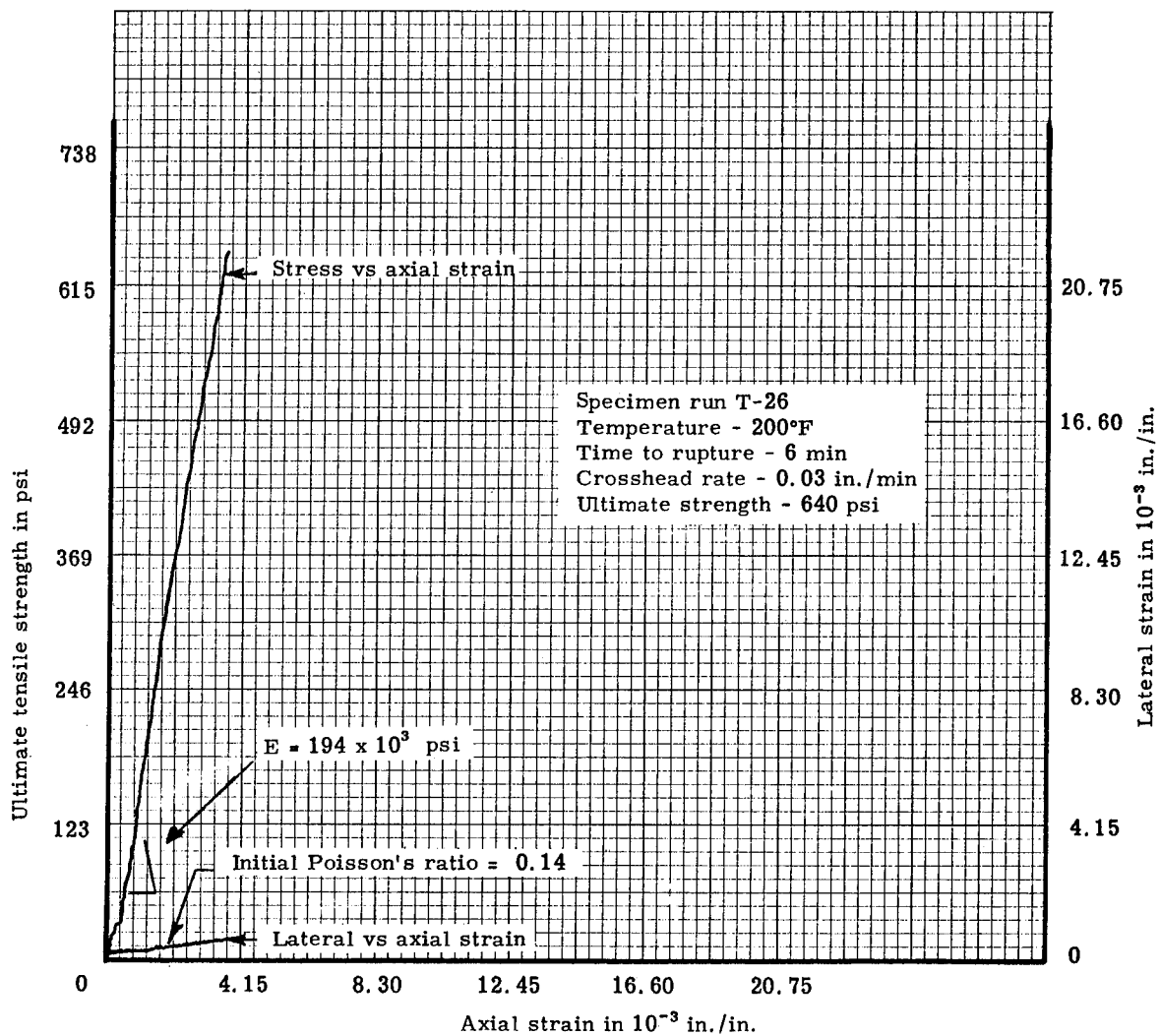
Figure C19. Axial tensile stress-strain and bi-directional strains at -200°F for a virgin low-density phenolic-nylon

Figure C20. Axial tensile stress-strain and bi-directional strains
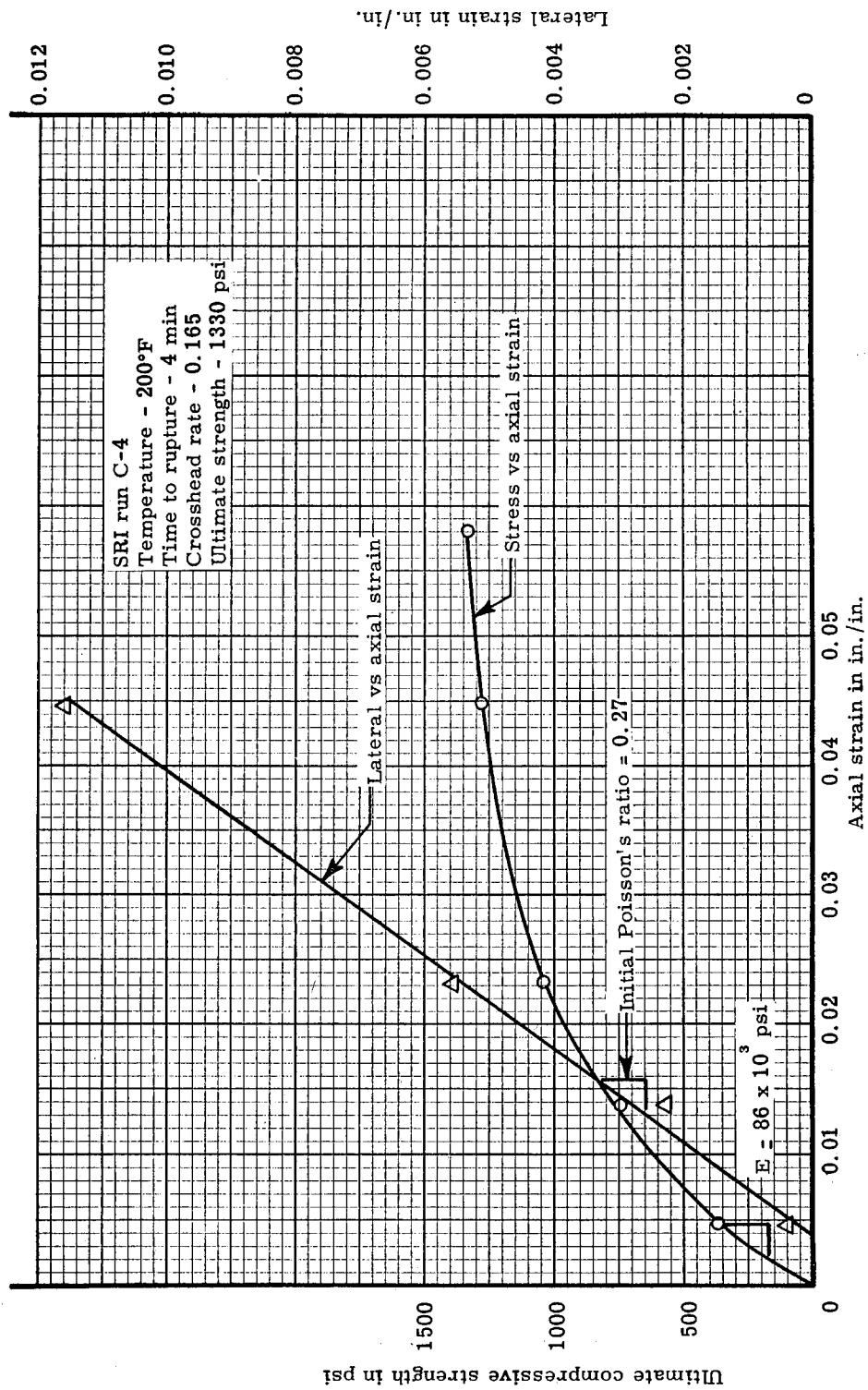at -200°F for a virgin low-density phenolic-nylon

89

Figure C21. Axial tensile stress-strain and bi-directional strains at -100°F
for a virgin low-density phenolic-nylon

Figure C22. Axial tensile stress-strain and bi-directional strains at -200°F
for a virgin low-density phenolic-nylon

Figure C23. Axial compressive stress-strain and bi-directional strains at 70°F for a virgin low-density phenolic-nylon
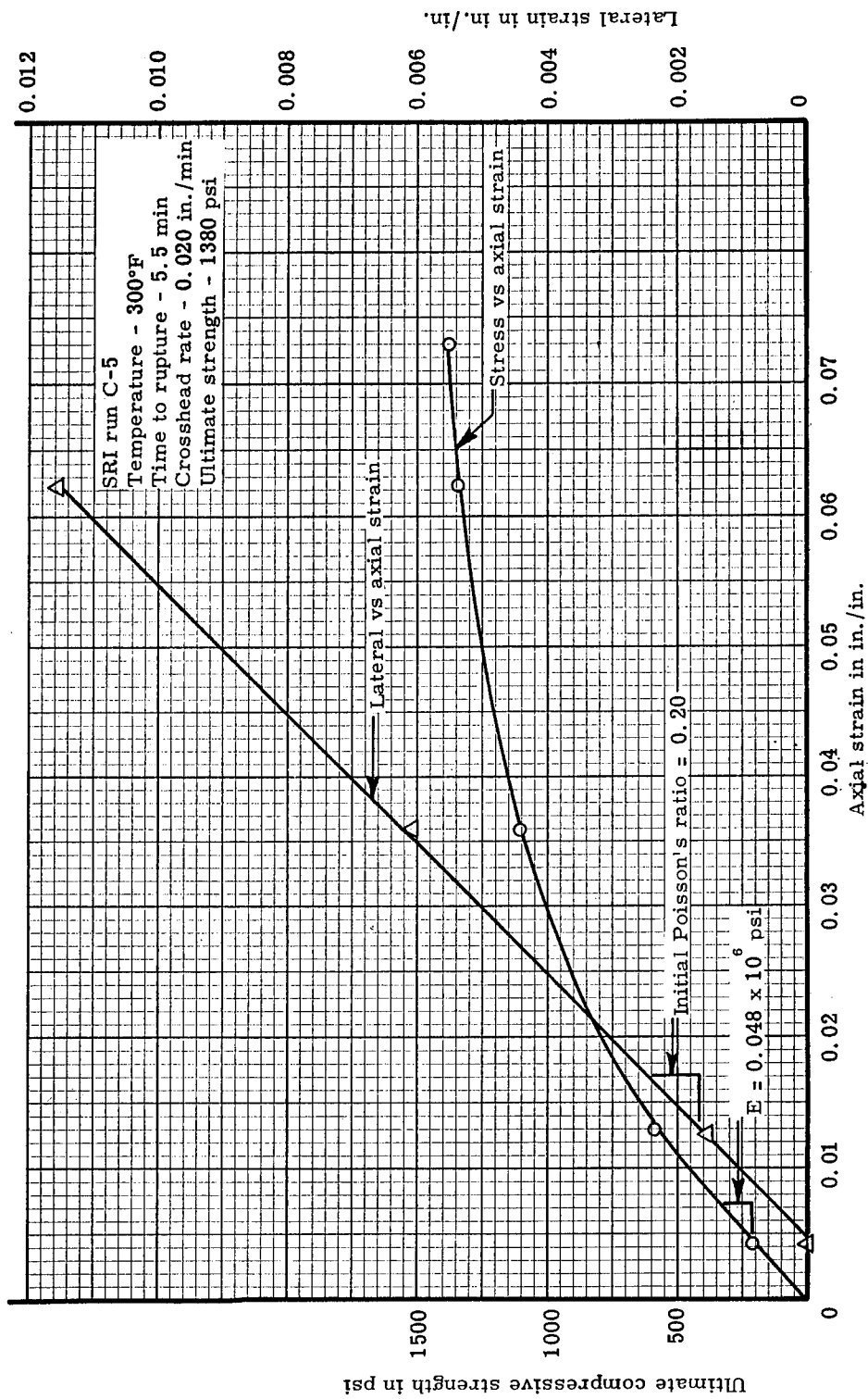
92

Figure C24. Axial compressive stress–strain and bi-directional strains at 70°F for a virgin low–density phenolic–nylon
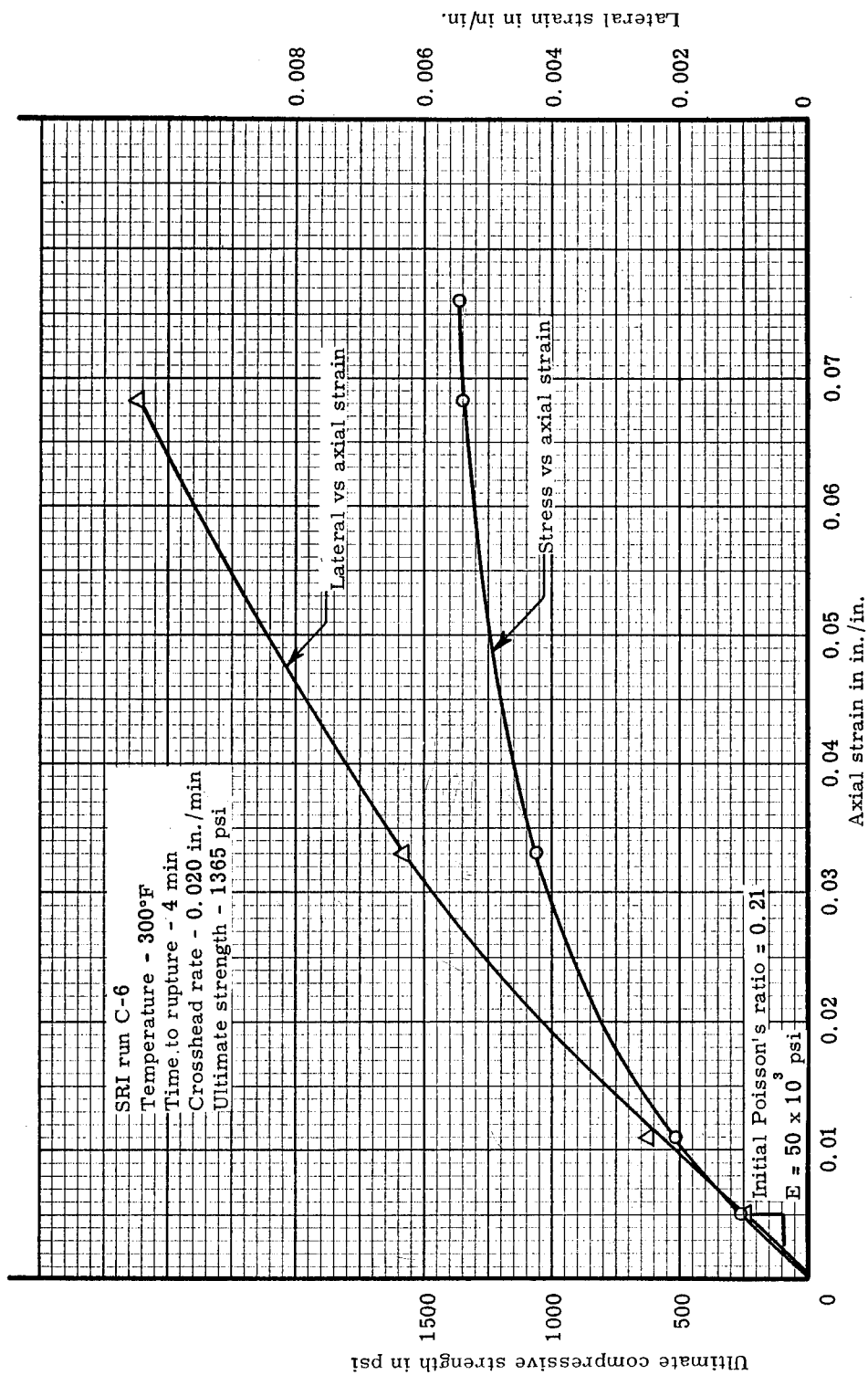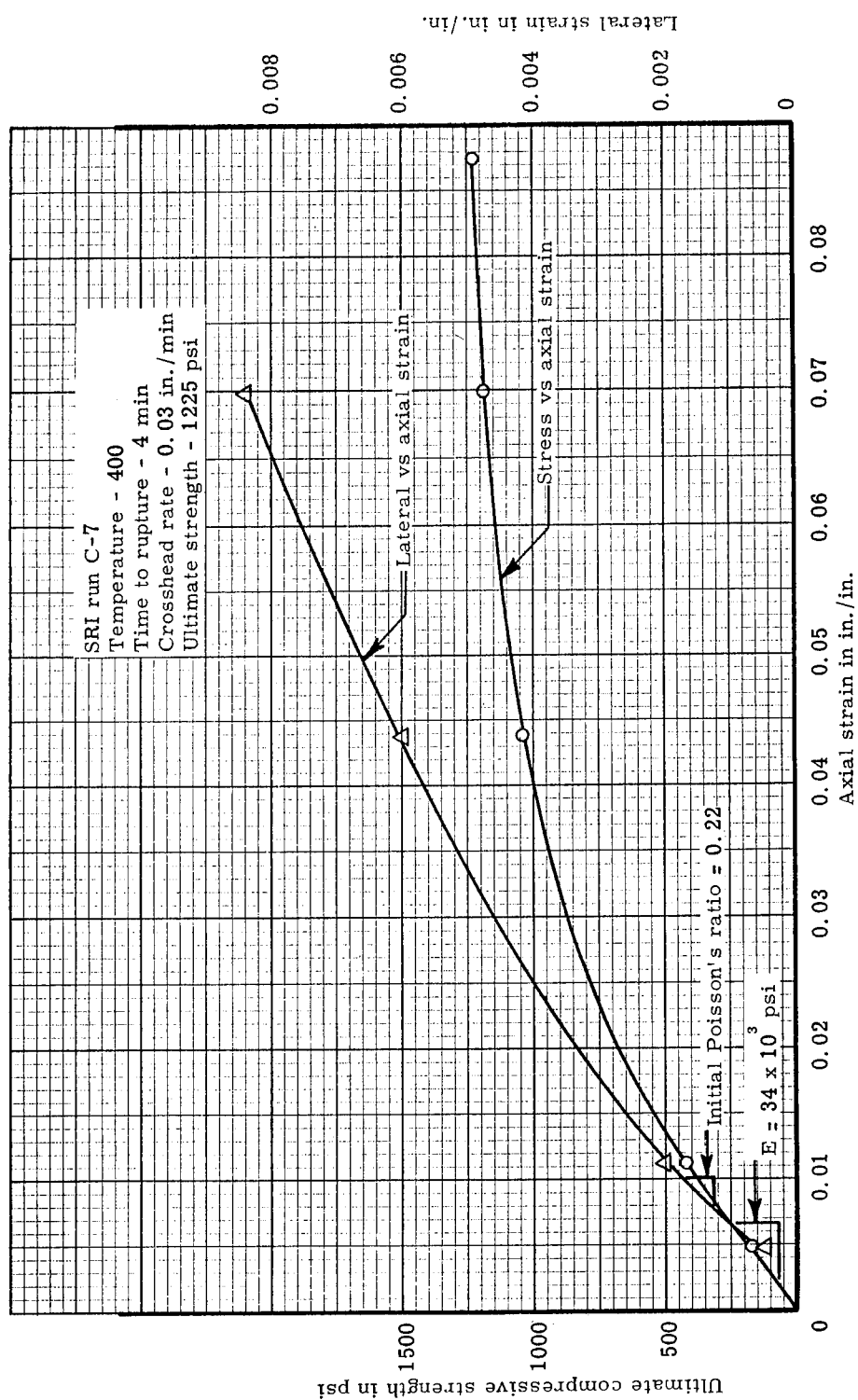
93

Figure C25. Axial compressive stress-strain and bi-directional strains at 200°F for a virgin low-density phenolic-nylon

Figure C26. Axial compressive stress–strain and bi–directional strain at 200°F for a virgin low–density phenolic–nylon

95

Figure C27. Axial compressive stress-strain and bi-directional strains at 300°F for a virgin low-density phenolic-nylon

SRI run C-5
Temperature - 300°F
Time to rupture - 5.5 min
Crosshead rate - 0.020 in./min
Ultimate strength - 1380 psi

Lateral vs axial strain

Stress vs axial strain

Initial Poisson's ratio = 0.20

$E = 0.048 \times 10^6$ psi

Lateral strain in in./in.

Axial strain in in./in.

Ultimate compressive strength in psi

96

Figure C28. Axial compressive stress-strain and bi-directional strains at 300°F for a virgin low-density phenolic-nylon

97

Figure C29. Axial compressive stress–strain and bi-directional strains at 400°F for a virgin low–density phenolic–nylon
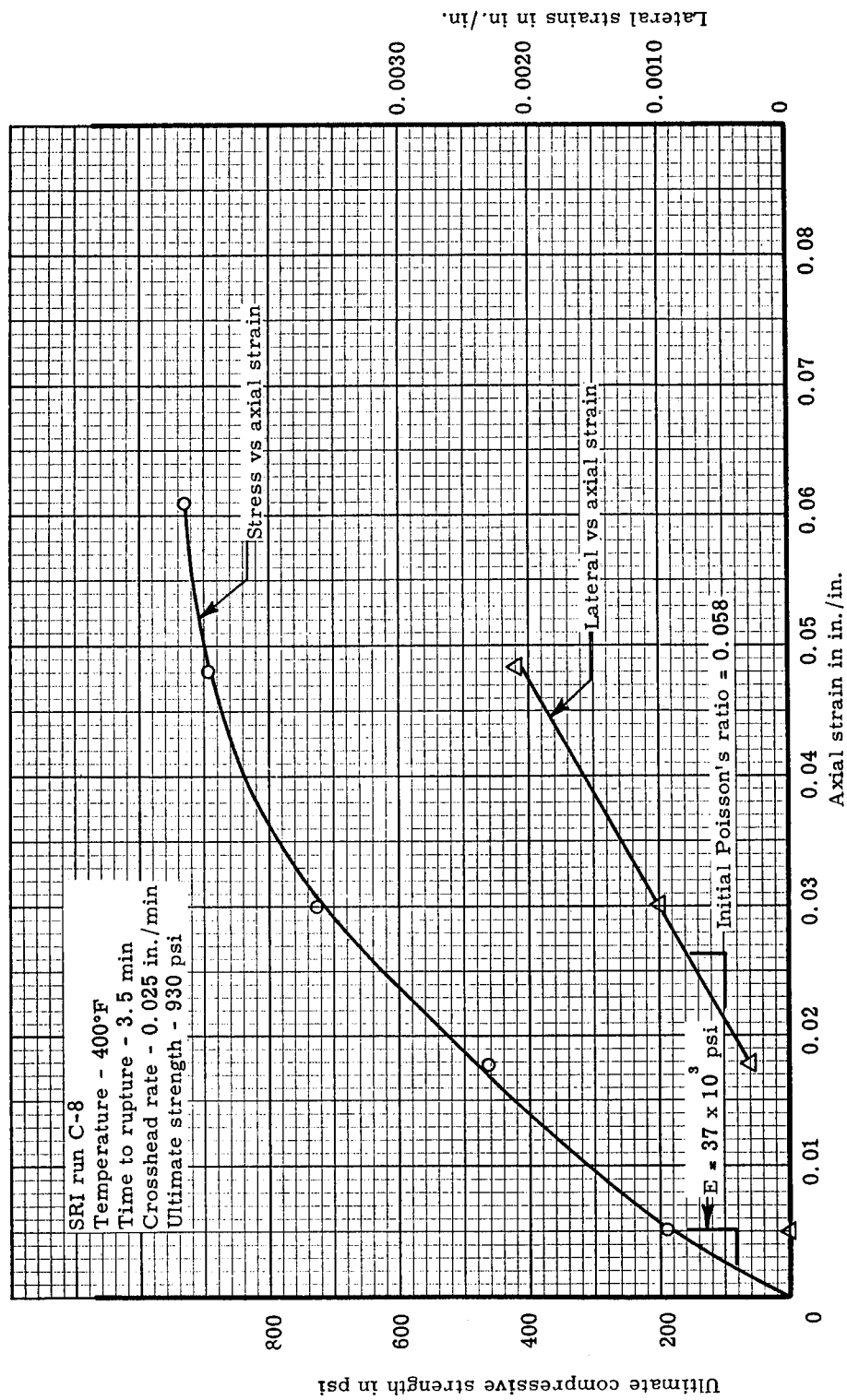
98

Figure C30. Axial compressive stress-strain and bi-directional strains at 400°F for a virgin low-density phenolic-nylon
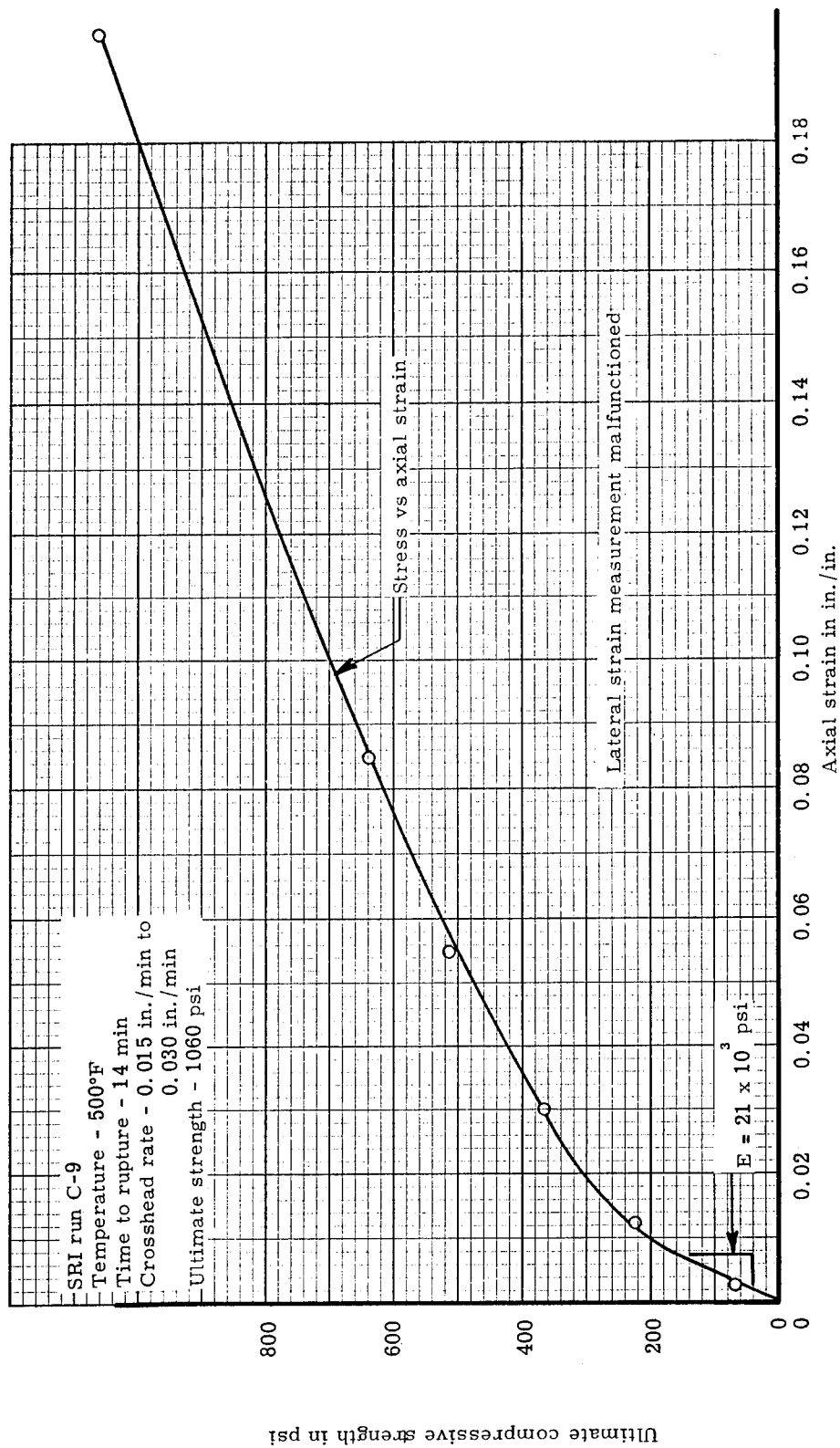
99

Figure C31. Axial compressive stress-strain at 500°F for a virgin low-density phenolic-nylon
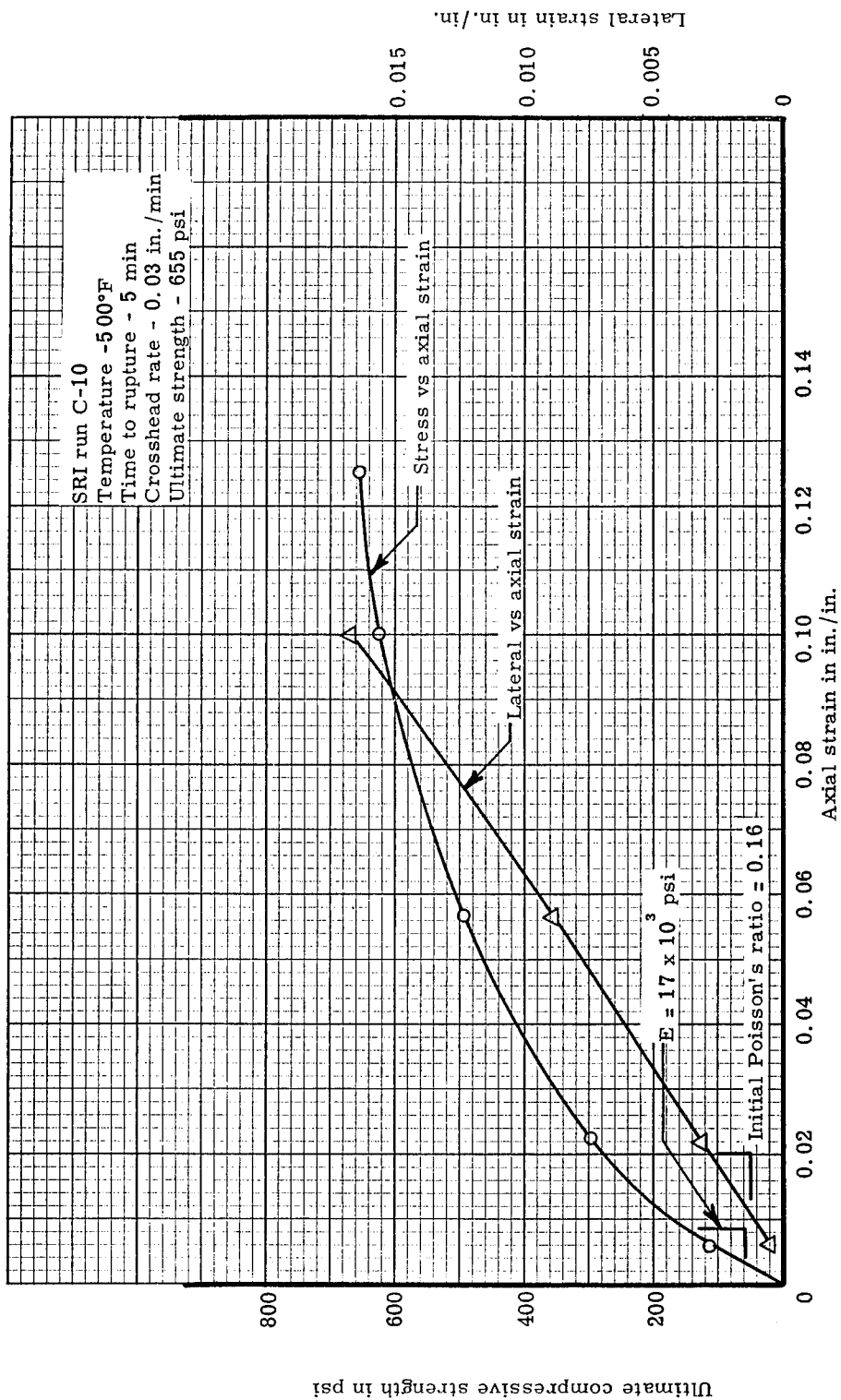
100

Figure C32. Axial compressive stress–strain and bi–directional strains at 500°F for a virgin low-density phenolic–nylon

Figure C33. Axial compressive stress-strain and bi-directional strains at 500°F for a virgin low-density phenolic-nylon
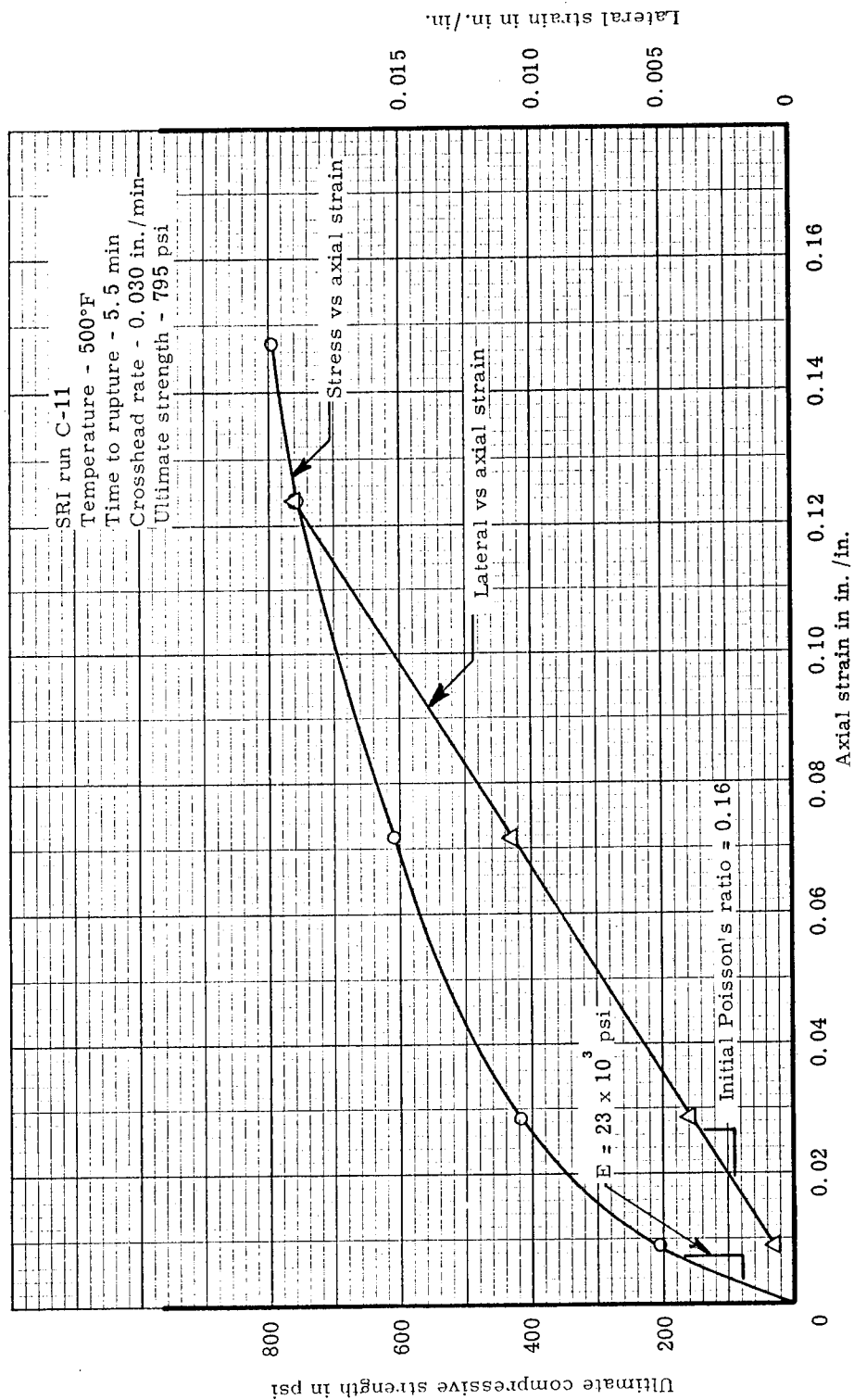
102
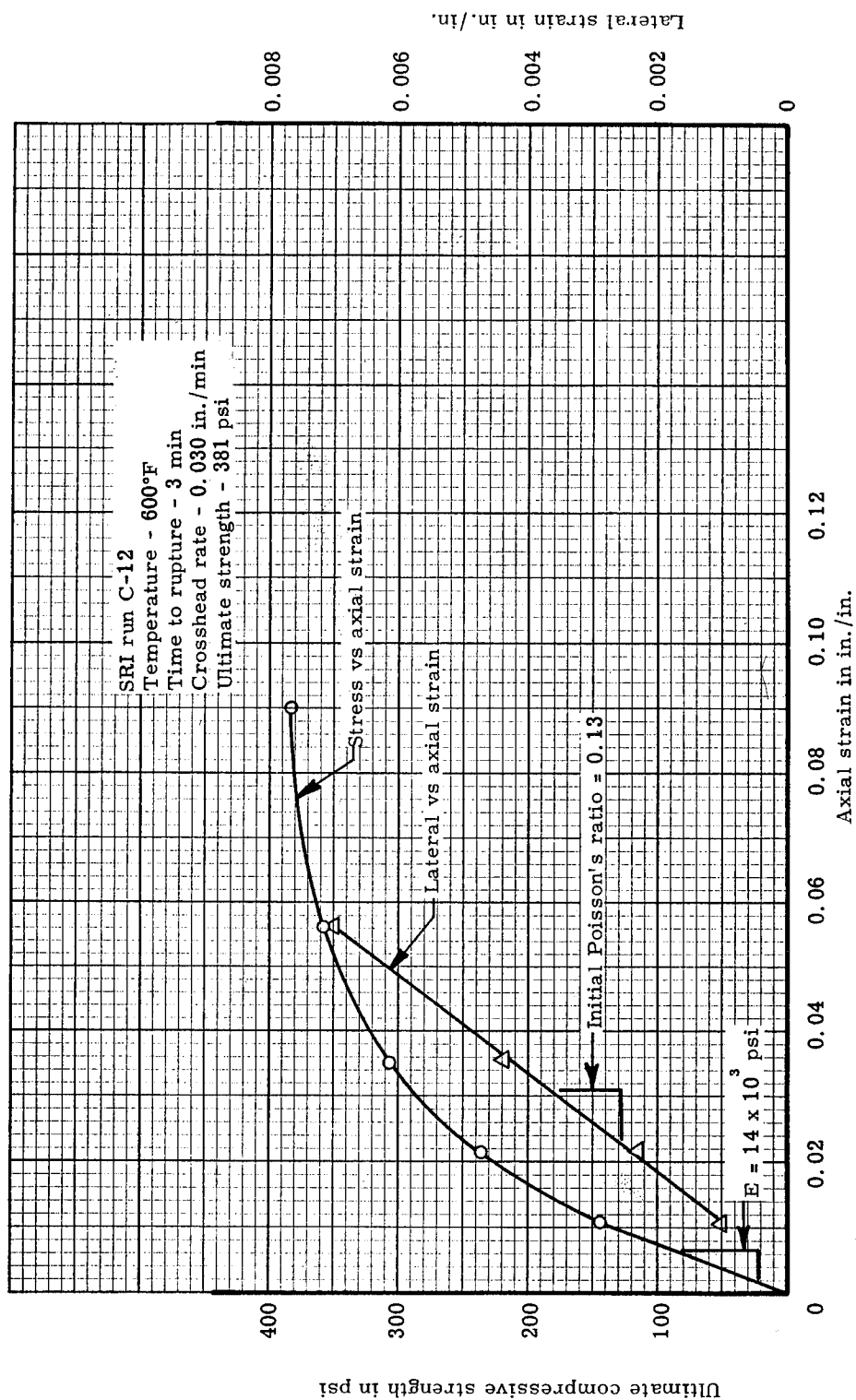
Figure C34. Axial compressive stress-strain and bi-directional strains at 600°F for a virgin low-density phenolic-nylon

SRI run C-12
Temperature - 600°F
Time to rupture - 3 min
Crosshead rate - 0.030 in./min
Ultimate strength - 381 psi

Stress vs axial strain

Lateral vs axial strain

Initial Poisson's ratio = 0.13

$E = 14 \times 10^{3}$ psi

Lateral strain in in./in.

Axial strain in in./in.

Ultimate compressive strength in psi

103

Figure C35. Axial compressive stress-strain and bi-directional strains at 600°F for a virgin low-density phenolic-nylon
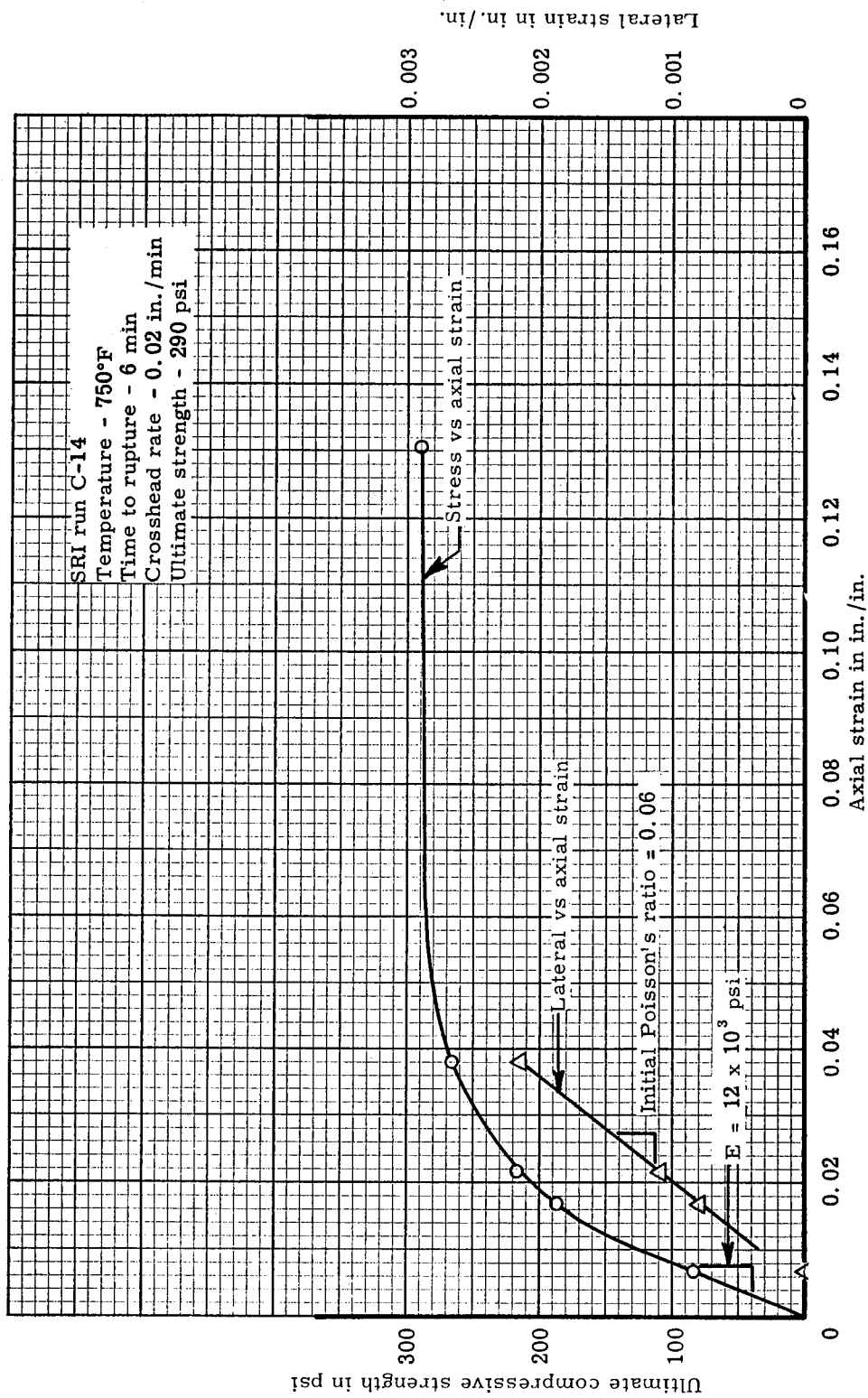
Figure C36. Axial compressive stress-strain and bi-directional strains at 750°F for a virgin low-density phenolic-nylon
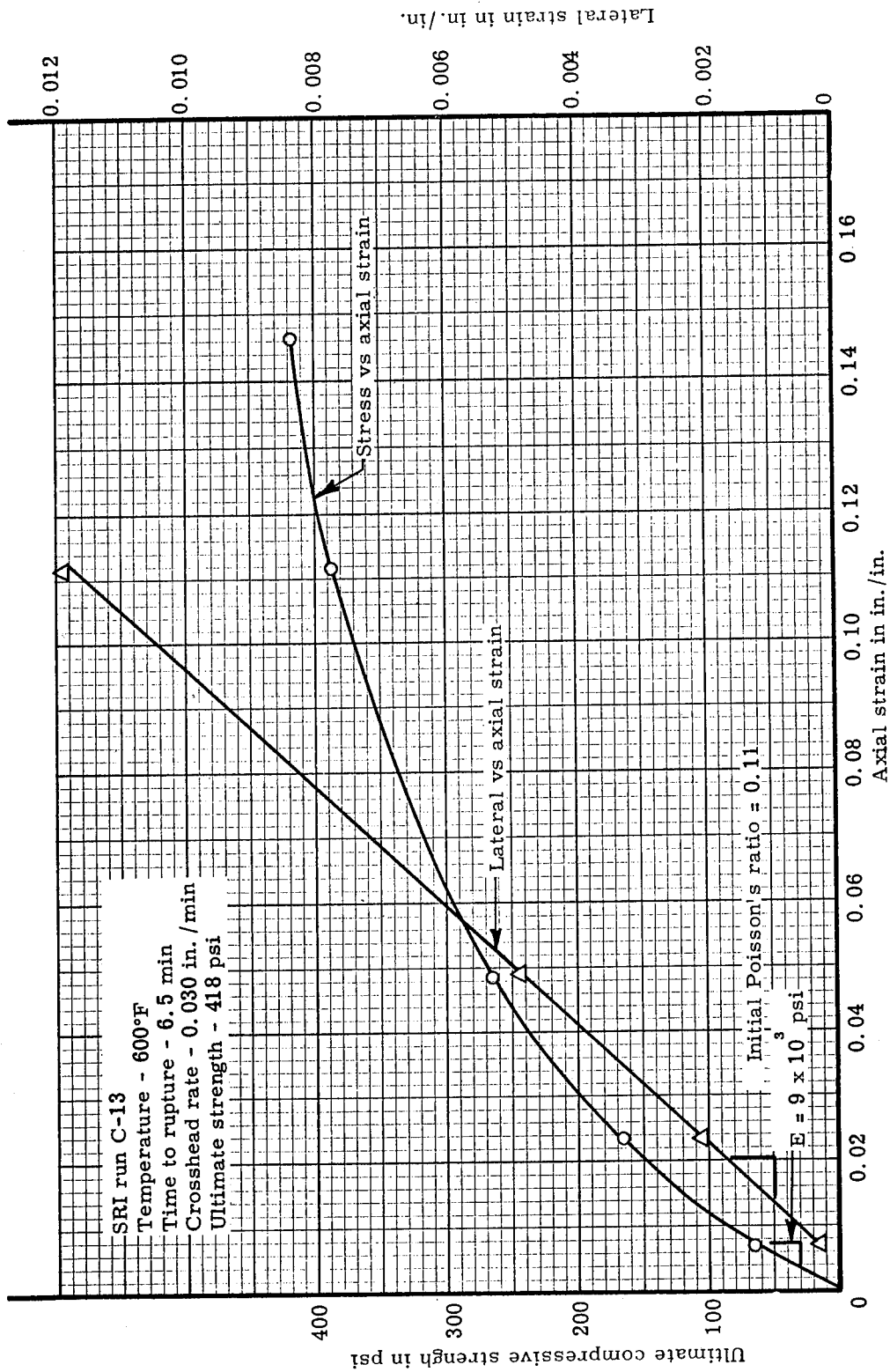
SRI run C-14
Temperature - 750°F
Time to rupture - 6 min
Crosshead rate - 0.02 in./min
Ultimate strength - 290 psi

Stress vs axial strain

Lateral vs axial strain

Initial Poisson's ratio = 0.06

$E = 12 \times 10^3$ psi

Lateral strain in in./in.

Axial strain in in./in.

Ultimate compressive strength in psi

105

Figure C37. Axial compressive stress-strain and bi-directional strains at 700°F for a virgin low-density phenolic-nylon

Figure C38. Axial compressive stress-strain and bi-directional strains at -200°F for a virgin low-density phenolic-nylon
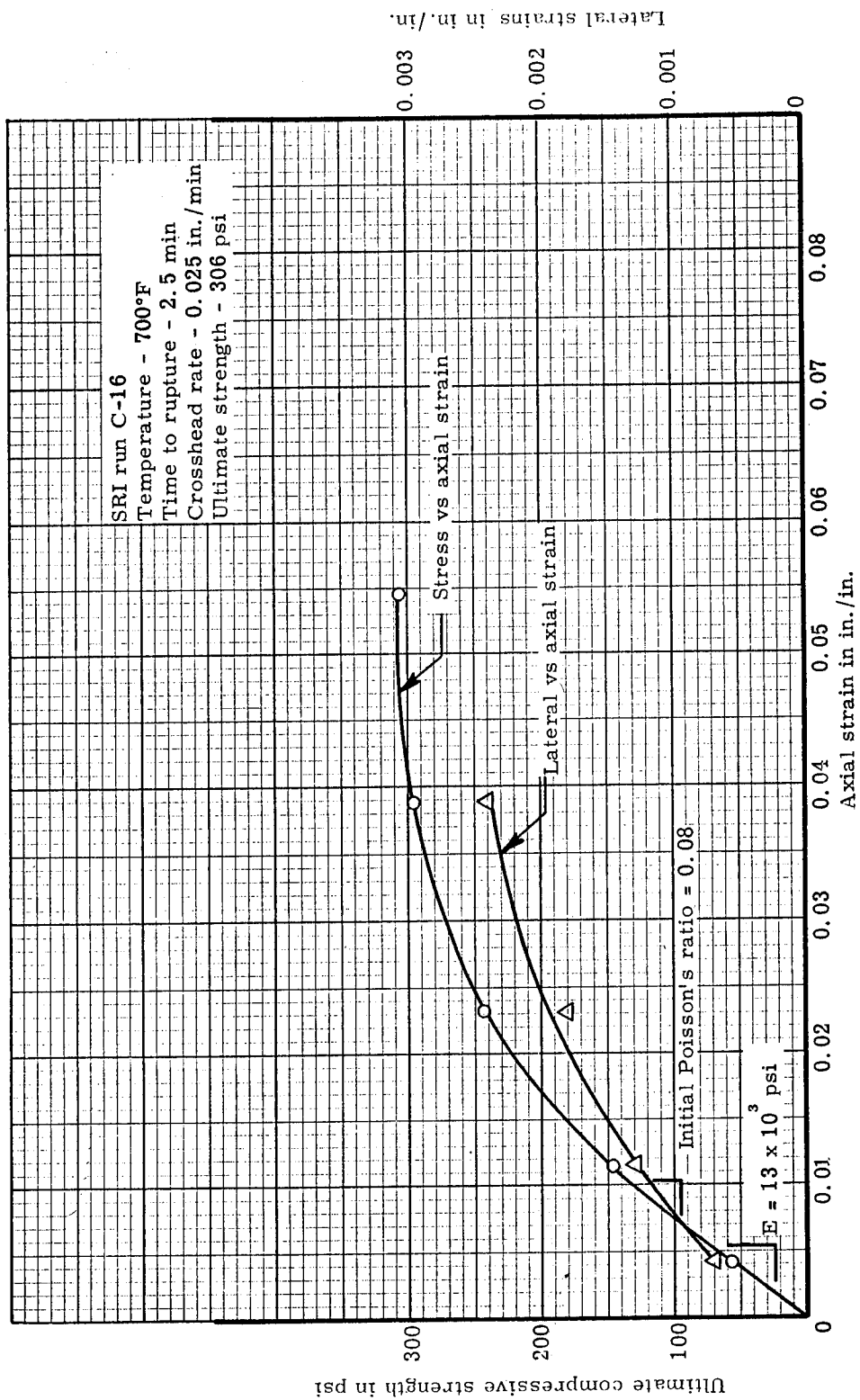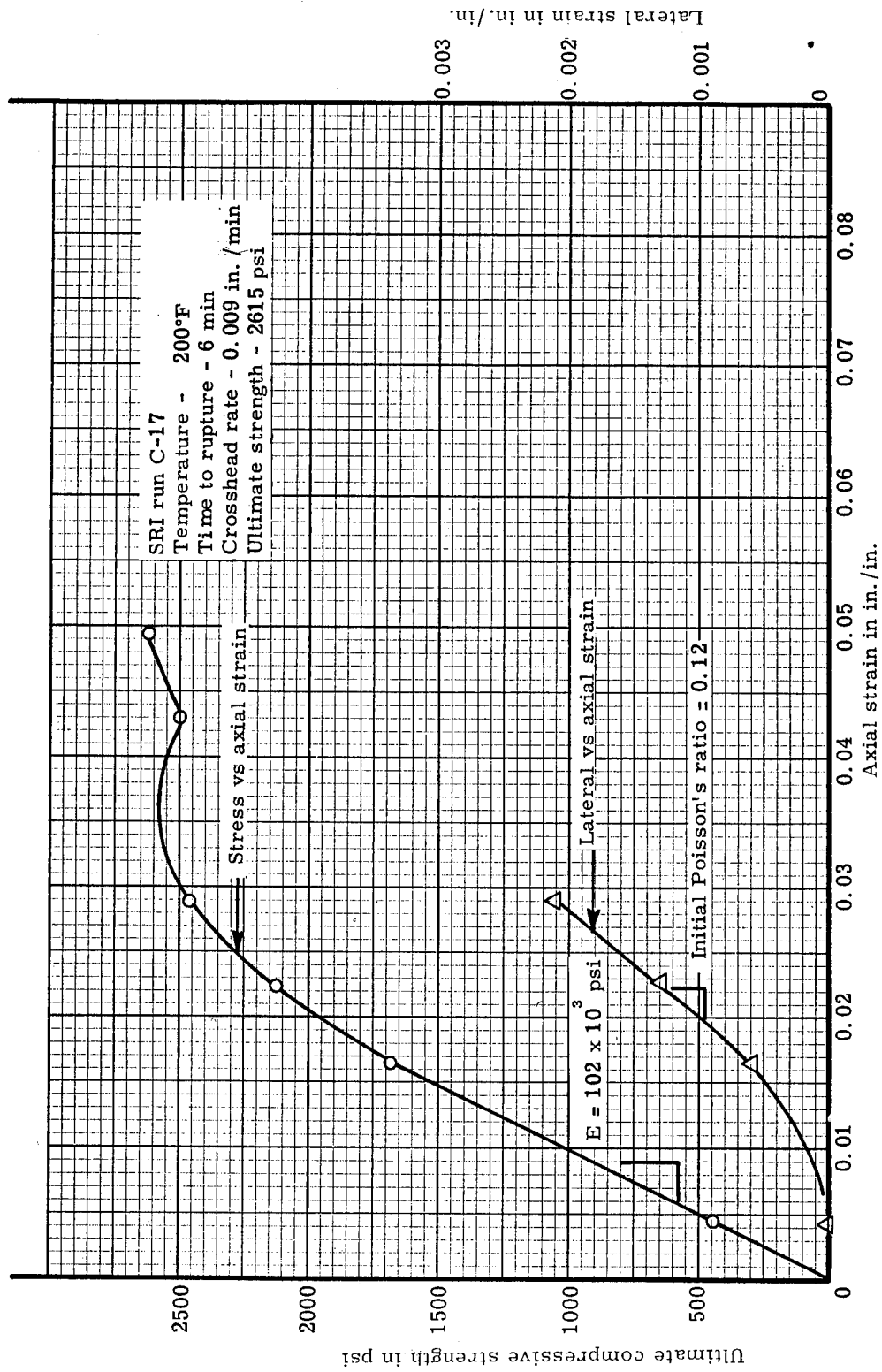
SRI run C-17
Temperature -   200°F
Time to rupture - 6 min
Crosshead rate - 0.009 in./min
Ultimate strength - 2615 psi

Stress vs axial strain

Lateral vs axial strain

Initial Poisson's ratio = 0.12

$E = 102 \times 10^3$ psi

Lateral strain in in./in.

0.003

0.002

0.001

0.08   0.07   0.06   0.05   0.04   0.03   0.02   0.01

Axial strain in in./in.
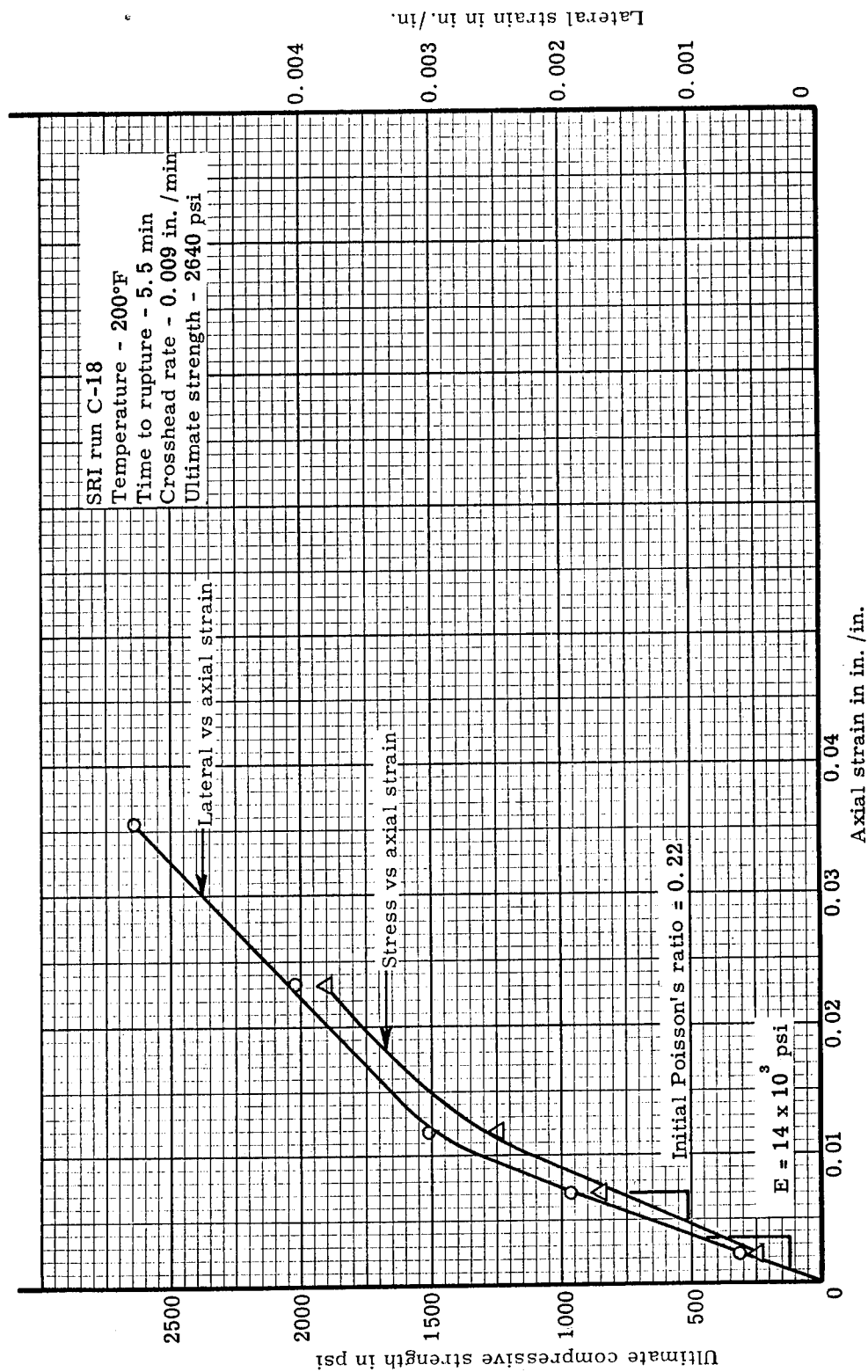
2500   2000   1500   1000   500

Ultimate compressive strength in psi

Figure C39. Axial compressive stress-strain and bi-directional strains at -200°F for a virgin low-density phenolic-nylon

SRI run C-18
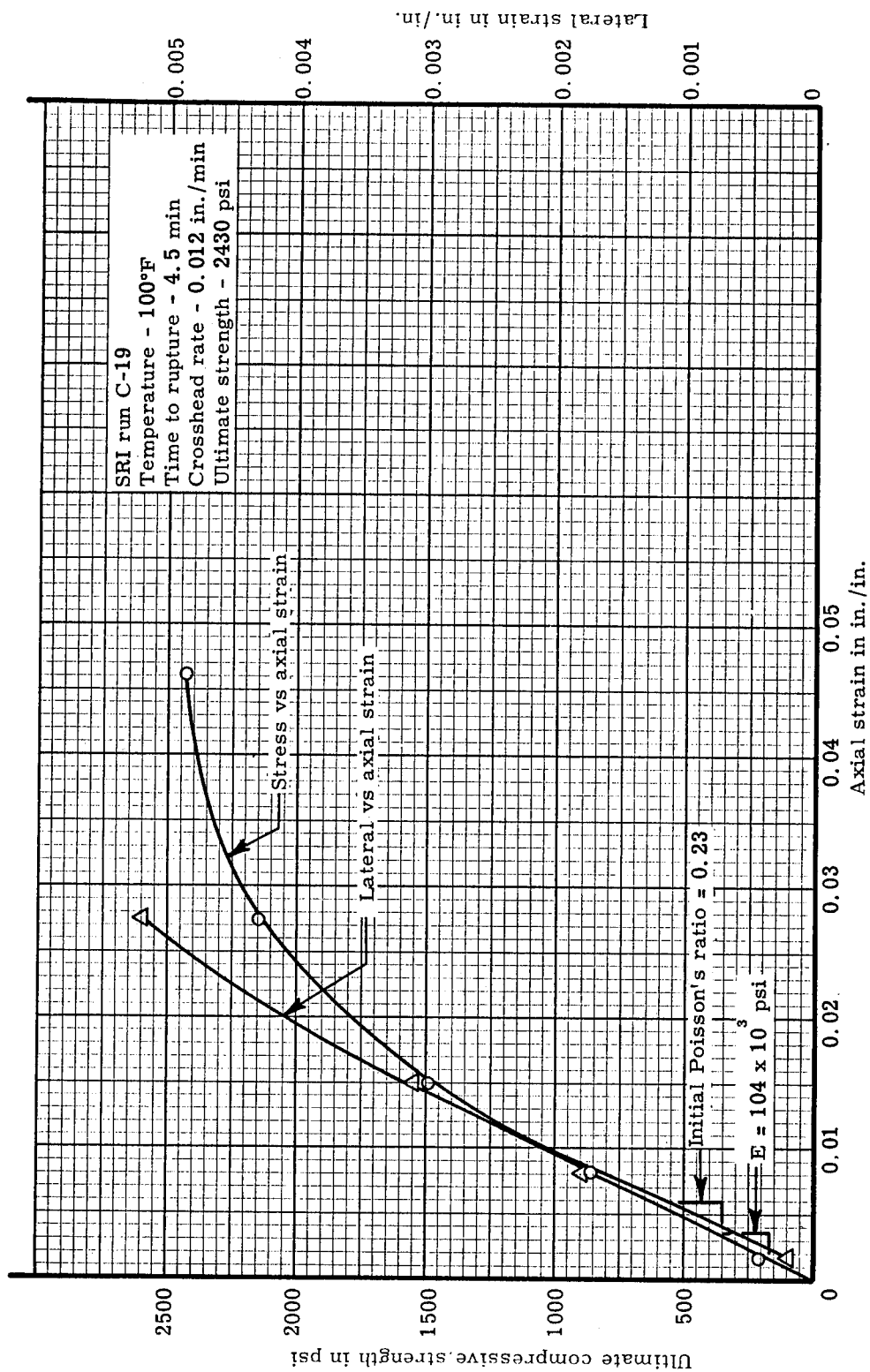Temperature - 200°F
Time to rupture - 5.5 min
Crosshead rate - 0.009 in./min
Ultimate strength - 2640 psi

Lateral vs axial strain

Stress vs axial strain

Initial Poisson's ratio = 0.22

E = 14 x 10³ psi

Lateral strain in in./in.

Axial strain in in./in.

Ultimate compressive strength in psi

Figure C40. Axial compressive stress–strain and bi-directional strains at -100°F for a virgin low-density phenolic–nylon

SRI run C-19
Temperature - 100°F
Time to rupture - 4.5 min
Crosshead rate - 0.012 in./min
Ultimate strength - 2430 psi

Stress vs axial strain

Lateral vs axial strain

Initial Poisson's ratio = 0.23

$E = 104 \times 10^3$ psi

Lateral strain in in./in.

Axial strain in in./in.

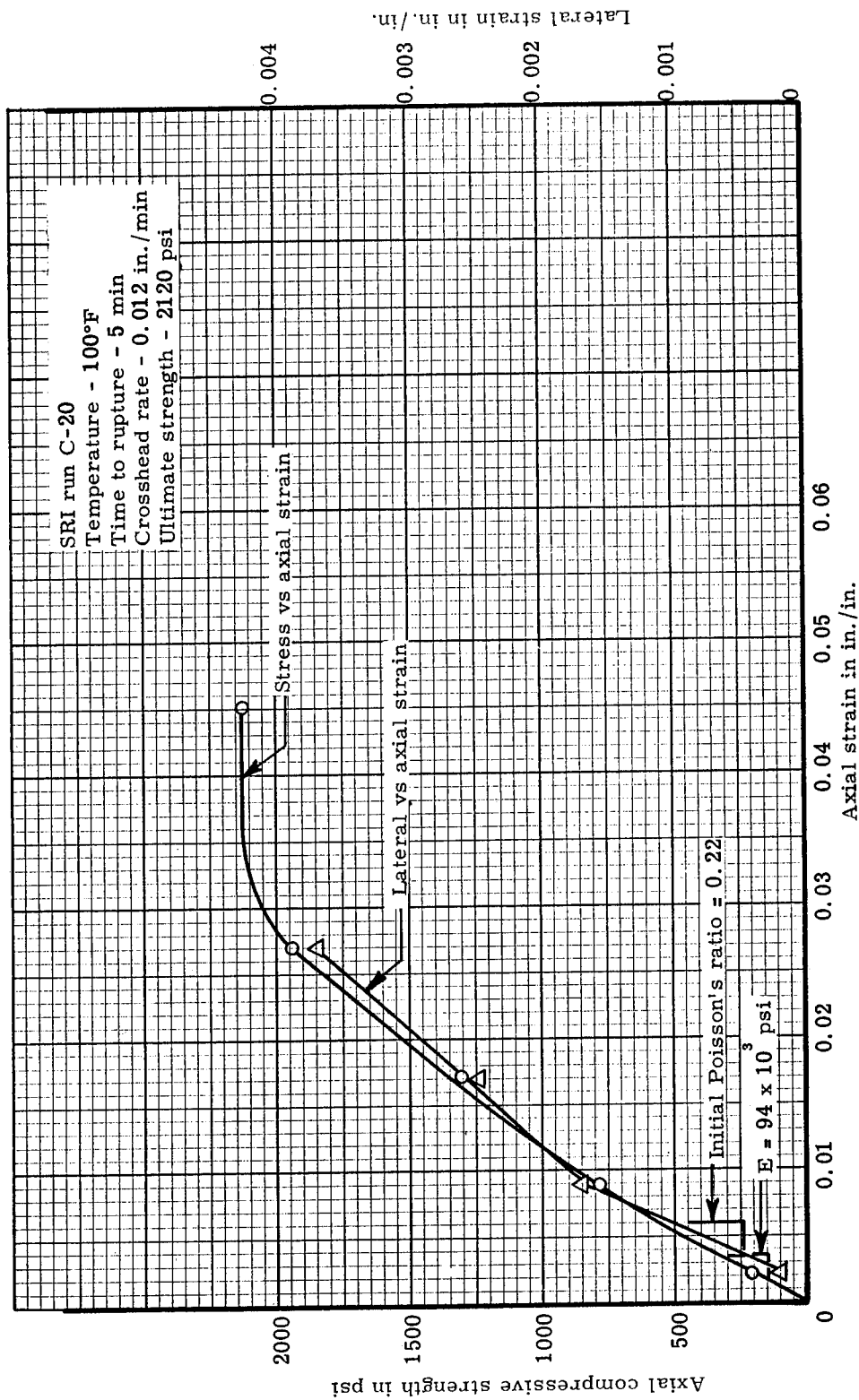Ultimate compressive strength in psi

109

Figure C41. Axial compressive stress-strain and bi-directional strains at -100°F for a virgin low-density phenolic-nylon
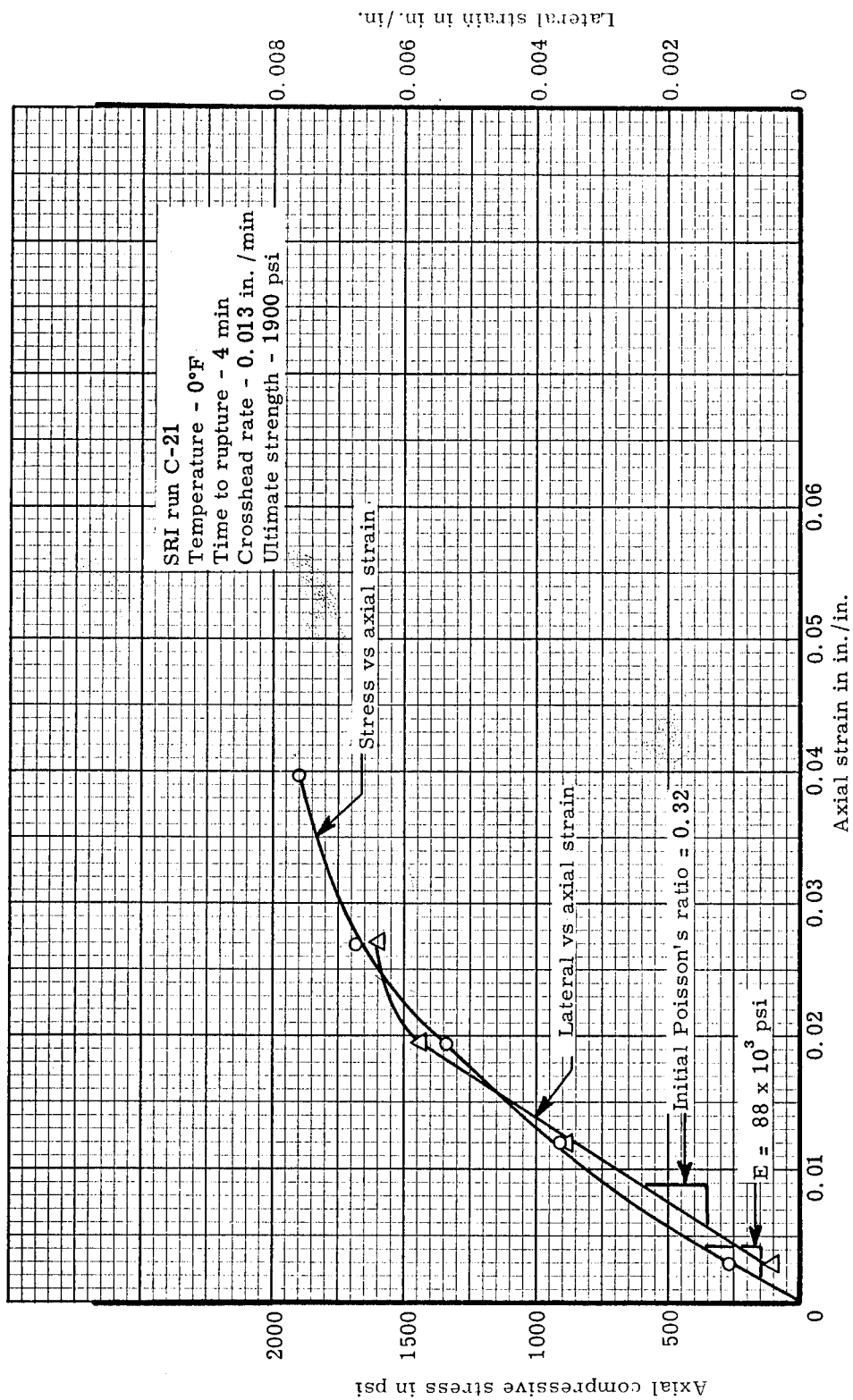
110

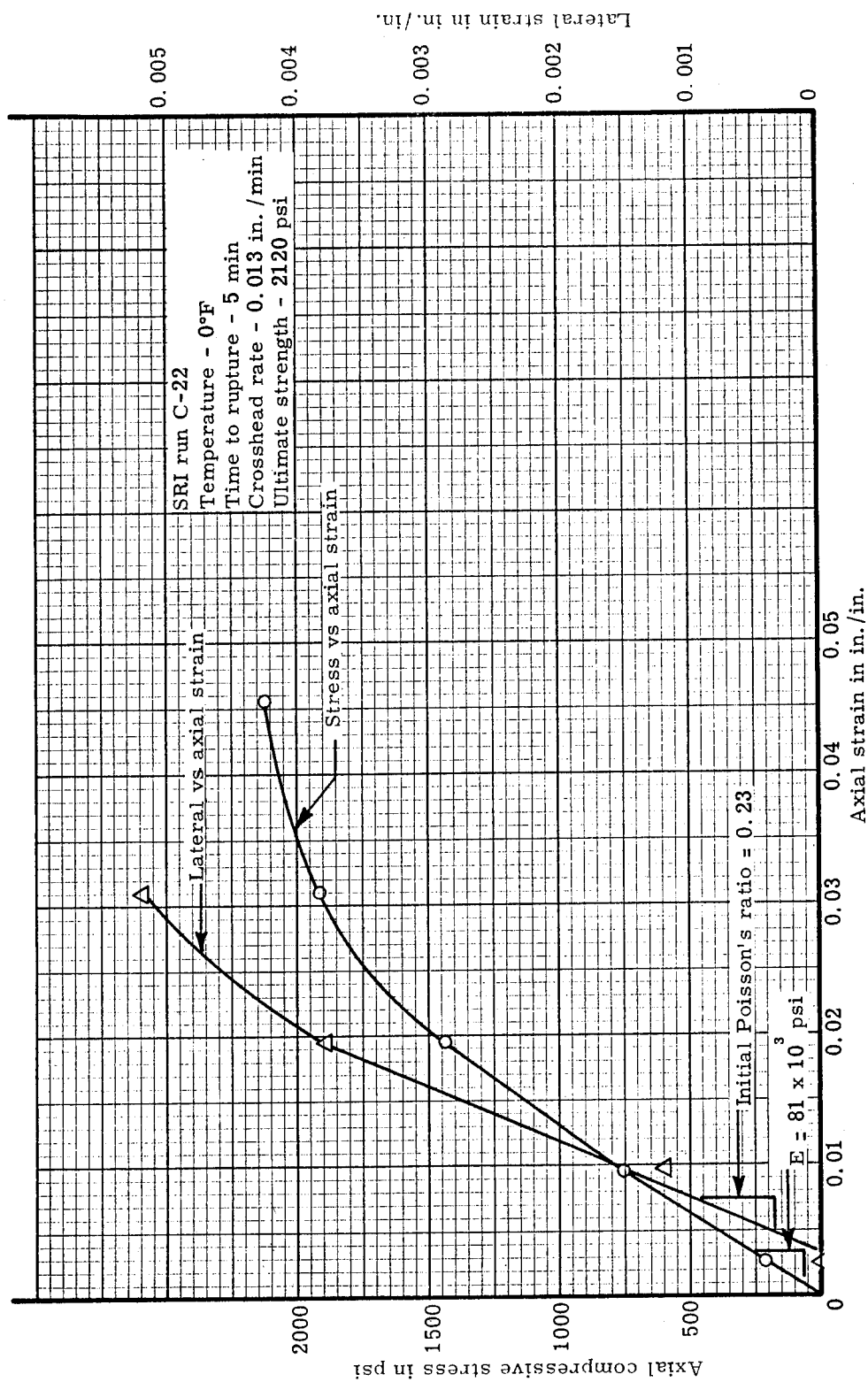Figure C42. Axial compressive stress-strain and bi-directional strains at 0°F for a virgin low-density phenolic-nylon

111

Figure C43. Axial compressive stress-strain and bi-directional strains at 0°F for a virgin low-density phenolic-nylon

The following text labels appear within the figure:

Lateral strain in in./in.

0.005   0.004   0.003   0.002   0.001   0

SRI run C-22
Temperature - 0°F
Time to rupture - 5 min
Crosshead rate - 0.013 in./min
Ultimate strength - 2120 psi

Stress vs axial strain

Lateral vs axial strain

Axial strain in in./in.

0.01   0.02   0.03   0.04   0.05

Initial Poisson's ratio = 0.23

$E = 81 \times 10^3$ psi

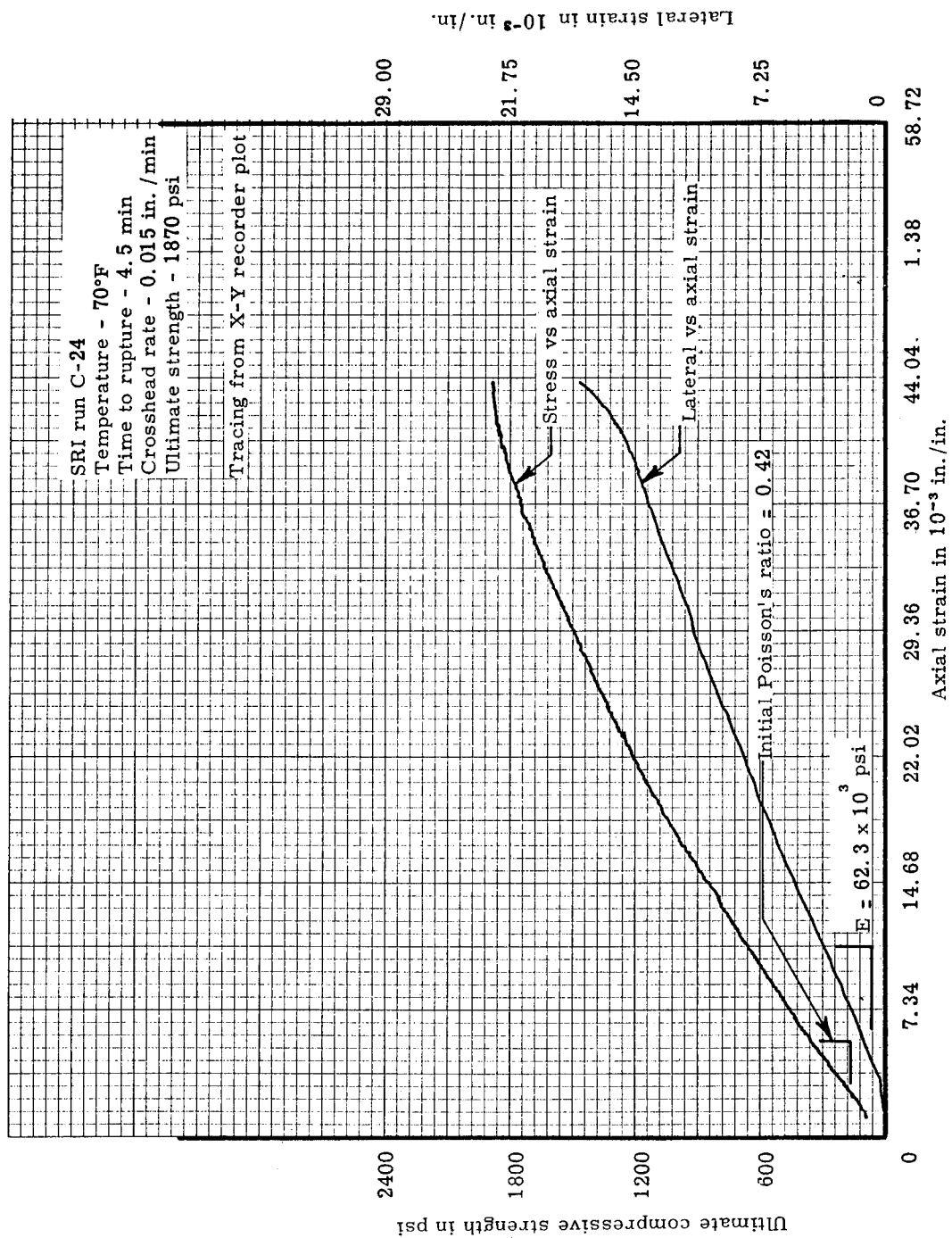Axial compressive stress in psi

2000   1500   1000   500   0

Figure C44. Axial compressive stress-strain and bi-directional strains at 70°F for a virgin low-density phenolic-nylon

113

Figure C45. Axial compressive stress-strain and bi-directional strains at 70°F for a virgin low-density phenolic-nylon
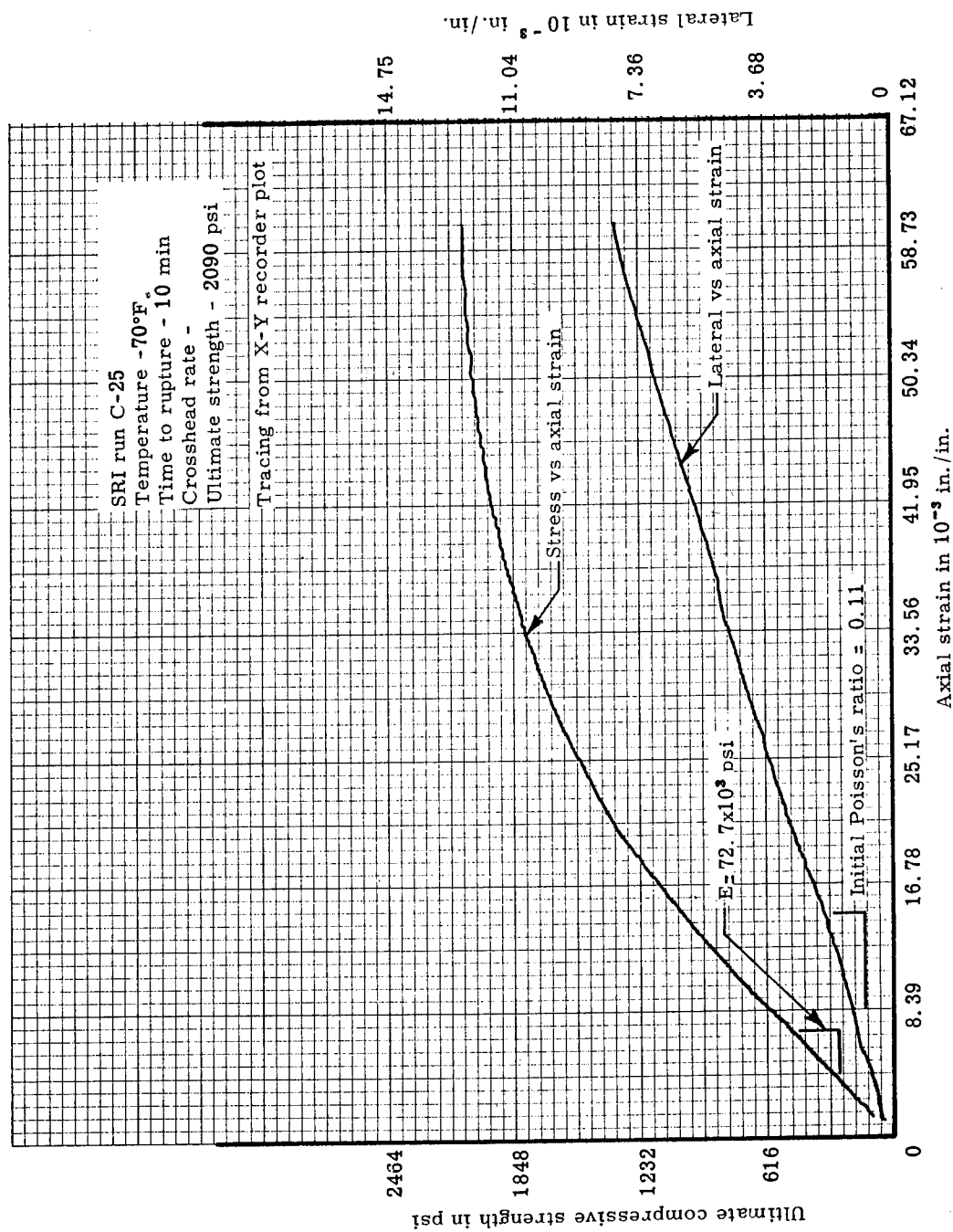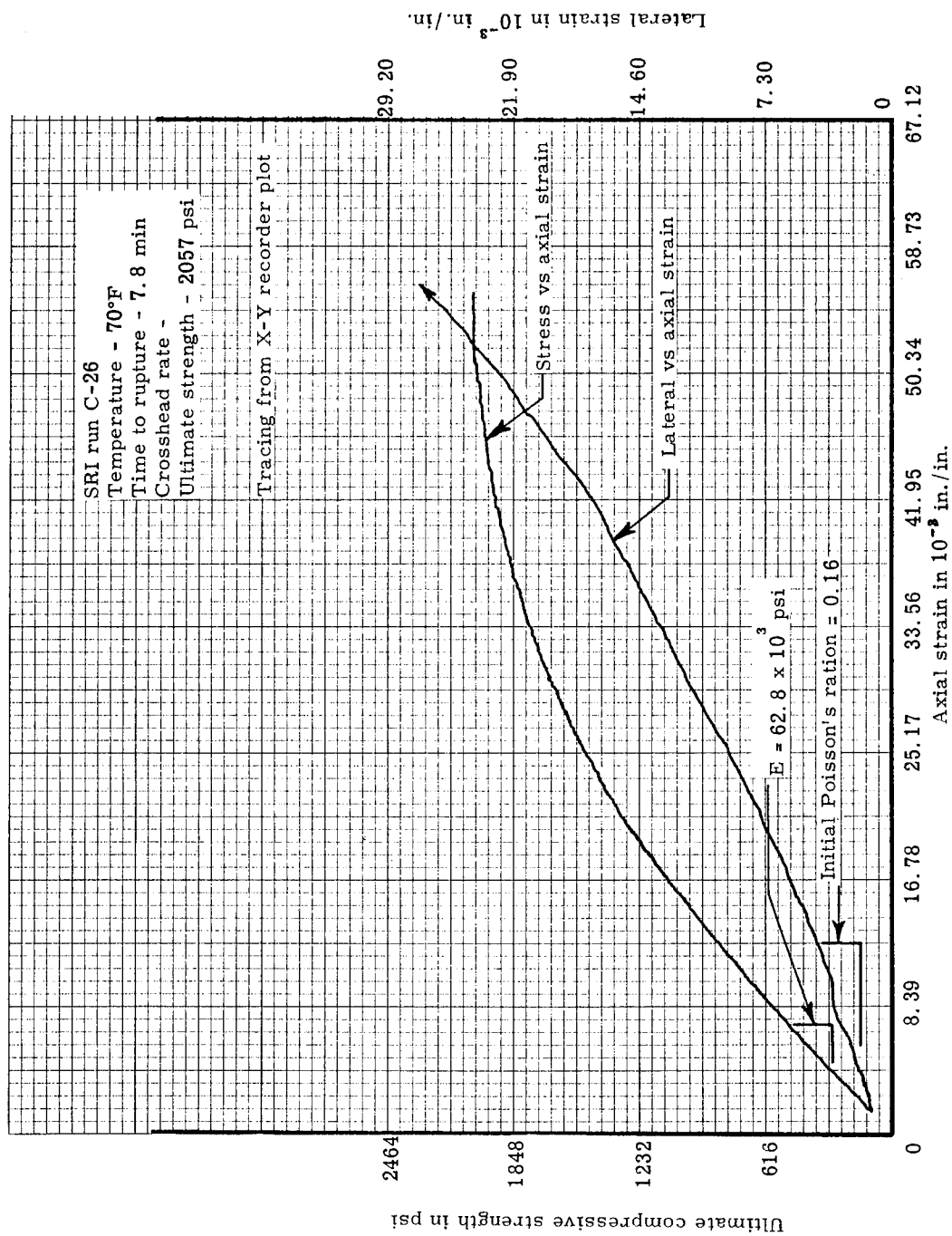
Chart labels and annotations:

Lateral strain in 10^{-3} in./in.

SRI run C-25
Temperature -70°F
Time to rupture - 10 min
Crosshead rate -
Ultimate strength - 2090 psi

Tracing from X-Y recorder plot

Stress vs axial strain

Lateral vs axial strain

E = 72.7×10³ psi

Initial Poisson's ratio = 0.11

Axial strain in 10^{-3} in./in.

Ultimate compressive strength in psi

114

Figure C46. Axial compressive stress-strain and bi-driectional strains at 70°F for a virgin low-density phenolic-nylon

115

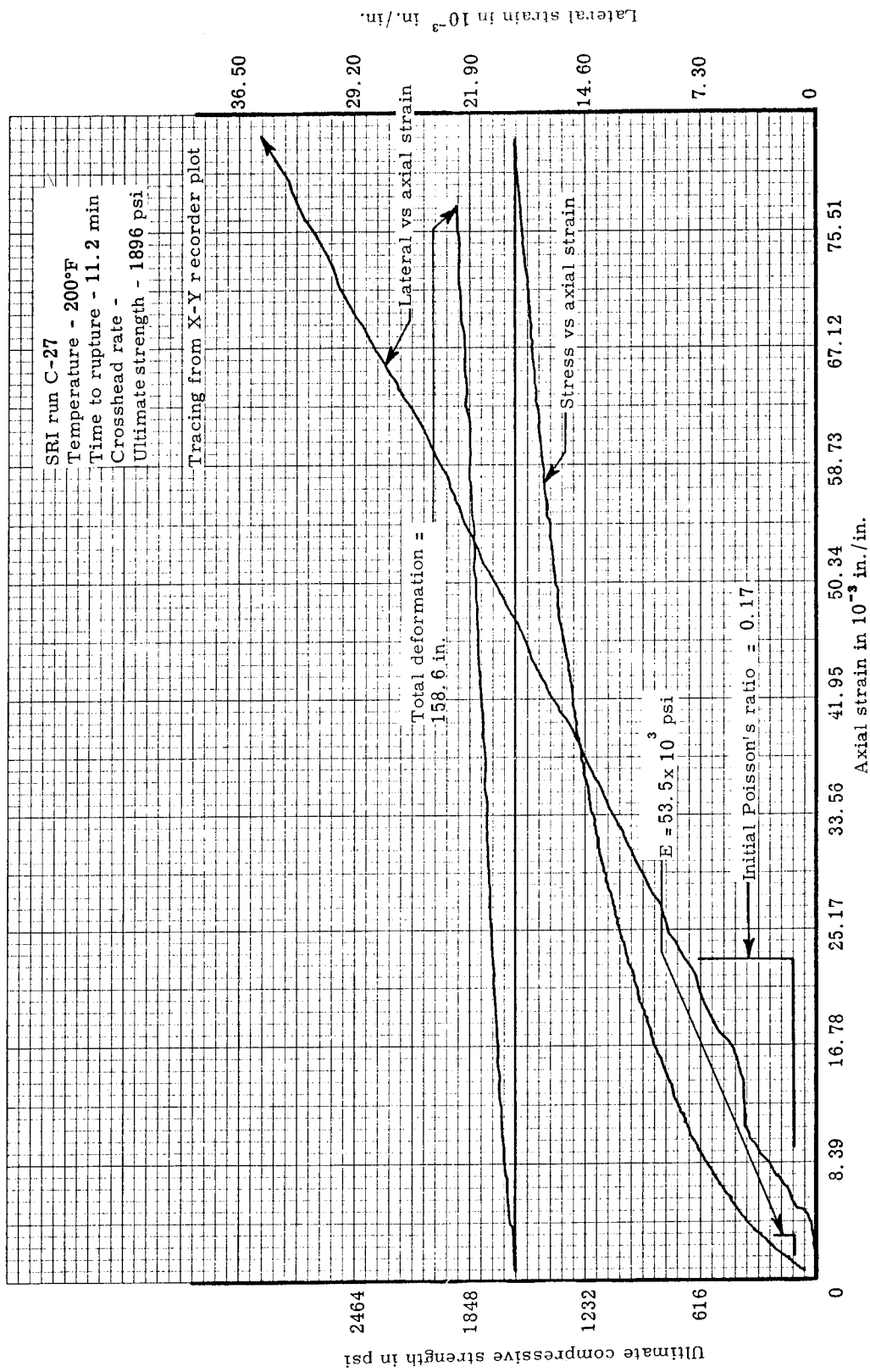Lateral strain in 10^{-3} in./in.

SRI run C-27
Temperature - 200°F
Time to rupture - 11.2 min
Crosshead rate -
Ultimate strength - 1896 psi

Tracing from X-Y recorder plot

Lateral vs axial strain

Stress vs axial strain

Total deformation =
158.6 in.

$E = 53.5 \times 10^3$ psi

Initial Poisson's ratio = 0.17

Ultimate compressive strength in psi

Axial strain in 10^{-3} in./in.

Figure C47. Axial compressive stress-strain and bi-directional strains at 200°F for a virgin low-density phenolic-nylon
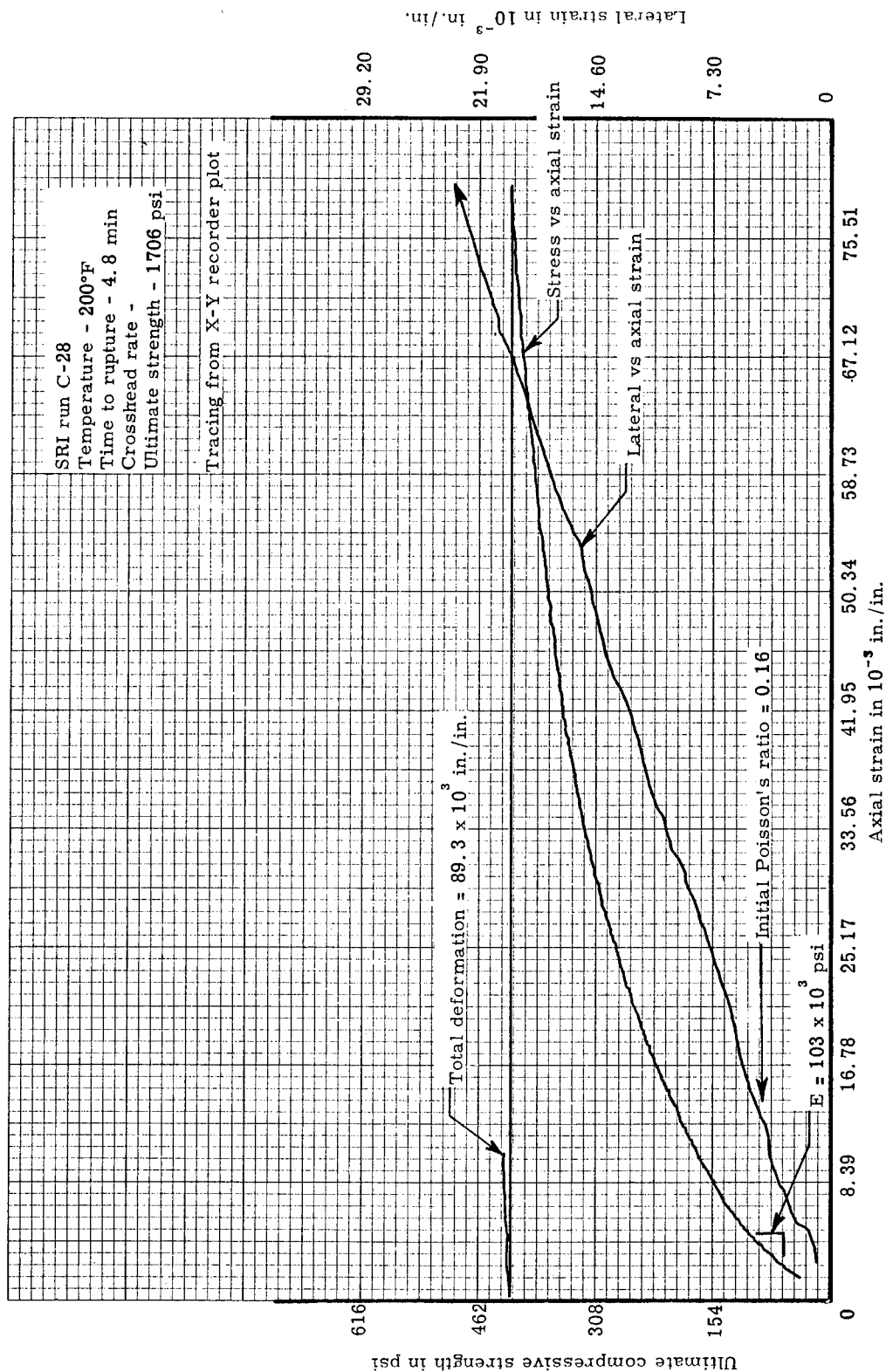
116

Figure C48. Axial compressive stress-strain and bi-directional strains at 200°F for a virgin low-density phenolic-nylon

"The aeronautical and space activities of the United States shall be conducted so as to contribute . . . to the expansion of human knowledge of phenomena in the atmosphere and space. The Administration shall provide for the widest practicable and appropriate dissemination of information concerning its activities and the results thereof."

—NATIONAL AERONAUTICS AND SPACE ACT OF 1958

NASA SCIENTIFIC AND TECHNICAL PUBLICATIONS

TECHNICAL REPORTS: Scientific and technical information considered important, complete, and a lasting contribution to existing knowledge.

TECHNICAL NOTES: Information less broad in scope but nevertheless of importance as a contribution to existing knowledge.

TECHNICAL MEMORANDUMS: Information receiving limited distribution because of preliminary data, security classification, or other reasons.

CONTRACTOR REPORTS: Scientific and technical information generated under a NASA contract or grant and considered an important contribution to existing knowledge.

TECHNICAL TRANSLATIONS: Information published in a foreign language considered to merit NASA distribution in English.

SPECIAL PUBLICATIONS: Information derived from or of value to NASA activities. Publications include conference proceedings, monographs, data compilations, handbooks, sourcebooks, and special bibliographies.

TECHNOLOGY UTILIZATION PUBLICATIONS: Information on technology used by NASA that may be of particular interest in commercial and other non-aerospace applications. Publications include Tech Briefs, Technology Utilization Reports and Notes, and Technology Surveys.

Details on the availability of these publications may be obtained from:

SCIENTIFIC AND TECHNICAL INFORMATION DIVISION

NATIONAL AERONAUTICS AND SPACE ADMINISTRATION

Washington, D.C. 20546